IN THIS ISSUE

Great Britain Journals Press

IMAGE: OBSERVATORY WITH STAR TRAILS ON MOUNTAINS FOR CLEAR SKY

www.journalspress.com

LONDON JOURNAL OF RESEARCH IN SCIENCE: NATURAL AND FORMAL

Print ISSN: 2631-8490
Online ISSN: 2631-8504
DOI: 10.17472/LJRS

Volume 23 | Issue 8 | Compilation 1.0

COMPILED IN UNITED KINGDOM

ENGLISH

London Journal of Research in Science: Natural and Formal

Volume 23 | Issue 8 | Compilation 1.0

PUBLISHER

Great Britain Journals Press
1210th, Waterside Dr,Opposite Arlington Building, Theale, Reading
Phone:+444 0118 965 4033 Pin: RG7-4TY United Kingdom

SUBSCRIPTION

Frequency: Quarterly

Print subscription
$280USD for 1 year
$500USD for 2 year
(*color copies including taxes and international shipping with TSA approved)*
Find more details at https://journalspress.com/journals/subscription

ENVIRONMENT

Great Britain Journals Press is intended about Protecting the environment. This journal is printed using led free environmental friendly ink and acid–free papers that are 100% recyclable.

Great Britain Journals Press Headquaters

1210th, Waterside Dr,
Opposite Arlington
Building, Theale, Reading
Phone:+444 0118 965 4033
Pin: RG7-4TY
United Kingdom

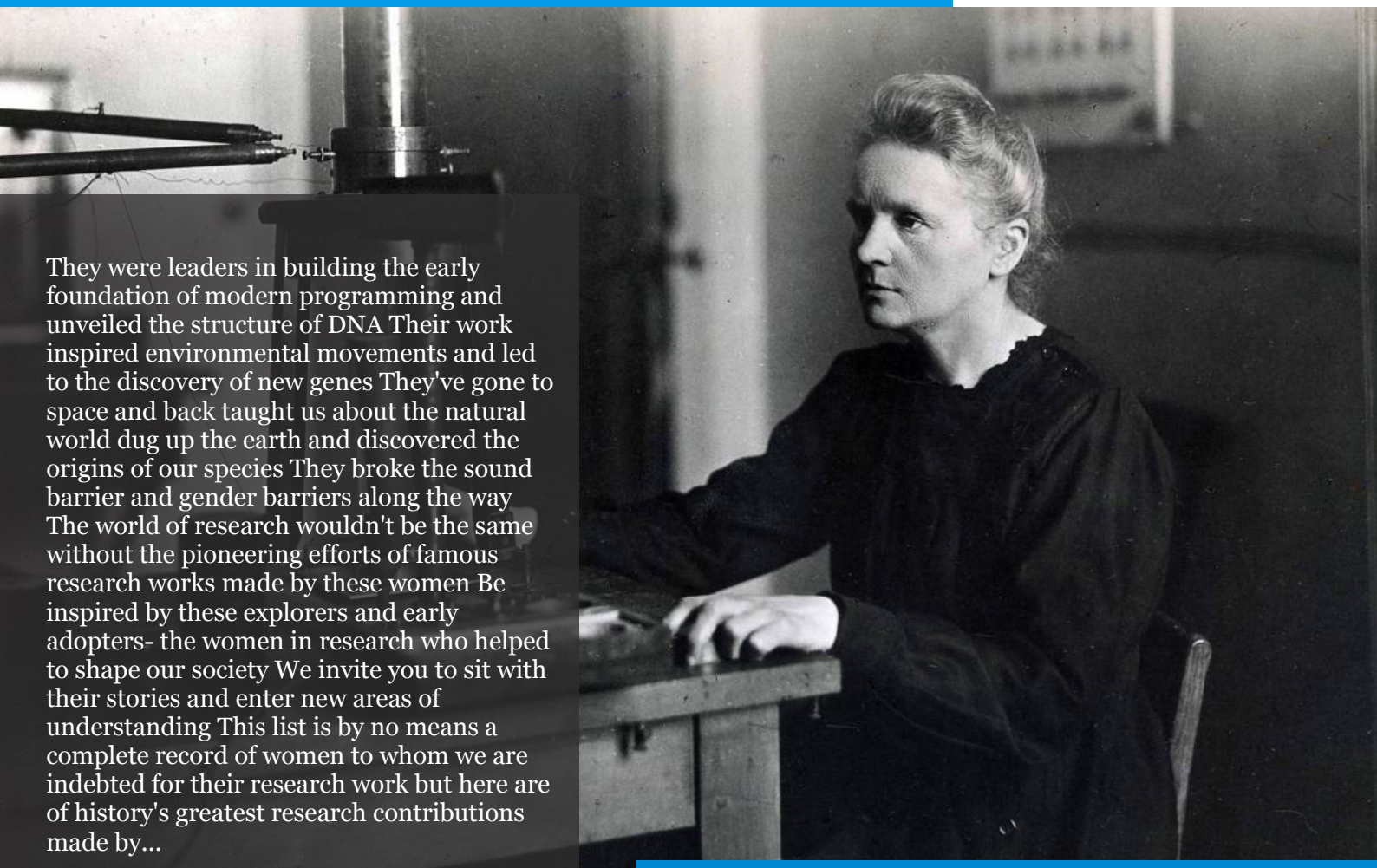

They were leaders in building the early foundation of modern programming and unveiled the structure of DNA Their work inspired environmental movements and led to the discovery of new genes They've gone to space and back taught us about the natural world dug up the earth and discovered the origins of our species They broke the sound barrier and gender barriers along the way The world of research wouldn't be the same without the pioneering efforts of famous research works made by these women Be inspired by these explorers and early adopters- the women in research who helped to shape our society We invite you to sit with their stories and enter new areas of understanding This list is by no means a complete record of women to whom we are indebted for their research work but here are of history's greatest research contributions made by...

Read complete here:
https://goo.gl/1vQ3lS

Women In Research

Computing in the cloud!

Cloud Computing is computing as a Service and not just as a Product Under Cloud Computing...

Read complete here:
https://goo.gl/VvHC72

Writing great research...

Prepare yourself before you start Before you start writing your paper or you start reading other...

Read complete here:
https://goo.gl/np73jP

Journal Content
In this Issue

Great Britain Journals Press

Editorial Board

Curated board members

Nicola Mastronardi

Consiglio Nazionaledelle Ricerche,
Ph.D. Applied Mathematics Katholieke
Universiteit Leuven
Belgium

Dr. Indranil Sen Gupta

Ph.D., Mathematics
Texas A & M University
Department of Mathematics
North Dakota State University
North Dakota, USA

Dr. Arvind Chhabra

University of Connecticut Health Center
USA Ph.D., Biotechnology Central
Drug Research Institute

Dr. Vladimir Burtman

Research Scientist
The University of Utah
Geophysics
Frederick Albert Sutton Building
115 S 1460 E Room 383
Salt Lake City, UT 84112, US

Dr. Xianghong Qi

University of Tennessee
Oak Ridge National Laboratory
Center for Molecular Biophysics
Oak Ridge National Laboratory
Knoxville, TN 37922
United States

Dr. Arshak Poghossian

Ph.D. Solid-State Physics
Leningrad Electrotechnical Institute, Russia
Institute of Nano and Biotechnologies
Aachen University of Applied Sciences, Germany

Dr. Bingyun Li

Ph.D. Fellow, IAES
Guest Researcher, NIOSH, CDC, Morgantown, WV
Institute of Nano and Biotechnologies
West Virginia University, US

Dr. Maria Gullo

Ph.D., Food Science, and Technology
University of Catania
Department of Agricultural and Food Sciences
University of Modena and Reggio Emilia, Italy

Dr. A. Heidari

Ph.D., D.Sc
Faculty of Chemistry
California South University (CSU), United States

Dr. Alicia Esther Ares

Ph.D. in Science and Technology,
University of General San Martin, Argentina
State University of Misiones, US

Research papers and articles

Volume 23 | Issue 8 | Compilation 1.0

On Some Spatial Considerations of the Tabulated (Categorical) Stationary Series (Natural Modelling; Probability Restrictions; Markovian Dependence)

Chrysoula Dimitriou-Fakalou

ABSTRACT

A spatial model for the strictly stationary series that have been discretized into a specified number of categories, is presented: special emphasis is concentrated on the finite two-sided Markovian structure. The new suggestion puts forward an all-random model, relying on a collection of unobserved series, with variables that are defined on different sample spaces. Imitating the linear ARMA series (that employ the spectral densities though), symmetry restrictions (via Bernoulli variables) and time reversal are explored and succeed to a certain extent. Subject to an, applicable to any distribution, assignment of variables' values into (k +1) ranges, and to the selection of the serial order p and q, the general Table Auto-Linear Moving-Average (k, p, q) equation provides for the spatial, all-moments stationary as well as infinite homogeneous Markovian, dependence.

Keywords: auto-linear; bernoulli; categorization; latent equalizer predictor; strictly stationary.

Classification: LCC Code: QA1-QA939

Language: English

Great Britain Journals Press

LJP Copyright ID: 925681
Print ISSN: 2631-8490
Online ISSN: 2631-8504

London Journal of Research in Science: Natural and Formal

Volume 22 | Issue 8 | Compilation 1.0

On Some Spatial Considerations of the Tabulated (Categorical) Stationary Series (Natural Modelling; Probability Restrictions; Markovian Dependence)

Chrysoula Dimitriou-Fakalou

ABSTRACT

A spatial model for the strictly stationary series that have been discretized into a specified number of categories, is presented: special emphasis is concentrated on the finite two-sided Markovian structure. The new suggestion puts forward an all-random model, relying on a collection of unobserved series, with variables that are defined on different sample spaces. Imitating the linear ARMA series (that employ the spectral densities though), symmetry restrictions (via Bernoulli variables) and time reversal are explored and succeed to a certain extent. Subject to an, applicable to any distribution, assignment of variables' values into (k +1) ranges, and to the selection of the serial order p and q, the general Table Auto-Linear Moving-Average (k, p, q) equation provides for the spatial, all-moments stationary as well as infinite homogeneous Markovian, dependence.

Keywords: auto-linear; bernoulli; categorization; latent equalizer predictor; strictly stationary.

Author: Chrysoula Dimitriou-Fakalou, self-employed scholar, 1st floor, 6 Kastelorizou Street, Ano Voula Attikis, Athens 16673, Greece. email: my.submission@mail.com

I. INTRODUCTION

Up to this day, the theory of the other than ARMA-modelled stationary time series has been enriched with some decent attempts: the direct aim of Lomnicki and Zaremba (1955) or Keenan (1982), was on the strictly stationary processes by reducing to categorical $0-1$ dependencies; the Discrete ARMA models of Jacobs and Lewis (1978) have placed the focus on general mixtures; the bilinear model with deterministic coefficients offers a net solution, by writing the variable as a sum of products of its lagged and error lagged values raised to natural powers, but suffers from a lack of interpretation and demands some immediate action regarding measurability; both the INARMA model (for instance, find a primary form in McKenzie (1985) and then Du and Li (1991)) and the suggestion of Cui and Lund (2009) work for count data, with the first one crossing the variables of interest with errors, and the second one only conveniently combining information from discrete time renewal processes.

London Journal of Research in Science: Natural and Formal

Evidently, blending the different equations in order to escape the linear series modelling, has been a common mentality: for example, one could catch up on switching between different ARMA equations in Francq and Zakoïan (2001). The threshold models, an excellent account of which resides in Tong (1990), may be considered as a world popular illustration of non-linearity that caused a lot of this. Finally, the latest suggestion of a TARMA model by Dimitriou-Fakalou (2019) is to fulfil the promise of encompassing the strictly stationary dependence, via a 'non-parametric' assignment of the variables' values into a fixed number of ranges: under causality, Markov chain conditional probability approaches become its special case. Since this paper will be translating the TARMA merits for the spatial series in the line transect, a reminder of existing transitions from time to space must follow.

For the linear series, two main streams developed in the past: the simultaneous bilateral auto-regressive models of Whittle (1954) and the conditional auto-normal processes of Besag (1974). The first exhibited what happens when the standard ARMA model uses its variables from both past and future: the high risks for the inference were exposed and the causal solution has been treasured as the right way to go, subject to the unilateral (more than one) index ordering of Whittle (1954). Besag (1974), on the other hand, worked with conditional arguments and proposed a Gaussian model that equally treats both ends of the axis; that second approach would often relate to a parameterization with intrinsic restrictions. Remaining in the 'best linear predictor' series department, those authentic definitions triggered Dimitriou-Fakalou (2010) to introduce the term 'auto-linear', combining the simultaneous (rather than conditional) element from Whittle (1954) together with the spatial (rather than unilateral) element from Besag (1974).

Trying to record some attempts for the spatial modelling outside the Gaussian distribution, Besag (1974) also introduced the auto-logistic schemes (for a fixated number of sites in space rather than a process in the transect) applied on Bernoulli variables that do, in general, exhibit a higher than second-order dependence: nevertheless, those definitions were accompanied by the assumption that the quantities

relating more than two variables were set as null (leaving the analysis only to *cliques consisting of single sites and pairs of sites*) and shattered any hope of going further than the relevant pairwise elements. The reader is encouraged to look at Cressie (1993) for a beautiful description of the different perspectives in spatial statistics, which is rich in diverse material: nevertheless when working in space, the dilemma of either sticking to linearity for the infinite lattice processes, or resorting to conditional probability arguments and under the knowledge of a basic distribution for the finite lattice variables, remains.

Hence a discretized strictly stationary series indexed regularly in the straight line is to be modelled: a two-sided, random coefficient equation is the proposed solution satisfying the spatial needs. Due to the severe difficulties that arise when scrutinizing the spatial dependencies, the assumption of causality that frees the 'future' errors from any dependence with 'present' and 'past' variables will still be wrapped inside the new definitions. Section 3 introduces a special case of the model, which results in the spatial pth order conditional probabilities, and Section 3.1 explains the thinking that supports the new models: the arguments relate to writing the *latent equalizer predictor*, as this has been explained already in Section 2. Section 3.2 is looking for ways to get to the restrictions that tie Bernoulli variables in space, and Section 3.3 examines whether time reversal can be achieved when one goes higher than the Gaussianity of random variables and there is no moment generating function to ease the derivations; this is versus the spectral density of an ARMA(p, q) series that reveals how 2^{p+q} different ARMA equations share the same auto-covariance function (Brockwell and Davis (1991)). Finally, *Definition 1* in Section 4 introduces the Table Auto-Linear Moving-Average model and perfects the previous suggestions, by approximating the infinite spatial Markovian dependence.

II. REMINDERS: THE 'LATENT EQUALIZER PREDICTOR' APPROACH

Suppose that $\{X_t,\ t \in \mathbb{Z}\}$ is a strictly stationary time series which, either naturally or by discretization, takes the values 0, v_1,...v_k with probability one. For a fixed positive integer p, this could be modelled as

$$X_t := I_t^{(X_{t-1},\ldots,X_{t-p})}, \tag{1}$$

where $\{I_t^{(i_1,\ldots,i_p)},\ t \in \mathbb{Z}\}$, $i_1,\ldots,i_p = 0, v_1,\ldots,v_k$ are sequences of independent in time and identically distributed random vectors with marginal probability masses

$$\pi_w^{(i_1,\ldots,i_p)} := \mathbb{P}(I_t^{(i_1,\ldots,i_p)} = w),\ w = 0, v_1,\ldots,v_k.$$

If the index functions

$$f_x(y) = \frac{\prod_{x^*=0,v_1,\ldots,v_k,\ x^*\neq x}(y-x^*)}{\prod_{x^*=0,v_1,\ldots,v_k,\ x^*\neq x}(x-x^*)} = \begin{cases} 1, & \text{if } y = x \\ 0, & \text{if } y = 0, v_1,\ldots,v_k,\ y \neq x \end{cases}$$

are considered, then (1) is equivalent to

$$f_x(X_t) = \sum_{i_1,\ldots,i_p=0,v_1,\ldots,v_k} f_x(I_t^{(i_1,\ldots,i_p)}) \cdot f_{i_1}(X_{t-1})\ldots f_{i_p}(X_{t-p}),\ x = 0, v_1,\ldots,v_k. \tag{2}$$

Under the condition of (*table*) causality (see Dimitriou-Fakalou (2019)), it is secured that $I_t^{(\ldots)}$ is independent of X_{t-l}, $l > 0$, so that (1) implies that

$$\mathbb{P}(X_t = x \mid X_{t-n} = x_n,\ n \in \mathbb{N}) \equiv \mathbb{P}(X_t = x \mid X_{t-n} = x_n,\ n = 1,\ldots,p) = \pi_x^{(x_1,\ldots,x_n)} \tag{3}$$

for $x, x_n = 0, v_1,\ldots,v_k$, $n \in \mathbb{N}$, and hence $\{X_t\}$ exhibits the pth order (homogeneous) Markovian structure.

Model (1) uses the *latent equalizer predictor* to define $\{X_t,\ t \in \mathbb{Z}\}$ and this is explained here further. For the linear series, we write the best (linear) predictor of X_t based on, say, X_{t-i} for some decided values of the $i \neq 0$: this is a linear function of the X_{t-i} with deterministic coefficients, i.e. a random variable; knowledge of the X_{t-i} leads to a realization of the predictor. The difference of X_t minus the predictor is defined as the *prediction error*, so that what singles out the best linear predictor as unique amongst other linear functions, is that *the best linear prediction error is uncorrelated with the relevant* X_{t-i}.

For the discretized series, we write the latent equalizer predictor of X_t based on X_{t-i}, $i \neq 0$, which is a random variable that is set *equal* to X_t, using the information according to X_{t-i} as it is their function; for each one of their combined value an X_t variable is assigned and, hence, knowledge of the X_{t-i} leads to a random variable, say, the conditional predictor with known distribution. What has characterized the latent equalizer predictor of X_t based on X_{t-i}, $i \neq 0$, is that the distribution of the conditional predictor remains unchanged under the presence of the relevant condition or not, implying some form of *independence* with it: for instance, in this section $\mathbb{P}(I_t^{(i_1,\ldots,i_p)} = w \mid X_{t-1} = i_1, \ldots, X_{t-p} = i_p) = \mathbb{P}(I_t^{(i_1,\ldots,i_p)} = w)$ verifies that $I_t^{(i_1,\ldots,i_p)}$ is independent of $f_{i_1}(X_{t-1}) \ldots f_{i_p}(X_{t-p})$.

Prediction examples: The best linear prediction of X_t based on some X_{t-i}, $i \neq 0$, is a linear function of the X_{t-i}; the intercept and coefficients are determined according to the first and second moments of the variables (parameters which are known or to be estimated). The latent equalizer prediction (of X_t based on some X_{t-i}, $i \neq 0$) is the realization of a random variable; its (discrete) distribution are the parameters which are known or to be estimated. In this section's notation, when $X_{t-1} = i_1$,...$X_{t-p} = i_p$ the latent equalizer prediction of X_t can be the realization of a random variable with identical distribution as that of $I_t^{(i_1,\ldots,i_p)}$.

III. SPATIAL MODELING

Next suppose that instead of the time axis, the strictly stationary process of interest, say $\{X_s,\ s \in \mathbb{Z}\}$ takes place in the spatial line transect (see Whittle, 1954); this can still be expressed as in (1), yielding a unilateral representation based on the variables of one side of the transect X_{s-i}, $i > 0$, but it is explored here what is the spatial analogue. Subject to the condition of causality that links (1) to an adequate strictly stationary process $\{X_s\}$, it is now written that

$$X_s := Y_s^{[(X_{s-p},\ldots,X_{s-1});(X_{s+1},\ldots,X_{s+p})]}, \tag{4}$$

where for $\mathbf{i}_P = (i_{P,p}, \ldots, i_{P,1})$ (and $\mathbf{i}_P^\tau = (i_{P,1}, \ldots, i_{P,p})$ still a row vector), $\mathbf{i}_F = (i_{F,1}, \ldots, i_{F,p})$, it holds that (set any $i_{P,1}, \ldots, i_{P,p}$, $i_{F,1}, \ldots, i_{F,p} = 0, v_1, \ldots, v_k$)

$$m_s^{[\mathbf{i}_P;\mathbf{i}_F]} \cdot Y_s^{[\mathbf{i}_P;\mathbf{i}_F]} := M_s^{[\mathbf{i}_P;\mathbf{i}_F]}, \tag{5}$$

which must be accompanied by

$$m_s^{[\mathbf{i}_P;\mathbf{i}_F]} := \sum_{w=0,v_1,\ldots,v_k} f_w(I_s^{(\mathbf{i}_P^\tau)}) \cdot f_{i_{F,1}}(I_{s+1}^{(w,i_{P,1},\ldots,i_{P,p-1})}) \ldots f_{i_{F,p}}(I_{s+p}^{(i_{F,p-1},\ldots,i_{F,1},w)})$$

and

$$M_s^{[\mathbf{i}_P;\mathbf{i}_F]} := I_s^{(\mathbf{i}_P^\tau)} \cdot f_{i_{F,1}}(I_{s+1}^{(I_s^{(\mathbf{i}_P^\tau)},i_{P,1},\ldots,i_{P,p-1})}) \ldots f_{i_{F,p}}(I_{s+p}^{(i_{F,p-1},\ldots,i_{F,1},I_s^{(\mathbf{i}_P^\tau)})});$$

the last equation results in

$$\begin{aligned} f_w(M_s^{[\mathbf{i}_P;\mathbf{i}_F]}) &= f_w(I_s^{(\mathbf{i}_P^\tau)}) \cdot f_{i_{F,1}}(I_{s+1}^{(w,i_{P,1},\ldots,i_{P,p-1})}) \ldots f_{i_{F,p}}(I_{s+p}^{(i_{F,p-1},\ldots,i_{F,1},w)}),\ w = v_1,\ldots,v_k, \\ f_0(M_s^{[\mathbf{i}_P;\mathbf{i}_F]}) &= 1 - \sum_{w=v_1,\ldots,v_k} f_w(M_s^{[\mathbf{i}_P;\mathbf{i}_F]}). \end{aligned}$$

Note that if $m_s^{[\mathbf{i}_P;\mathbf{i}_F]} = 0$ then $M_s^{[\mathbf{i}_P;\mathbf{i}_F]} \equiv I_s^{(\mathbf{i}_P^\tau)} \cdot m_s^{[\mathbf{i}_P;\mathbf{i}_F]}$ is equal to zero as well. Hence, it is clarified that if the system (5) is null, then the variable Y cannot be considered at all, i.e. $Y_s^{[\mathbf{i}_P;\mathbf{i}_F]}$ is defined on the sample space $\{m_s^{[\mathbf{i}_P;\mathbf{i}_F]} = 1\}$. Provided that $m_s^{[\mathbf{i}_P;\mathbf{i}_F]} = 1$, (5) can be replaced by $f_y(Y_s^{[\mathbf{i}_P;\mathbf{i}_F]}) = f_y(M_s^{[\mathbf{i}_P;\mathbf{i}_F]})$.

In addition, (4) is equivalent to

$$\begin{aligned} f_y(X_s) = \sum_{i_{P,p},\ldots,i_{P,1},i_{F,1},\ldots i_{F,p}=0,v_1,\ldots,v_k} & f_y(Y_s^{([\mathbf{i}_P;\mathbf{i}_F])} \cdot f_{i_{P,p}}(X_{s-p}) \ldots f_{i_{P,1}}(X_{s-1}) \\ & f_{i_{F,1}}(X_{s+1}) \ldots f_{i_{F,p}}(X_{s+p}) \end{aligned} \quad (6)$$

for all $y = 0, v_1, \ldots, v_k$. Directly from (6), it can be deduced that for any $y = 0, v_1, \ldots, v_k$, it holds that

$$\begin{aligned} &\mathbb{P}(X_s = y \mid X_{s-p} = i_{P,p}, \ldots, X_{s-1} = i_{P,1}, X_{s+1} = i_{F,1}, \ldots, X_{s+p} = i_{F,p}) = \\ &\mathbb{P}(Y_s^{[\mathbf{i}_P;\mathbf{i}_F]} = y \mid X_{s-p} = i_{P,p}, \ldots, X_{s-1} = i_{P,1}, X_{s+1} = i_{F,1}, \ldots, X_{s+p} = i_{F,p}) \quad (7) \end{aligned}$$

$$(\{X_{s-1} = i_{P,1}, \ldots, X_{s-p} = i_{P,p}, X_{s+1} = i_{F,1}, \ldots, X_{s+p} = i_{F,p}\} \subseteq \{m_s^{[\mathbf{i}_P;\mathbf{i}_F]} = 1\}).$$

3.1 Interpretations

The variable $m_s^{[\mathbf{i}_P;\mathbf{i}_F]}$ is Bernoulli and it holds that

$$\mathbb{P}(m_s^{[\mathbf{i}_P;\mathbf{i}_F]}=1)=\sum_{w=0,v_1,\ldots,v_k}\mathbb{E}\{f_w(I_s^{(\mathbf{i}_P^\tau)})\}\,\mathbb{E}\{f_{i_{F,1}}(I_{s+1}^{(w,i_{P,1},\ldots,i_{P,p-1})})\}\ldots\mathbb{E}\{f_{i_{F,p}}(I_{s+p}^{(i_{F,p-1},\ldots,i_{F,1},w)})\} \tag{8}$$

(remember that I are assumed to be 'serially' independent on different spots of the line transect). The variable $M_s^{[\mathbf{i}_P;\mathbf{i}_F]}$ is 0 or $1\cdot w$, $w=0,v_1,\ldots,v_k$, and it holds that

$$\begin{aligned}&\mathbb{P}(M_s^{[\mathbf{i}_P;\mathbf{i}_F]}=w,m_s^{[\mathbf{i}_P;\mathbf{i}_F]}=1)=\\&\mathbb{E}\{f_w(I_s^{(\mathbf{i}_P^\tau)})\}\,\mathbb{E}\{f_{i_{F,1}}(I_{s+1}^{(w,i_{P,1},\ldots,i_{P,p-1})})\}\ldots\mathbb{E}\{f_{i_{F,p}}(I_{s+p}^{(i_{F,p-1},\ldots,i_{F,1},w)})\}\end{aligned} \tag{9}$$

(for $w=v_1,\ldots,v_k$, it holds additionally that $\mathbb{P}(M_s^{[\mathbf{i}_P;\mathbf{i}_F]}=w)=\mathbb{P}(M_s^{[\mathbf{i}_P;\mathbf{i}_F]}=w,m_s^{[\mathbf{i}_P;\mathbf{i}_F]}=1)$). It can be written, in general, then

$$\begin{aligned}\mathbb{P}(Y_s^{[\mathbf{i}_P;\mathbf{i}_F]}=w)\;\equiv\;&\mathbb{P}(Y_s^{[\mathbf{i}_P;\mathbf{i}_F]}=w\mid m_s^{[\mathbf{i}_P;\mathbf{i}_F]}=1)=\mathbb{P}(M_s^{[\mathbf{i}_P;\mathbf{i}_F]}=w\mid m_s^{[\mathbf{i}_P;\mathbf{i}_F]}=1)=\\&\frac{\mathbb{P}(M_s^{[\mathbf{i}_P;\mathbf{i}_F]}=w,m_s^{[\mathbf{i}_P;\mathbf{i}_F]}=1)}{\mathbb{P}(m_s^{[\mathbf{i}_P;\mathbf{i}_F]}=1)},\;w=0,v_1,\ldots,v_k.\end{aligned} \tag{10}$$

In the other hand, it holds that

$$\begin{aligned}&\mathbb{P}(X_s=w\mid(X_{s-1},\ldots,X_{s-p})=\mathbf{i}_P^\tau,(X_{s+1},\ldots,X_{s+p})=\mathbf{i}_F)=\\&\frac{\mathbb{P}(X_s=w,X_{s+1}=i_{F,1},\ldots,X_{s+p}=i_{F,p}\mid X_{s-1}=i_{P,1},\ldots,X_{s-p}=i_{P,p})}{\sum_{w^*=0,v_1,\ldots,v_k}\mathbb{P}(X_s=w^*,X_{s+1}=i_{F,1},\ldots,X_{s+p}=i_{F,p}\mid X_{s-1}=i_{P,1},\ldots,X_{s-p}=i_{P,p})}=\\&\frac{\mathbb{E}\{f_w(I_s^{(i_{P,1},\ldots,i_{P,p})})f_{i_{F,1}}(I_{s+1}^{(w,i_{P,1},\ldots,i_{P,p-1})})\ldots f_{i_{F,p}}(I_{s+p}^{(i_{F,p-1},\ldots,i_{F,1},w)})\}}{\sum_{w^*=0,v_1,\ldots,v_k}\mathbb{E}\{f_{w^*}(I_s^{(i_{P,1},\ldots,i_{P,p})})f_{i_{F,1}}(I_{s+1}^{(w^*,i_{P,1},\ldots,i_{P,p-1})})\ldots f_{i_{F,p}}(I_{s+p}^{(i_{F,p-1},\ldots,i_{F,1},w^*)})\}}\end{aligned}$$

based on the representation $X_s=I_s^{(X_{s-1},\ldots,X_{s-p})}$. By combining the derivation above together with (7) as well as (8), (9) and (10), it can be concluded that

$$\mathbb{P}(Y_s^{[\mathbf{i}_P;\mathbf{i}_F]}=w)=\mathbb{P}(Y_s^{[\mathbf{i}_P;\mathbf{i}_F]}=w\mid(X_{s-1},\ldots,X_{s-p})=\mathbf{i}_P^\tau,(X_{s+1},\ldots,X_{s+p})=\mathbf{i}_F). \tag{11}$$

In fact using similar arguments, it can be shown (for any $x_l=0,v_1,\ldots,v_k$, $|l|=p+1,p+2,\ldots$), that

$$\begin{aligned}\mathbb{P}(Y_s^{[\mathbf{i}_P;\mathbf{i}_F]}=w)=\mathbb{P}(Y_s^{[\mathbf{i}_P;\mathbf{i}_F]}=w\mid\;&(X_{s-1},\ldots,X_{s-p})=\mathbf{i}_P^\tau,\\&(X_{s+1},\ldots,X_{s+p})=\mathbf{i}_F,X_{s-l}=x_l,\;|l|=p+1,p+2,\ldots).\end{aligned} \tag{12}$$

It has been obvious already that $Y_s^{[\mathbf{i}_P;\mathbf{i}_F]}$ (properly defined) is independent of X_{s-i}, $i > 0$, as the former is a function of I_{s+j}, $j \in \mathbb{N}_0$ and the latter is a function of I_{s-i-j}, $j \in \mathbb{N}_0$: this is no improvement over what was there before defining Y_s, i.e. the random variable I_s being independent of X_{s-i}, $i > 0$. The additional element that the equation (11) (together with (12)) brings in, is that it allows the probability of Y to remain unchanged under the condition of interest or not (implying a form of independence of $Y_s^{[\mathbf{i}_P;\mathbf{i}_F]}$ with each Bernoulli variable on the set $\{(X_{s-1},\dots,X_{s-p}) = \mathbf{i}_P^{\tau},\ (X_{s+1},\dots,X_{s+p}) = \mathbf{i}_F, X_{s-l} = x_l,\ |l| = (p+1),\dots,(p+n)\},\ n \in \mathbb{N}_0$), subject to shrinking the sample space for the variable; this seems to justify $Y_s^{[(X_{s-p},\dots,X_{s-1});(X_{s+1},\dots,X_{s+p})]}$ being a latent equalizer predictor of X_s based on X_{s-i}, $|i| \in \mathbb{N}$.

3.2 Symmetrical Probabilities

For variables with two values only ($k = 1$), say v_0, v_1 ($v_0 \neq v_1$), there is interest whether it holds that

$$\mathbb{P}(Y_s^{[\mathbf{i}_P;\mathbf{i}_F]} = w) \equiv \mathbb{P}(Y_s^{[\mathbf{i}_F^{\tau};\mathbf{i}_P^{\tau}]} = w),\ w = v_0, v_1 \tag{13}$$

(it is reminded that the two random variables are defined on different spaces and the index 's' for both is used 'loosely'). If (13) takes place, then

$$\frac{\mathbb{E}\{f_w(I_s^{(i_{P,1},\dots,i_{P,p})}) f_{i_{F,1}}(I_{s+1}^{(w,i_{P,1},\dots,i_{P,p-1})}) \dots f_{i_{F,p}}(I_{s+p}^{(i_{F,p-1},\dots,i_{F,1},w)})\}}{\sum_{w^*=v_0,v_1} \mathbb{E}\{f_{w^*}(I_s^{(i_{P,1},\dots,i_{P,p})}) f_{i_{F,1}}(I_{s+1}^{(w^*,i_{P,1},\dots,i_{P,p-1})}) \dots f_{i_{F,p}}(I_{s+p}^{(i_{F,p-1},\dots,i_{F,1},w^*)})\}} =$$
$$\frac{\mathbb{E}\{f_w(I_s^{(i_{F,1},\dots,i_{F,p})}) f_{i_{P,1}}(I_{s+1}^{(w,i_{F,1},\dots,i_{F,p-1})}) \dots f_{i_{P,p}}(I_{s+p}^{(i_{P,p-1},\dots,i_{P,1},w)})\}}{\sum_{w^*=v_0,v_1} \mathbb{E}\{f_{w^*}(I_s^{(i_{F,1},\dots,i_{F,p})}) f_{i_{P,1}}(I_{s+1}^{(w^*,i_{F,1},\dots,i_{F,p-1})}) \dots f_{i_{P,p}}(I_{s+p}^{(i_{P,p-1},\dots,i_{P,1},w^*)})\}}$$

and, consequently, (13) results in the key equality

$$\begin{aligned}
&\mathbb{E}\{f_{v_0}(I_s^{(i_{P,1},\dots,i_{P,p})}) f_{i_{F,1}}(I_{s+1}^{(v_0,i_{P,1},\dots,i_{P,p-1})}) \dots f_{i_{F,p}}(I_{s+p}^{(i_{F,p-1},\dots,i_{F,1},v_0)})\}\\
&\mathbb{E}\{f_{v_1}(I_s^{(i_{F,1},\dots,i_{F,p})}) f_{i_{P,1}}(I_{s+1}^{(v_1,i_{F,1},\dots,i_{F,p-1})}) \dots f_{i_{P,p}}(I_{s+p}^{(i_{P,p-1},\dots,i_{P,1},v_1)})\} =\\
&\mathbb{E}\{f_{v_1}(I_s^{(i_{P,1},\dots,i_{P,p})}) f_{i_{F,1}}(I_{s+1}^{(v_1,i_{P,1},\dots,i_{P,p-1})}) \dots f_{i_{F,p}}(I_{s+p}^{(i_{F,p-1},\dots,i_{F,1},v_1)})\}\\
&\mathbb{E}\{f_{v_0}(I_s^{(i_{F,1},\dots,i_{F,p})}) f_{i_{P,1}}(I_{s+1}^{(v_0,i_{F,1},\dots,i_{F,p-1})}) \dots f_{i_{P,p}}(I_{s+p}^{(i_{P,p-1},\dots,i_{P,1},v_0)})\}.
\end{aligned} \tag{14}$$

Lemma 1: If the order $p=1$ or $p=2$ then (13) definitely holds.

Proof: For $p=1$, (14) becomes

$$\mathbb{E}\{f_{v_0}(I_s^{(i_{P,1})})f_{i_{F,1}}(I_{s+1}^{(v_0)})\}\mathbb{E}\{f_{v_1}(I_s^{(i_{F,1})})f_{i_{P,1}}(I_{s+1}^{(v_1)})\}=$$
$$\mathbb{E}\{f_{v_1}(I_s^{(i_{P,1})})f_{i_{F,1}}(I_{s+1}^{(v_1)})\}\mathbb{E}\{f_{v_0}(I_s^{(i_{F,1})})f_{i_{P,1}}(I_{s+1}^{(v_0)})\}$$

or $\pi_{v_0}^{(i_{P,1})}\pi_{i_{F,1}}^{(v_0)}\pi_{v_1}^{(i_{F,1})}\pi_{i_{P,1}}^{(v_1)}=\pi_{v_1}^{(i_{P,1})}\pi_{i_{F,1}}^{(v_1)}\pi_{v_0}^{(i_{F,1})}\pi_{i_{P,1}}^{(v_0)}$, which holds when $i_{P,1}=i_{F,1}$ as well as when $v_1=i_{P,1}\neq i_{F,1}=v_0$ or $v_0=i_{P,1}\neq i_{F,1}=v_1$.

For $p=2$, the equality under question reduces to

$$\pi_{v_0}^{(i_{P,1},i_{P,2})}\,\pi_{i_{F,1}}^{(v_0,i_{P,1})}\pi_{i_{F,2}}^{(i_{F,1},v_0)}\cdot\pi_{v_1}^{(i_{F,1},i_{F,2})}\pi_{i_{P,1}}^{(v_1,i_{F,1})}\pi_{i_{P,2}}^{(i_{P,1},v_1)}=$$
$$\pi_{v_1}^{(i_{P,1},i_{P,2})}\pi_{i_{F,1}}^{(v_1,i_{P,1})}\pi_{i_{F,2}}^{(i_{F,1},v_1)}\cdot\pi_{v_0}^{(i_{F,1},i_{F,2})}\pi_{i_{P,1}}^{(v_0,i_{F,1})}\pi_{i_{P,2}}^{(i_{P,1},v_0)}$$

and the reader may try all different values to verify its validity. □

Next it is explained why (13) is investigated whether it holds. If it is true, it may be derived as well that

$$\mathbb{P}(X_s=w\mid(X_{s-1},\ldots,X_{s-p})=\mathbf{i}_P^{\tau},(X_{s+1},\ldots,X_{s+p})=\mathbf{i}_F)=$$
$$\mathbb{P}(X_s=w\mid(X_{s-1},\ldots,X_{s-p})=\mathbf{i}_F,(X_{s+1},\ldots,X_{s+p})=\mathbf{i}_P^{\tau}).\qquad(15)$$

In fact, it was Besag (1974) crystallizing that symmetry conditions often take place regarding the deterministic coefficients for spatial models of interest: for the auto-normal schemes (i.e. Gaussian variables that are characterized by an up to second-order dependence), those coefficients would be found in $\mathbb{E}\{X_s|X_{s-i},\ i=\pm1,\ldots,\pm p\}$. Later, in the simultaneous Auto-Linear model of Dimitriou-Fakalou (2010), the symmetrical coefficients were demonstrated to be (proportional to) the auto-covariances of the Y latent process, which was a moving-average series with pairs of variables uncorrelated when more than p (i.e. the order of the model) steps away. Hence the short investigation that took place here regarding Y symmetrical probabilities is natural and just.

For Bernoulli variables and $p=1$, the dependence is still linear (the conditional expectation of X_s given X_{s-i}, $i\geq1$ is a linear function of X_{s-1}, the conditional variance is no constant though), so that an even auto-covariance function might describe it. The material point is that

$$\mathbb{E}\{X_{s-n}^{(v_P)} X_s^{(w)} X_{s+n}^{(v_F)}\} = \mathbb{E}\{X_{s-n}^{(v_F)} X_s^{(w)} X_{s+n}^{(v_P)}\}, \quad n \in \mathbb{N}, \tag{16}$$

for any $w, v_P, v_F = 0, 1$, where the operator $X^{(i)}$, $i = 0, 1$ generates either X $(i = 1)$ or $1 - X$ $(i = 0)$, when X is in $\{0, 1\}$. The general Bernoulli property (16) results in

$$\mathbb{P}(X_s = w \mid X_{s-n} = v_P, X_{s+n} = v_F) = \mathbb{P}(X_s = w \mid X_{s-n} = v_F,\ X_{s+n} = v_P),$$

which easily justifies all symmetrical probabilities (15) for $p = 1$.

Lemma 2: For any fixed order $p \in \mathbb{N}$ ($k = 1$ and values v_0, v_1), it holds that

$$\begin{aligned}&\mathbb{P}(X_s = v_1 \mid X_{s-n} = v_1,\ X_{s+n} = v_0,\ n = 1, \ldots, p) = \\ &\mathbb{P}(X_s = v_1 \mid X_{s-n} = v_0, X_{s+n} = v_1,\ n = 1, \ldots, p) \equiv \frac{\pi_{v_1}^{(v_1,\ldots,v_1)}}{\pi_{v_1}^{(v_1,\ldots,v_1)} + \pi_{v_0}^{(v_0,\ldots,v_0)}},\end{aligned} \tag{17}$$

which can be linked to a natural interpretation.

Proof: Obvious. □

Lemma 3: For any fixed order $p \in \mathbb{N}$ ($k = 1$ and values v_0, v_1), it is true that the 'oscillating' conditional probabilities are symmetrical, i.e.

$$\begin{aligned}&\mathbb{P}(X_s = w \mid X_{s-1} = v_1, X_{s+1} = v_0, X_{s-2} = v_0, X_{s+2} = v_1, \ldots \\ &\qquad (X_{s+p-1} =) X_{s-p} \neq X_{s+p} (= X_{s-p+1})) = \\ &\mathbb{P}(X_s = w \mid X_{s-1} = v_0, X_{s+1} = v_1, X_{s-2} = v_1, X_{s+2} = v_0, \ldots \\ &\qquad (X_{s+p-1} =) X_{s-p} \neq X_{s+p} (= X_{s-p+1}))\end{aligned}$$

holds for both $w = v_0, v_1$.

Proof: If p is even, it holds (for either $w = v_0, v_1$) that

$$\begin{aligned}&\mathbb{P}(X_s = w, X_{s+1} = v_0, X_{s+2} = v_1, \ldots X_{s+p} = v_1 \mid X_{s-1} = v_1, \ldots, X_{s-p} = v_0) = \\ &\mathbb{P}(X_s = w, X_{s+1} = v_1, X_{s+2} = v_0, \ldots, X_{s+p} = v_0 \mid X_{s-1} = v_0, \ldots, X_{s-p} = v_1);\end{aligned}$$

if p is odd, it can be shown that

$$\frac{\mathbb{P}(X_s = w, X_{s+1} = v_0, X_{s+2} = v_1, \ldots, X_{s+p} = v_0 \mid X_{s-1} = v_1, \ldots, X_{s-p} = v_1)}{\mathbb{P}(X_s = w, X_{s+1} = v_1, X_{s+2} = v_0, \ldots, X_{s+p} = v_1 \mid X_{s-1} = v_0, \ldots, X_{s-p} = v_0)} = \frac{\pi_{v_0}^{(v_1 \ v_0 \ldots v_1)}}{\pi_{v_1}^{(v_0 \ v_1 \ldots v_0)}}, \ w = v_0, v_1. \quad \square$$

In addition to the Y latent series of the auto-linear model (Dimitriou-Fakalou, 2010), for any $p, k \in \mathbb{N}$, the variables Y as defined in Section 2 also follow a moving-average like pattern, in the sense that Y_s is *independent* of Y_{s+i}, $|i| \geq p+1$ (p-dependence). Due to the discretization within a finite number of categories and the extensive use of index variables, it is possible to compute joint probabilities of the Y variables. It is reminded that symmetry conditions for the original X modelled naturally in space, such as (15) when it holds, translate for the spatial latent equalizer predictors Y, such as (13), respectively. Nevertheless, the varying conditions under which the different Y series are considered could be making an essential difference to the various equalities, so the probabilities of Y or M should be computed with care. Below, there is a couple of examples of unobvious restrictions on the parameter probabilities of the spatial Y or M.

Probability restriction examples: We consider Bernoulli variables and order $p = 1$. We start with

$$\mathbb{P}(M_s^{[0;1]} = 1) = \pi_1^{(0)} \ \pi_1^{(1)} \neq \pi_1^{(1)}(1 - \pi_1^{(1)}) \equiv \mathbb{P}(M_s^{[1;0]} = 1), \tag{18}$$

as opposed to the special case of (13) when we know that

$$\mathbb{P}(Y_s^{[0;1]} = 1) = \frac{\pi_1^{(0)}\pi_1^{(1)}}{\pi_1^{(0)}\pi_1^{(1)} + (1 - \pi_1^{(0)})\pi_1^{(0)}} = \frac{\pi_1^{(1)}(1 - \pi_1^{(1)})}{\pi_1^{(1)}(1 - \pi_1^{(1)}) + (1 - \pi_1^{(1)})(1 - \pi_1^{(0)})} \equiv \mathbb{P}(Y_s^{[1;0]} = 1) : \tag{19}$$

though the left-hand or right-hand side of (18) seems to be 'proportional' to the left-hand or right-hand, respectively, side of (19), an equality does not become apparent from (18); $Y_s^{[0;1]}$ and $Y_s^{[1;0]}$ are defined on different spaces resulting, here, in $\mathbb{P}(m_s^{[0;1]} = 1) \neq \mathbb{P}(m_s^{[1;0]} = 1)$.

We continue with interest in moments (probabilities) of two random variables, and we try to discover analogues to the *even* auto-covariance function of the auto-linear Y latent series by Dimitriou-Fakalou (2010). Hence we consider the case $\{M_s^{[0;1]} = 1, M_{s+1}^{[1;0]} = 1\}$ and compare it to $\{M_s^{[1;0]} = 0, M_{s+1}^{[0;1]} = 0\}$, in terms of probability: this seems to be the closest possible to reversing the order in the transect of the two M-variables, i.e. $M^{[0;1]}$ and $M^{[1;0]}$.

An adequate space must be taking place for either case. In the first case, we write $\{mm_s^{[0;1][1;0]} = 1\} := \left\{I_s^{(0)} = 1, I_{s+2}^{(I_{s+1}^{(1)})} = 0\right\}$ ('mm' is one symbol), with probability of occurrence

$$\begin{aligned}\mathbb{P}(mm_s^{[0;1][1;0]} = 1) &= \pi_1^{(0)}\,[\mathbb{P}(I_{s+1}^{(1)} = 1)\,\mathbb{P}(I_{s+2}^{(1)} = 0) + \mathbb{P}(I_{s+1}^{(1)} = 0)\,\mathbb{P}(I_{s+2}^{(0)} = 0)] \\ &= \pi_1^{(0)}\,(1 - \pi_1^{(1)})\,(\pi_1^{(1)} + 1 - \pi_1^{(0)}),\end{aligned}$$

and followed by

$$\begin{aligned}\mathbb{P}(M_s^{[0;1]} = 1, M_{s+1}^{[1;0]} = 1 \mid mm_s^{[0;1][1;0]} = 1) &\equiv \frac{\mathbb{P}(I_s^{(0)} = 1,\ I_{s+1}^{(1)} = 1,\ I_{s+2}^{(1)} = 0)}{\mathbb{P}(mm_s^{[0;1][1;0]} = 1)} \\ &= \frac{\pi_1^{(1)}}{1 - \pi_1^{(0)} + \pi_1^{(1)}}.\end{aligned}$$

In the other hand, we write $\{mm_s^{[1;0][0;1]} = 1\} := \left\{I_s^{(1)} = 0, I_{s+2}^{(I_{s+1}^{(0)})} = 1\right\}$, and consider the events $\{M_s^{[1;0]} = 0\} = \{I_s^{(1)} = 0\} \cup \{I_{s+1}^{(I_s^{(1)})} = 1\}$ and $\{M_{s+1}^{[0;1]} = 0\} = \{I_{s+1}^{(0)} = 0\} \cup \{I_{s+2}^{(I_{s+1}^{(0)})} = 0\}$. Observe that

$$\mathbb{P}(M_s^{[1;0]} = 0, M_{s+1}^{[0;1]} = 0 \mid mm_s^{[1;0][0;1]} = 1) = \frac{\mathbb{P}(I_s^{(1)} = 0, I_{s+1}^{(0)} = 0, I_{s+2}^{(0)} = 1)}{\mathbb{P}(mm_s^{[1;0][0;1]} = 1)} =$$

$$\frac{(1 - \pi_1^{(1)})\,(1 - \pi_1^{(0)})\,\pi_1^{(0)}}{(1 - \pi_1^{(1)})\,\pi_1^{(0)}\,[\pi_1^{(1)} + (1 - \pi_1^{(0)})]} \equiv \frac{(1 - \pi_1^{(0)})}{\pi_1^{(1)} + 1 - \pi_1^{(0)}}.$$

Not only is the sum of the two conditional probabilities equal to unity (this might be attributed to the fact that the realizations 0 and 1 have to switch as well), but even more so it is true that

$$\begin{aligned}\mathbb{P}(M_s^{[0;1]}=1, M_{s+1}^{[1;0]}=1 \mid mm_s^{[0;1][1;0]}=1) &= \mathbb{P}(X_s=1 \mid X_{s-1}=1, X_{s+1}=0)\\ &\equiv \mathbb{P}(X_s=1 \mid X_{s-1}=0, X_{s+1}=1),\\ \mathbb{P}(M_s^{[1;0]}=0, M_{s+1}^{[0;1]}=0 \mid mm_s^{[1;0][0;1]}=1) &= \mathbb{P}(X_s=0 \mid X_{s-1}=1, X_{s+1}=0)\\ &\equiv \mathbb{P}(X_s=0 \mid X_{s-1}=0, X_{s+1}=1),\end{aligned}$$

((17) might be referred to) and the relation between the symmetrical conditional (from past and future) probabilities of X, translates to the joint probabilities of M-adjusted (Y-like variables). This basic result can be considered as one of a plethora of unobvious restrictions that do take place regarding the Y series dependence: those might concern joint probabilities of not necessarilly just two variables (especially for $p \geq 2$). Thanks to the model (4), with Y defined from (5), following M and m defined from the I series, there should be no danger that the restrictions might be overlooked by the spatial parameterization. The building block of the I series (hiding behind the m, M and Y) should make sure that any probability is computable and any relationship in the probabilities may reveal itself.

3.3 Time Reversal

It is easily demonstrated that once the pth order Markovian dependence resulting from the 'causal' representation in the transect takes place, the same holds for the unilateral representation from the other side: hence, for any $n \in \mathbb{N}_0$, it holds that

$$\begin{aligned}&\mathbb{P}(X_s=x_0 \mid X_{s+1}=x_1,\ldots,X_{s+p}=x_p,\ldots,X_{s+p+n}=x_{p+n}) =\\ &\frac{\mathbb{P}(X_s=x_0, X_{s+1}=x_1,\ldots,X_{s+p}=x_p,\ldots,X_{s+p+n}=x_{p+n})}{\mathbb{P}(X_{s+1}=x_1,\ldots,X_{s+p}=x_p,\ldots,X_{s+p+n}=x_{p+n})} =\\ &\frac{\mathbb{P}(X_s=x_0, X_{s+1}=x_1,\ldots,X_{s+p}=x_p)}{\mathbb{P}(X_{s+1}=x_1,\ldots,X_{s+p}=x_p)}\cdot\\ &\frac{\mathbb{P}(X_{s+p+n}=x_{p+n},\ldots,X_{s+p+1}=x_{p+1} \mid X_{s+p}=x_p,\ldots,X_{s+1}=x_1,X_s=x_0)}{\mathbb{P}(X_{s+p+n}=x_{p+n},\ldots,X_{s+p+1}=x_{p+1} \mid X_{s+p}=x_p,\ldots,X_{s+1}=x_1)},\end{aligned}$$

where straight from the p-variate memoryless property (3), the last ratio is equal to unity, so that one can continue by writing

$$\frac{\mathbb{P}(X_s = x_0, X_{s+1} = x_1, \ldots, X_{s+p} = x_p)}{\mathbb{P}(X_{s+1} = x_1, \ldots, X_{s+p} = x_p)} = \mathbb{P}(X_s = x_0 \mid X_{s+1} = x_1, \ldots, X_{s+p} = x_p),$$

i.e. a causal $\{X_s,\ s \in \mathbb{Z}\}$ satisfying (3) also satisfies

$$\begin{aligned}&\mathbb{P}(X_s = x_0 \mid X_{s+1} = x_1, \ldots, X_{s+p} = x_p, \ldots, X_{s+p+n} = x_{p+n}) = \\ &\mathbb{P}(X_s = x_0 \mid X_{s+1} = x_1, \ldots, X_{s+p} = x_p),\ \text{for any } n \in \mathbb{N}_0. \end{aligned} \tag{20}$$

Additionally, a more general statement concerning a series of variables that occur holds as well, i.e.

$$\begin{aligned}&\mathbb{P}(X_{s-n} = x_{-n}, \ldots, X_{s-1} = x_{-1},\ X_s = x_0 \mid X_{s+1} = x_1, \ldots, X_{s+p} = x_p) = \\ &\prod_{m=0}^{n} \mathbb{P}(X_{s-m} = x_{-m} \mid X_{s-m+1} = x_{-m+1}, \ldots, X_{s-m+p} = x_{-m+p}\ ),\ \text{for any } n \in \mathbb{N}_0. \end{aligned} \tag{21}$$

Thanks to (20) and (21), we may *continue under the following assumption*: there can also be $(k+1)^p$ sequences, say $\{J_s^{(j_1,\ldots,j_p)},\ s \in \mathbb{Z}\}$, $j_1, \ldots, j_p = 0, v_1, \ldots, v_k$ of independent (on different points of the transect and from either sequence) and identically distributed variables, with marginal distributions

$$\rho_w^{(j_1,\ldots,j_p)} := \mathbb{P}(J_s^{(j_1,\ldots,j_p)} = w) \equiv \mathbb{P}(X_s = w \mid X_{s+1} = j_1, \ldots, X_{s+p} = j_p)$$

for $w = 0, v_1, \ldots, v_k$, *such that it can be written for any* $s \in \mathbb{Z}$, that

$$X_s \equiv J_s^{(X_{s+1},\ldots,X_{s+p})}. \tag{22}$$

Then it *must* hold that

$$\rho_w^{(j_1,\ldots,j_p)} \equiv \pi_{j_p}^{(j_{p-1},\ldots,j_1,w)} \cdot \frac{\boldsymbol{\psi}_{(j_{p-1},\ldots,j_1,w)}}{\boldsymbol{\psi}_{(j_p,\ldots,j_1)}}, \tag{23}$$

where $\boldsymbol{\psi}_{(i_1,\ldots,i_p)} := \mathbb{P}(X_{s-1} = i_1, \ldots, X_{s-p} = i_p)$ are the 'stationary' probabilities, which have been obtained as a unique solution to the linear system (i.e. satisfying)

$$\boldsymbol{\psi}_{(i_1,\ldots,i_p)} = \sum_w \pi_{i_1}^{(i_2,\ldots,i_p,w)} \cdot \boldsymbol{\psi}_{(i_2,\ldots,i_p,w)}.$$

The linear system

$$\boldsymbol{\psi}^*_{(i_1,\ldots,i_p)} = \sum_w \rho_{i_p}^{(i_{p-1},\ldots,i_1,w)} \cdot \boldsymbol{\psi}^*_{(w,i_1,\ldots,i_{p-1})}$$

must yield the same stationary distribution $\boldsymbol{\psi}^* = \boldsymbol{\psi}$ to be the unique solution: by substitution in the system above of $\rho_{i_p}^{(i_{p-1},\ldots,i_1,w)}$ according to (23), it is easy to verify that $\boldsymbol{\psi}$ is a solution indeed. Additionally, $\{X_s\}$ must be a 'causal' (from the 'future') process based on $\{J_s^{(\ldots)}\}$ (see Dimitriou-Fakalou (2019)).

Following an identical argument as from the I to the Y, it can be written

$$n_s^{[\mathbf{i}_F^\tau;\mathbf{i}_P^\tau]} := \sum_{w=0,v_1,\ldots,v_k} f_w(J_s^{(\mathbf{i}_F)}) \cdot f_{i_{P,1}}(J_{s-1}^{(w,i_{F,1},\ldots,i_{F,p-1})}) \ldots f_{i_{P,p}}(J_{s-p}^{(i_{P,p-1},\ldots,i_{P,1},w)})$$

and

$$N_s^{[\mathbf{i}_F^\tau;\mathbf{i}_P^\tau]} := J_s^{(\mathbf{i}_F)} \cdot f_{i_{P,1}}(J_{s-1}^{(J_s^{(\mathbf{i}_F)},i_{F,1},\ldots,i_{F,p-1})}) \ldots f_{i_{P,p}}(J_{s-p}^{(i_{P,p-1},\ldots,i_{P,1},J_s^{(\mathbf{i}_F)})}),$$

so that it is defined

$$n_s^{[\mathbf{i}_F^\tau;\mathbf{i}_P^\tau]} \cdot Y_s^{*[\mathbf{i}_F^\tau;\mathbf{i}_P^\tau]} := N_s^{[\mathbf{i}_F^\tau;\mathbf{i}_P^\tau]}, \tag{24}$$

i.e. $Y_s^{*[\mathbf{i}_F^\tau;\mathbf{i}_P^\tau]}$ is defined on the sample space $\{n_s^{[\mathbf{i}_F^\tau;\mathbf{i}_P^\tau]} = 1\}$. Then it *must* hold that

$$X_s = Y_s^{*[(X_{s+p},\ldots,X_{s+1});(X_{s-1},\ldots,X_{s-p})]} \equiv Y_s^{[(X_{s-p},\ldots,X_{s-1});(X_{s+1},\ldots,X_{s+p})]}. \tag{25}$$

Equation (25) sets $J_s^{(\mathbf{i}_F)} \equiv I_s^{(\mathbf{i}_P^\tau)}$ but only *provided that* $X_{s-n} = i_{P,n}$, $X_{s+n} = i_{F,n}$, $n = 1,\ldots,p$.

In fact, regardless of the values of X_{s-n}, $n = \pm 1,\ldots,\pm p$, it could be considered *for every* $\mathbf{i}_P$ and $\mathbf{i}_F$, whether it holds that $m_s^{[\mathbf{i}_P;\mathbf{i}_F]} = n_s^{[\mathbf{i}_F^\tau;\mathbf{i}_P^\tau]} \equiv 1$; then, provided that

$$\begin{aligned}
&\mathbb{P}(Y_s^{[\mathbf{i}_P;\mathbf{i}_F]} = Y_s^{*[\mathbf{i}_F^\tau;\mathbf{i}_P^\tau]} = w \mid m_s^{[\mathbf{i}_P;\mathbf{i}_F]} = n_s^{[\mathbf{i}_F^\tau;\mathbf{i}_P^\tau]} \equiv 1) = \\
&\mathbb{P}(I_s^{(\mathbf{i}_P^\tau)} = J_s^{(\mathbf{i}_F)} = w \mid m_s^{[\mathbf{i}_P;\mathbf{i}_F]} = n_s^{[\mathbf{i}_F^\tau;\mathbf{i}_P^\tau]} \equiv 1) = \\
&\mathbb{P}(X_s = w \mid (X_{s-1},\ldots,X_{s-p}) = \mathbf{i}_P^\tau, (X_{s+1},\ldots,X_{s+p}) = \mathbf{i}_F)
\end{aligned} \tag{26}$$

holds for all $w = 0, v_1, \ldots, v_k$, it would be fair to conclude that $Y_s^{[\mathbf{i}_P;\mathbf{i}_F]} = Y_s^{*[\mathbf{i}_F^\tau;\mathbf{i}_P^\tau]}$ (defined on the intersection of sample spaces) has all the elements, to take the role of the (conditional) latent equalizer predictor of X_s given $X_{s-n} = i_{P,n}$, $X_{s+n} = i_{F,n}$, $n = 1, \ldots, p$ and X_{s-n}, $|n| \geq p+1$: as it has been explained already, $Y_s^{[\ldots;\ldots]}$ (properly defined) is independent of X_{s-n}, $n \in \mathbb{N}$ and, for the same reasons, $Y_s^{*[\ldots;\ldots]}$ (properly defined) would be independent of X_{s+n}, $n \in \mathbb{N}$. It is mandatory for every $s \in \mathbb{Z}$, that for *at least one* out of the $(k+1)^{2p}$ possible $i_{P,1}, \ldots, i_{P,p}$, $i_{F,1}, \ldots, i_{F,p} = 0, v_1, \ldots, v_k$, it holds that $m_s = 1$ and $n_s = 1$ and $Y_s = Y_s^*$, together with

$$\mathbb{P}(Y_s^{[(X_{s-p},\ldots,X_{s-1});(X_{s+1},\ldots,X_{s+p})]} = Y_s^{*[(X_{s+p},\ldots,X_{s+1});(X_{s-1},\ldots,X_{s-p})]} = w \mid X_{s-i},\ i \neq 0) =$$
$$\mathbb{P}(Y_s^{[(X_{s-p},\ldots,X_{s-1});(X_{s+1},\ldots,X_{s+p})]} = w \mid X_{s-i},\ i \neq 0) \equiv$$
$$\mathbb{P}(Y_s^{*[(X_{s+p},\ldots,X_{s+1});(X_{s-1},\ldots,X_{s-p})]} = w \mid X_{s-i},\ i \neq 0);$$

it remains a question to be answered though, whether (26) can or should be attempted to hold. Formally, one would be able to consider for every $s \in \mathbb{Z}$, that the latent equalizer predictor of X_s based on X_{s-n}, $|n| \in \mathbb{N}$, is $Y_s^{[(X_{s-p},\ldots,X_{s-1});(X_{s+1},\ldots,X_{s+p})]} = Y_s^{*[(X_{s+p},\ldots,X_{s+1});(X_{s-1},\ldots,X_{s-p})]}$ and should proceed conditionally via Y *or* Y^*.

IV. AN INTRODUCTION TO THE TALMA

Write $\mathbf{j}_P = (j_{P,q}, \ldots, j_{P,1})$ (and $\mathbf{j}_P^\tau = (j_{P,1}, \ldots, j_{P,q})$), $\mathbf{j}_F = (j_{F,1}, \ldots, j_{F,q})$ and consider $\{I_s^{(\mathbf{i}_P^\tau|\mathbf{j}_P^\tau)},\ s \in \mathbb{Z}\}$ to be a series of independent and identically distributed $(k+1)^{p+q}$-vectors $(i_{P,1}, \ldots, i_{P,p},\ j_{P,1}, \ldots, j_{P,q} = 0, v_1, \ldots, v_k)$, which will be used as a building block for the series of interest. Write

$$\pi_x^{(\mathbf{i}_P^\tau|\mathbf{j}_P^\tau)} := \mathbb{P}(I_s^{(\mathbf{i}_P^\tau|\mathbf{j}_P^\tau)} = x),\ x = 0, v_1, \ldots, v_k, \sum_{x=0,v_1,\ldots,v_k} \pi_x^{(\mathbf{i}_P^\tau|\mathbf{j}_P^\tau)} = 1,$$

as well as $I_s^{(\mathbf{0}_p|\mathbf{0}_q)} \equiv I_s$ and $\pi_x^{(\mathbf{0}_p|\mathbf{0}_q)} \equiv \pi_x$.

Definition 1: $\{X_s,\ s \in \mathbb{Z}\}$ will be called a Table Auto-Linear Moving-Average process of order (k, p, q) and it will be written $\{X_s\} \sim \text{TALMA}(k, p, q)$, if it holds that

$$X_s := Y_s^{([(X_{s-p},...,X_{s-1});(X_{s+1},...,X_{s+p})]|[(Y_{s-q},...,Y_{s-1});(Y_{s+1},...,Y_{s+q})])},\ s\in\mathbb{Z}, \tag{27}$$

paired with

$$Y_s := y_s^{([(X_{s-p},...,X_{s-1});(X_{s+1},...,X_{s+p})]|[(Y_{s-q},...,Y_{s-1});(Y_{s+1},...,Y_{s+q})])},\ s\in\mathbb{Z},$$

where, for every $\mathbf{i}_P$, $\mathbf{i}_F$, $\mathbf{j}_P$ and $\mathbf{j}_F$, it is set

$$\begin{aligned} m_s^{([\mathbf{i}_P;\mathbf{i}_F]|[\mathbf{j}_P;\mathbf{j}_F])} := {} & f_{j_{F,1}}(I_{s+1})\cdot\ldots\cdot f_{j_{F,q}}(I_{s+q})\cdot \\ & f_{i_{F,1}}(I_{s+1}^{((I_s^{(\mathbf{i}_P^\tau|\mathbf{j}_P^\tau)}),i_{P,1},...,i_{P,p-1})|(I_s,j_{P,1},...,j_{P,q-1}))}\cdot\ldots\cdot \\ & f_{i_{F,p}}(I_{s+p}^{((i_{F,p-1},...,i_{F,1},I_s^{(\mathbf{i}_P^\tau|\mathbf{j}_P^\tau)})|(I_{s+p-1}(?=j_F),...,j_{F,1},I_s,j_{P,1},...,j_P))}), \end{aligned} \tag{28}$$

followed by defining on the sample space $\{m_s^{([\mathbf{i}_P;\mathbf{i}_F]|[\mathbf{j}_P;\mathbf{j}_F])}=1\}$ only, the variables

$$y_s^{([\mathbf{i}_P;\mathbf{i}_F]|[\mathbf{j}_P;\mathbf{j}_F])} := I_s, \quad \text{and} \quad Y_s^{([\mathbf{i}_P;\mathbf{i}_F]|[\mathbf{j}_P;\mathbf{j}_F])} := I_s^{(\mathbf{i}_P^\tau|\mathbf{j}_P^\tau)}.$$

1. *Definition 1* presents the spatial analogue to the Table ARMA (k,p,q) equation (see Dimitriou-Fakalou (2019)), which models the infinite Markovian dependence (see Dimitriou-Fakalou (2022)), in the same way that the standard time series ARMA is an AR(∞). Indeed it can be verified for the process of interest $\{X_s,\ s\in\mathbb{Z}\}$ that $X_s = I_s^{((X_{s-1},...,X_{s-p})|(I_{s-1},...,I_{s-q}))}$, $s\in\mathbb{Z}$: it is a prerequisite that this is causal, implying strictly stationary, (as in Dimitriou-Fakalou (2019)) and invertible (as in Dimitriou-Fakalou (2022)). Additionally, the main latent process $\{I_s\}$ converts into $\{Y_s\}$, which shares the same realizations but, each time, the y-value is picked from a different probability rule, depending on the fixed values of X and I from both sides. Note that, if (28) is re-written as

$$\begin{aligned} & f_{j_{F,1}}(Y_{s+1})\cdot\ldots\cdot f_{j_{F,q}}(Y_{s+q})\cdot \\ & f_{i_{F,1}}(I_{s+1}^{((I_s^{(\mathbf{i}_P^\tau|\mathbf{j}_P^\tau)}),i_{P,1},...,i_{P,p-1})|(I_s,j_{P,1},...,j_{P,q-1}))}\cdot\ldots\cdot \\ & f_{i_{F,p}}(I_{s+p}^{((i_{F,p-1},...,i_{F,1},I_s^{(\mathbf{i}_P^\tau|\mathbf{j}_P^\tau)})|(I_{s+p-1}(?=j_F),...,j_{F,1},I_s,j_{P,1},...,j_P))}), \end{aligned}$$

then the definition of $y_s^{([\mathbf{i}_P;\mathbf{i}_F]\|[\mathbf{j}_P;\mathbf{j}_F])}$ resembles that of a TARMA (k,q,p) caused *from the future*, though the comparisons should be done with care (this is due to merging the different y processes into one Y for the 'AR' part and considering a p-dependence for the 'MA' part). Still, it should be clear that X_s and $y_{s+l}^{([\mathbf{i}_P;\mathbf{i}_F]\|[\mathbf{j}_P;\mathbf{j}_F])}$, $Y_{s+l}^{([\mathbf{i}_P;\mathbf{i}_F]\|[\mathbf{j}_P;\mathbf{j}_F])}$, for *positive* (and valid) l, are independent (in the same way that X_s and I_{s+l}, $l>0$, are independent).

To exhibit the independence of X_s and $y_{s-l}^{([\mathbf{i}_P;\mathbf{i}_F]\|[\mathbf{j}_P;\mathbf{j}_F])}$, $Y_{s-l}^{([\mathbf{i}_P;\mathbf{i}_F]\|[\mathbf{j}_P;\mathbf{j}_F])}$, $l>0$, some form of time reversal would be required, i.e. writing X_s as a 'causal' (from the future) function of another sequence of, say J, iid variables, with the same variables from the past only determining the values of y, Y. Nevertheless, not only would time reversal be expected to be an arduous (if not impossible) task, but also it is *not* really needed, in order to solidify the vital property of the TALMA model (as in (29) and the statement following it, which conclude this point).

So without resorting to any other than the I building blocks, first see that

$$\{X_{s-1}=i_{P,1},\dots,X_{s-p}=i_{P,p},\ X_{s+1}=i_{F,1},\dots,X_{s+p}=i_{F,p},$$
$$I_{s-1}=j_{P,1},\dots,I_{s-q}=j_{P,q},\ I_{s+1}=j_{F,1},\dots,I_{s+q}=j_{F,q}\}\subseteq$$
$$\{m_s^{([\mathbf{i}_P;\mathbf{i}_F]\|[\mathbf{j}_P;\mathbf{j}_F])}=1\}.$$

Secondly, it is easy to spot

$$\begin{aligned}\mathbb{P}(X_s=x,Y_s=y\ \ |\ \ & X_{s-1}=i_{P,1},\dots,X_{s-p}=i_{P,p},\ X_{s+1}=i_{F,1},\dots,X_{s+p}=i_{F,p},\\ & I_{s-1}=j_{P,1},\dots,I_{s-q}=j_{P,q},\ I_{s+1}=j_{F,1},\dots,I_{s+q}=j_{F,q})=\\ \mathbb{P}(I_s^{(\mathbf{i}_P^\tau|\mathbf{j}_P^\tau)}=x,\ I_s=y\ \ |\ \ & X_{s-1}=i_{P,1},\dots,X_{s-p}=i_{P,p},\ I_{s-1}=j_{P,1},\dots,I_{s-q}=j_{P,q},\\ & m_s^{([\mathbf{i}_P;\mathbf{i}_F]\|[\mathbf{j}_P;\mathbf{j}_F])}=1)\equiv\\ \mathbb{P}(I_s^{(\mathbf{i}_P^\tau|\mathbf{j}_P^\tau)}=x,I_s=y\ \ |\ \ & m_s^{([\mathbf{i}_P;\mathbf{i}_F]\|[\mathbf{j}_P;\mathbf{j}_F])}=1),\end{aligned}$$

where the last equality is due to the fact that X_{s-l}, I_{s-n}, $l,n>0$ are jointly independent of $I_s^{(\dots)}$, $m_s^{(\dots)}$. Identical arguments write, for any $l_1,m_1\in\mathbb{N}$, that

$$\mathbb{P}(X_s = x, Y_s = y \;\;|\;\; X_{s-1} = i_{P,1}, \ldots, X_{s-p} = i_{P,p},\; X_{s+1} = i_{F,1}, \ldots, X_{s+p} = i_{F,p},$$
$$I_{s-1} = j_{P,1}, \ldots, I_{s-q} = j_{P,q},\; I_{s+1} = j_{F,1}, \ldots, I_{s+q} = j_{F,q},$$
$$X_{s-p-l},\; l = 1, \ldots, l_1,\; I_{s-q-m},\; m = 1, \ldots, m_1) =$$
$$\mathbb{P}(I_s^{(\mathbf{i}_P^\tau|\mathbf{j}_P^\tau)} = x, I_s = y \;\;|\;\; m_s^{([\mathbf{i}_P;\mathbf{i}_F]|[\mathbf{j}_P;\mathbf{j}_F])} = 1).$$

Thirdly, set for convenience $o := \max\{p, q\}$, $\mathbf{i}_F^* = (\mathbf{i}_F, i_{F,p+1}, \ldots, i_{F,o})$, $\mathbf{j}_F^* = (\mathbf{j}_F, j_{F,q+1}, \ldots, j_{F,o})$, and slightly shrink the sample space to $\{m_s^{*([\mathbf{i}_P;\mathbf{i}_F^*]|[\mathbf{j}_P;\mathbf{j}_F^*])} = 1\} \subseteq \{m_s^{([\mathbf{i}_P;\mathbf{i}_F]|[\mathbf{j}_P;\mathbf{j}_F])} = 1\}$, where

$$\begin{aligned} m_s^{*([\mathbf{i}_P;\mathbf{i}_F^*]|[\mathbf{j}_P;\mathbf{j}_F^*])} \;:=\; & f_{j_{F,1}}(I_{s+1}) \cdot \ldots \cdot f_{j_{F,o}}(I_{s+o}) \cdot \\ & f_{i_{F,1}}(I_{s+1}^{((I_s^{(\mathbf{i}_P^\tau|\mathbf{j}_P^\tau)}, i_{P,1}, \ldots, i_{P,p-1})|(I_s, j_{P,1}, \ldots, j_{P,q-1}))}) \cdot \ldots \cdot \\ & f_{i_{F,p}}(I_{s+p}^{((i_{F,p-1}, \ldots, i_{F,1}, I_s^{(\mathbf{i}_P^\tau|\mathbf{j}_P^\tau)})|(j_{F,p-1}, \ldots, j_{F,1}, I_s, j_{P,1}, \ldots, j_{P,p}))}) \cdot \ldots \cdot \\ & f_{i_{F,o}}(I_{s+o}^{((i_{F,o-1}, \ldots)|(j_{F,o-1}, \ldots, j_{F,1}, I_s))}) \end{aligned}$$

(the first line fixes the case $p - 1 > q$, so that $j_{F,p-1}$ exists, and the $\cdot \ldots \cdot$ last line takes care of when $q > p$, so that 'I_s' is the last entry in the MA part), so that it becomes clear why it holds that

$$\mathbb{P}(I_s^{(\mathbf{i}_P^\tau|\mathbf{j}_P^\tau)} = x, I_s = y \;\;|\;\; X_{s-1} = i_{P,1}, \ldots, X_{s-p} = i_{P,p},\; I_{s-1} = j_{P,1}, \ldots, I_{s-q} = j_{P,q},$$
$$m_s^{*([\mathbf{i}_P;\mathbf{i}_F^*]|[\mathbf{j}_P;\mathbf{j}_F^*])} = 1) \equiv$$
$$\mathbb{P}(I_s^{(\mathbf{i}_P^\tau|\mathbf{j}_P^\tau)} = x, I_s = y \;\;|\;\; X_{s-1} = i_{P,1}, \ldots, X_{s-p} = i_{P,p},\; I_{s-1} = j_{P,1}, \ldots, I_{s-q} = j_{P,q},$$
$$m_s^{*([\mathbf{i}_P;\mathbf{i}_F^*]|[\mathbf{j}_P;\mathbf{j}_F^*])} = 1,$$
$$X_{s+o+n},\; n = 1, \ldots, n_1,\; I_{s+o+n^*},\; n^* = 1, \ldots, n_2),$$

for any $n_1, n_2 \in \mathbb{N}$: a similar relation can be found in Section 3.1.

To sum it up, the TALMA(k, p, q) model for $\{X_s\}$, is such that the probability

$$\begin{aligned} \mathbb{P}(X_s = x, Y_s = y \;\;|\;\; & X_{s-1} = i_{P,1}, \ldots, X_{s-p} = i_{P,p},\; X_{s-p-l},\; l = 1, \ldots, l_1, \\ & Y_{s-1} = j_{P,1}, \ldots, Y_{s-q} = j_{P,q},\; Y_{s-q-m},\; m = 1, \ldots, m_1, \\ & X_{s+1} = i_{F,1}, \ldots, X_{s+o} = i_{F,o},\; X_{s+o+n},\; n = 1, \ldots, n_1, \\ & Y_{s+1} = j_{F,1}, \ldots, Y_{s+o} = j_{F,o},\; Y_{s+o+n^*},\; n^* = 1, \ldots, n_2), \end{aligned} \tag{29}$$

remains *unchanged* for any l_1, m_1, n_1, $n_2 \in \mathbb{N}_0$.

The adjustment from m_s to m_s^* (which is not the case for the linear series) might be attributed to the fact that the model is multiplicative on the AL and MA parts, i.e. those two are tangled together.

2. It is clarified next how to employ the special merit of the TALMA equation, which has been attached to the use of the partitioned Y latent series. When $q = 0$, the TAL(k, p) process is none other than what was described in Section 3. It is accustomed that the inclusion of the moving-average part with order $q \in \mathbb{N}$, offers a parsimonious way to model the *infinite Markovian dependence*: its *spatial version* is what the TALMA is all about.

   To demonstrate how to approximate it, first for any $n \in \mathbb{N}_0$, write the 'conditions'

$$\mathcal{P}_{s,(n)}(x_{-\mu},\ \mu = (n+1), \ldots, (n+p),\ y_{-\nu},\ \nu = (n+1), \ldots, (n+q)) :=$$
$$\{X_{s-\mu} = x_{-\mu},\ \mu = (n+1), \ldots, (n+p),\ Y_{s-\nu} = y_{-\nu},\ \nu = (n+1), \ldots, (n+q)\},$$

   and

$$\mathcal{F}_{s,(n)}(x_m,\ y_m,\ m = (n+1), \ldots, (n+o)) :=$$
$$\{X_{s+m} = x_m,\ Y_{s+m} = y_m,\ m = (n+1), \ldots, (n+o)\}.$$

   Then define the probabilities

$$\omega_{(x_0,y_0)}^{([(x_{-p},\ldots,x_{-1});(x_1,\ldots,x_o)]|[(y_{-q},\ldots,y_{-1});(y_1,\ldots,y_o)])} := \mathbb{P}(X_s = x_0, Y_s = y_0 \mid \mathcal{P}_{s,(0)},\ \mathcal{F}_{s,(0)}).$$

   More specifically, for any $n \in \mathbb{N}_0$, the quantity

$$\mathbb{P}(X_s = x_0 \mid X_{s+m} = x_m,\ m = \pm 1, \ldots, \pm n,\ X_{s+\mu} = x_\mu,\ \mu = -(n+p), \ldots$$
$$-(n+1), (n+1), \ldots, (n+o),\ Y_{s+\nu} = y_\nu,\ \nu = -(n+q), \ldots, -(n+1),$$
$$(n+1), \ldots, (n+o)) \tag{30}$$

will be of interest. To compute (30), first re-write it as

$$\{\sum_{y_m,\ m=0,\pm1,\ldots,\pm n} \mathbb{P}(X_s = x_0,\ Y_s = y_0,\ X_{s+m} = x_m,\ Y_{s+m} = y_m,\ m = \pm1,\ldots,\pm n \mid$$
$$X_{s+\mu} = x_\mu,\ \mu = -(n+p),\ldots,-(n+1),(n+1),\ldots,(n+o),$$
$$Y_{s+\nu} = y_\nu,\ \nu = -(n+q),\ldots,-(n+1),(n+1),\ldots,(n+o)\ )\}\ /$$
$$\{\sum_{x_0^*,y_m,\ m=0,\pm1,\ldots,\pm n} \mathbb{P}(X_s = x_0^*,\ Y_s = y_0,\ X_{s+m} = x_m,\ Y_{s+m} = y_m,\ m = \pm1,\ldots,\pm n \mid$$
$$X_{s+\mu} = x_\mu,\ \mu = -(n+p),\ldots,-(n+1),(n+1),\ldots,(n+o),$$
$$Y_{s+\nu} = y_\nu,\ \nu = -(n+q),\ldots,-(n+1),(n+1),\ldots,(n+o)\ )\};$$

then observe the important relation

$$\frac{\mathbb{P}(X_{s+m} = xx_m,\ Y_{s+m} = yy_m,\ m = 0,\pm1,\ldots,\pm n \mid \mathcal{P}_{s,(n)}, \mathcal{F}_{s,(n)})}{\mathbb{P}(X_{s+m} = xx_m^*,\ Y_{s+m} = yy_m^*,\ m = 0,\pm1,\ldots,\pm n \mid \mathcal{P}_{s,(n)}, \mathcal{F}_{s,(n)})} = \prod_{i=-n}^{n}$$
$$\{\mathbb{P}(X_{s+i} = xx_i, Y_{s+i} = yy_i \mid \mathcal{P}_{s,(n)},\ X_{s+j} = xx_j,\ Y_{s+j} = yy_j,\ j = -n,$$
$$\ldots,i-1,\ X_{s+j^*} = xx_{j^*}^*,\ Y_{s+j^*} = yy_{j^*}^*,\ j^* = i+1,\ldots,n,\ \mathcal{F}_{s,(n)})\}\ /$$
$$\{\mathbb{P}(X_{s+i} = xx_i^*, Y_{s+i} = yy_i^* \mid \mathcal{P}_{s,(n)},\ X_{s+j} = xx_j,\ Y_{s+j} = yy_j,\ j = -n,$$
$$\ldots,i-1,\ X_{s+j^*} = xx_{j^*}^*,\ Y_{s+j^*} = yy_{j^*}^*,\ j^* = i+1,\ldots,n,\ \mathcal{F}_{s,(n)})\},\quad (31)$$

which finds its roots in Besag (1974) together with a sketch of proof. Indeed, by taking its right-hand side, it can be re-written

$$\prod_{i=-n}^{n} \{\mathbb{P}(X_{s+j} = xx_j,\ Y_{s+j} = yy_j,\ j = -n,\ldots,i,$$
$$X_{s+j^*} = xx_{j^*}^*,\ Y_{s+j^*} = yy_{j^*}^*,\ j^* = i+1,\ldots,n \mid \mathcal{P}_{s,(n)},\ \mathcal{F}_{s,(n)})\}\ /$$
$$\{\mathbb{P}(X_{s+j} = xx_j,\ Y_{s+j} = yy_j,\ j = -n,\ldots,i-1,$$
$$X_{s+j^*} = xx_{j^*}^*,\ Y_{s+j^*} = yy_{j^*}^*,\ j^* = i,\ldots,n \mid \mathcal{P}_{s,(n)},\ \mathcal{F}_{s,(n)})\};$$

for $i = -n$, the factor becomes

$$\{\mathbb{P}(X_{s-n} = xx_{-n},\ Y_{s-n} = yy_{-n},\ X_{s+j^*} = xx_{j^*}^*,\ Y_{s+j^*} = yy_{j^*}^*,$$
$$j^* = -n+1,\ldots,n \mid \mathcal{P}_{s,(n)},\ \mathcal{F}_{s,(n)})\}\ /$$
$$\{\mathbb{P}(X_{s+j^*} = xx_{j^*}^*,\ Y_{s+j^*} = yy_{j^*}^*,\ j^* = -n,\ldots,n \mid \mathcal{P}_{s,(n)},\ \mathcal{F}_{s,(n)})\}$$

with its denominator being exactly what is wanted and the numerator will cancel with the denominator of the next factor (for $i = -n+1$), which is altogether

$$\{\mathbb{P}(X_{s-n} = xx_{-n},\ Y_{s-n} = yy_{-n},\ X_{s-n+1} = xx_{-n+1},\ Y_{s-n+1} = yy_{-n+1},$$
$$X_{s+j^*} = xx^*_{j^*},\ Y_{s+j^*} = yy^*_{j^*},\ j^* = -n+2,\dots,n \mid \mathcal{P}_{s,(n)},\ \mathcal{F}_{s,(n)})\}\ /$$
$$\{\mathbb{P}(X_{s-n} = xx_{-n},\ Y_{s-n} = yy_{-n},\ X_{s+j^*} = xx^*_{j^*},\ Y_{s+j^*} = yy^*_{j^*},$$
$$j^* = -n+1,\dots,n \mid \mathcal{P}_{s,(n)},\ \mathcal{F}_{s,(n)})\}$$

and so on. Similarly, the one before the end factor ($i = n-1$)

$$\{\mathbb{P}(X_{s+j} = xx_j,\ Y_{s+j} = yy_j,\ j = -n,\dots,n-1,$$
$$X_{s+n} = xx^*_n,\ Y_{s+n} = yy^*_n \mid \mathcal{P}_{s,(n)},\ \mathcal{F}_{s,(n)})\}\ /$$
$$\{\mathbb{P}(X_{s+j} = xx_j,\ Y_{s+j} = yy_j,\ j = -n,\dots,n-2,\ X_{s+n-1} = xx^*_{n-1},$$
$$Y_{s+n-1} = yy^*_{n-1},\ X_{s+n} = xx^*_n,\ Y_{s+n} = yy^*_n \mid \mathcal{P}_{s,(n)},\ \mathcal{F}_{s,(n)})\},$$

will have its denominator cancelled with the numerator of the previous factor ($i = n-2$) and its numerator cancelled with the denominator of the last one for $i = n$, which is

$$\{\mathbb{P}(X_{s+j} = xx_j,\ Y_{s+j} = yy_j,\ j = -n,\dots,n \mid \mathcal{P}_{s,(n)},\ \mathcal{F}_{s,(n)})\}\ /$$
$$\{\mathbb{P}(X_{s+j} = xx_j,\ Y_{s+j} = yy_j,\ j = -n,\dots,n-1,$$
$$X_{s+n} = xx^*_n,\ Y_{s+n} = yy^*_n \mid \mathcal{P}_{s,(n)},\ \mathcal{F}_{s,(n)})\}:$$

as for the numerator of the last part above, together with the denominator of the first factor, those are combined to verify exactly the statement under question.

Once (31) is valid, given the same condition $\mathcal{P}_{s,(n)}$, $\mathcal{F}_{s,(n)}$, the distribution

$$\mathbb{P}(X_{s+m} = xx_m,\ Y_{s+m} = yy_m,\ m = 0, \pm 1,\dots,\pm n \mid \mathcal{P}_{s,(n)}, \mathcal{F}_{s,(n)}),$$

i.e. for any xx_m, yy_m, $m = 0, \pm 1, \ldots, \pm n$, can be determined: this should be obvious how. As for the right-hand side of (31), thanks to the conclusion regarding the probability (29) remaining unchanged, it suffices to know the probabilities ω to have at hand all that is required for it, then for (30). Straight from (30), the infinite spatial Markovian dependence is implied as $n \to \infty$, and the result is always contained within the prespecified TALMA parameters ω.

3. The parameters relating to *Definition 1* are none other than the probabilities ω, and those should be expressed in terms of the original π, i.e.

$$\begin{aligned}\omega_{(x,y)}^{([\mathbf{i}_P;\mathbf{i}_F^*]|[\mathbf{j}_P;\mathbf{j}_F^*])} &\equiv \mathbb{P}(I_s^{(\mathbf{i}_P^\tau|\mathbf{j}_P^\tau)} = x, I_s = y \mid m_s^{*([\mathbf{i}_P;\mathbf{i}_F^*]|[\mathbf{j}_P;\mathbf{j}_F^*])} = 1) \\ &= \mathbb{P}(I_s^{(\mathbf{i}_P^\tau|\mathbf{j}_P^\tau)} = x, I_s = y \mid I_{s+1} = j_{F,1}, \ldots, I_{s+o} = j_{F,o}, \\ I_{s+1}^{((I_s^{(\mathbf{i}_P^\tau|\mathbf{j}_P^\tau)}, i_{P,1}, \ldots, i_{P,p-1})|(I_s, j_{P,1}, \ldots, j_{P,q-1}))} &= i_{F,1}, \ldots, I_{s+o}^{((i_{F,o-1},\ldots)|(j_{F,o-1},\ldots,j_{F,1},I_s))} = i_{F,o}) :\end{aligned}$$

particular emphasis must be paid on making sure that the condition considered each time has a strictly *positive* probability of occuring (this can be referred to as *positivity* condition). For example, when it is set $(\mathbf{i}_P, \mathbf{j}_P) = \mathbf{0}_{p+q}$ (i.e. $I_s^{(\mathbf{i}_P|\mathbf{j}_P)} \equiv I_s$) this has to be accounted for in the condition first. Other cases $(\mathbf{i}_P, \mathbf{j}_P) \neq \mathbf{0}_{p+q}$ rely on the *interdependence* of $I_s^{(\mathbf{i}_P^\tau|\mathbf{j}_P^\tau)}$ and I_s, referring to variables at the same point $s \in \mathbb{Z}$ (rather than the independence of I when considered at different points of the transect): nothing has been said about that here, but the fixes for the causality (or invertibility) of the process usually demand that the distributions of the different $I_s^{(\ldots)}$ must be really near (see Dimitriou-Fakalou (2019) and Dimitriou-Fakalou (2022)).

V. FINAL POINTS: WHY TALMA?

Given the correspondence from the causal TARMA(k, p, q) to the TALMA(k, p, q) equation, as well as the fact that it is the usual tack, from a sample of observed values to derive optimal inference results via step-by-step projections on the *past* available, one might wonder, why bother with the TALMA model?

The reasons can be counted on three fingers, the first one being that it might be *desirable* to *understand* how the (stationary) spatial dependencies extend. Secondly, it might be *preferable* to *naturally clothe* the spatial relations using the TALMA not TARMA equation, when the variables of interest are indexed on more than one coordinates, mainly, in order to avoid the conventional (half-plane) unilateral order of Whittle (1954): instead of writing the conditional probability of one value based on its 'previous' ones, all (other than itself) values can contribute to the information. Finally, there is the *practical reason of prediction in spatial settings*: for example, the TAL($q = 0$) equation provides directly with the whole distribution of the variable of interest based on values from a finite number of 'neighbours' from all around, when additional information can be discarded.

In the cases of multi-indexed discretized stationary processes, it is still advised that simultaneous spatial models would better not be attempted directly: the previous care of causal arrangements in the lattice that will, nevertheless, remain hidden, is essential for the validity of the spatial considerations.

REFERENCES

1. Besag, J. (1974). Spatial Interaction and the Statistical Analysis of Lattice Systems (with discussion), Journal of the Royal Statistical Society, Series B, 36, 192-236.
2. Brockwell, P.J. and Davis, R.A. (1991). Time Series: Theory and Methods, second edition, Springer-Verlag, New-York.
3. Cressie, N.A.C. (1993). Statistics for Spatial Data, revised edition, Wiley, New York.
4. Cui, Y. and Lund, R.B. (2009). A new look at time series of counts, Biometrika, 96, 781-792.
5. Dimitriou-Fakalou, C. (2010). Statistical Inference for Spatial Auto-Linear Processes, Journal of Statistical Theory and Practice, 4, 345-365.
6. Dimitriou-Fakalou, C. (2019). The Table Auto-Regressive Moving-Average model for (categorical) stationary series: statistical properties (causality; from the all random to the conditional random), Journal of Nonparametric Statistics, 31, 31-63.
7. Dimitriou-Fakalou, C. (2022). The Table Auto-Regressive Moving-Average Model for (Categorical) Stationary Series: Mathematical Perspectives (Invertibility; Maximum Likelihood Estimation), Open Journal of Statistics, 12, 385-407.
8. Du, J.G. and Li, Y. (1991). The integer-valued auto-regressive (INAR(p)) model, Journal of Time Series Analysis, 12, 129-142.
9. Francq, C. and Zakoïan, J.-M. (2001). Stationarity of multivariate Markov-switching ARMA models, Journal of Econometrics, 102, 339-364.

10. Jacobs, P.A. and Lewis, P.A.W. (1978). Discrete time series generated by mixtures I: correlational and runs properties, Journal of the Royal Statistical Society, Series B, 40, 94-105.
11. Keenan, D.M. (1982). A time series analysis of binary data, Journal of the American Statistical Association, 77, 816-821.
12. Lomnicki, Z.A. and Zaremba, S.K. (1955). Some applications of zero-one processes, Journal of the Royal Statistical Society, Series B, 17, 243-255.
13. McKenzie, E. (1985). Some simple models for discrete variate time series, Water Resources Bulletin, 21, 645-650.
14. Tong, H. (1990). Non-linear Time Series: A Dynamical Systems Approach, Oxford University Press, Oxford.
15. Whittle, P. (1954). On Stationary Processes in the Plane, Biometrika, 41, 434-449.

This page is intentionally left blank

Finite Quantum-Field Theory and the Bosonic String Formalism: A Critical Point of View

P. Grange & J.F. Mathiot

Université de Montpellier

ABSTRACT

Basics of scalar and vector Finite Quantum Field Theories are recalled, stressing the importance of the quantization of classical physical fields as Operator-Valued- Distributions with specific fast decreasing test functions of the coordinates. The procedure respects full Lorentz and symmetry invariances and, due to the presence of test functions, leads to finite Feynman diagrams directly at the physical dimension D = 2.4. In dimension 2 it is only with such test function that the canonical quantization of the massless scalar field is found to be fully consistent with the most successfull Conformal Field Theoretic approach, pioneered by Belavin, Polyakov and Zamolodchikov in the early 1980's. The question is then raised how Poliakov's wordline path integral representation of the relativistic string could possibly lead tofinite Feynmann diagrams. The natural way of inquiries is through the extension of the string formalism with classical convoluted coordinates leading then to Operator-Valued-Distributions and thereby to Finite Quantum Field Theories. It is shown that in the process some age-old certitudes about quantized strings are somewhat jostled.

Keywords: NA

Classification: LCC Code: QC1-QC999

Language: English

Great Britain Journals Press

LJP Copyright ID: 925682
Print ISSN: 2631-8490
Online ISSN: 2631-8504

London Journal of Research in Science: Natural and Formal

Volume 22 | Issue 8 | Compilation 1.0

Finite Quantum-Field Theory and the Bosonic String Formalism: A Critical Point of View

P. Grangé[α] & J.F. Mathiot[σ]

ABSTRACT

Basics of scalar and vector Finite Quantum Field Theories are recalled, stressing the importance of the quantization of classical physical fields as Operator-Valued- Distributions with specific fast decreasing test functions of the coordinates. The procedure respects full Lorentz and symmetry invariances and, due to the presence of test functions, leads to finite Feynman diagrams directly at the physical dimension D = 2..4. In dimension 2 it is only with such test function that the canonical quantization of the massless scalar field is found to be fully consistent with the most successfull Conformal Field Theoretic approach, pioneered by Belavin, Polyakov and Zamolodchikov in the early 1980's. The question is then raised how Poliakov's wordline path integral representation of the relativistic string could possibly lead tofinite Feynmann diagrams. The natural way of inquiries is through the extension of the string formalism with classical convoluted coordinates leading then to Operator- Valued-Distributions and thereby to Finite Quantum Field Theories. It is shown that in the process some age-old certitudes about quantized strings are somewhat jostled.

Author α: Laboratoire Univers et Particules, Université de Montpellier, CNRS/IN2P3, Place E. Bataillon F-34095 Montpellier Cedex 05, France.
σ: Université de Clermont Auvergne, Laboratoire de Physique Corpusculaire, CNRS/IN2P3, BP10448, F-63000 Clermont-Ferrand, France.

I. INTRODUCTION

Finite Quantum Field Theories (FQFT) originate from the early causal and finite approach of Bogoliubov-Epstein-Glaser ($BEG-CSFT$) [1–7]. The inital steps are based on the early recognition that, in general, fields are not regular functions in the usual sense but distributions [8, 9]. However the setting up of a Lagrangian formalism in the QFT context encounters products of fields as distributions at the same space-time point, which are ill-defined and the later sources of crippling divergences. Past QFT history essentially deals with the search for counter-terms cancelling these anoying divergences. On the opposite the $BEG-CSFT$ approach under the forms of Refs. [6, 7] aims from the start at a Lagrangian formulation in keeping with the basic underlying classical differentiable structure of the space-time manifold. The taming of these divergencies involves regularization procedures which ought to preserve, to start with, the symmetry principles of the Lagrangian. Using a naïve cut-off for instance is known to violate Lorentz and gauge invariances, whereas Dimensional Regularization (DR) [10] and that of Ref. [7] -dubbed $TLRS$ here after- do preserve these fundamental symmetries. The two procedures have in common the distinctive aspect of their implementation

London Journal of Research in Science: Natural and Formal

prior to the construction of the Lagragian density. The use of DR does not however address directly to the origin of these divergencies but just avoids them in going to an hypothetical space in $D = 4-\epsilon$ dimensions. $TLRS$ was developped in Ref. [11,12]. Since the early applications of this scheme [13,14] the calculation of radiative corrections to the Higgs mass [15] and the treatment of the axial anomaly [16,17] are relevant illustrations of the practical use of the $TLRS$ procedure in the $D = 4$ context. It was shown recently how $TLRS$ solves the long-standing consistency problem [18] encountered between EqualTime (EQT) and Light-Front-Time (LFT) quantizations of bosonic two-dimensional massless fields. Our purpose here is to confront the findings of [18] with the standard bosonic string theory approach of [19, 20] and elaborate on the values of the critical dimension for the cancelation of the conformal anomaly.

II THE MATHEMATICAL SETTING

2.1. Classical wave equations

To the original classical field-distribution $\phi(x^0, x^1)$ is associatted a translation-convolution product $\Phi(\rho)$ built on a rapidly decreasing test functions $\rho(x^0, x^1)$, symmetric under reflexion in the variables x^0 and x^1. In Fourier-space variables this linear functional can be written as an integral with the proper bilinear form $\ll p, x \gg = p^a g_{a,\nu} x^\nu$ $(g_{a,\nu} = \mathrm{diag}\{1, -1\})$

$$(\Phi * \rho)(x^0, x^1) = \int \frac{dp_0 dp_1}{(2\pi)^2} e^{-\imath \ll p,x \gg} \tilde{\phi}(p_0, p_1) f(p_0^2, p_1^2),$$

where $\tilde{\phi}(p_0, p_1)$ (resp. $f(p_0^2, p_1^2)$) is the Fourier-space transform of $\phi(x^0, x^1)$ (resp. of $\rho(x^0, x^1)$). Hereafter $\mathbf{\Phi}(x^0, x^1)$ will stand for $(\Phi * \rho)(x^0, x^1)$.

The wave-equation for the classical convoluted distribution in space-time variables is obtained from the hyperbolic partial differential equation (HPDE)

$$\Box \mathbf{\Phi}(x^0, x^1) = \left[\partial_{x^0}^2 - \partial_{x^1}^2\right] \mathbf{\Phi}(x^0, x^1) = 0. \tag{2.1}$$

A solution of the Cauchy problem in the sense of convolution of tempered distributions is nothing else than D'Alembert's $(1717 - 1783)$ solution. It can be written as

$$\mathbf{\Phi}(x^0, x^1) = \frac{1}{2\pi} \int d^2p \delta(p_0^2 - p_1^2) \chi(p_0, p_1) \mathrm{e}^{-\imath \ll p,x \gg} f(p_0^2, p_1^2), \tag{2.2}$$

with $\chi(\pm|p_1|, p_1) = \chi_\pm(p_1)$. Canonical quantization of the zero mass scalar quantum operator valued-distribution (OPVD) field $\hat{\Phi}(x^0, x^1)$ proceeds from Eq.(2.2) via the correspondance, in terms of creation and annihilation operators, $\{\chi_-(p) \curvearrowright a^\dagger(p), \chi_+(p) \curvearrowright a(p)\}$, with commutator algebra $[a(p), a^+(q)] = 4\pi p \delta(p-q)$ and a vacuum $|\mathbf{0}>$ such that $a(p)\,|\mathbf{0}>= 0 \ \ \forall p$. That is

London Journal of Research in Science: Natural and Formal

$$\hat{\Phi}(x^0,x^1)=\frac{1}{4\pi}\int_0^\infty\frac{dp}{p}[a(p)e^{-\imath p(x^0-x^1)}+a^\dagger(p)e^{\imath p(x^0+x^1)}]f(p^2). \tag{2.3}$$

Then, one easily evaluates the commutator of two free scalar OPVD to

$$\left[\hat{\Phi}(x),\hat{\Phi}(0)\right]\equiv\imath\Delta(x)=-\frac{\imath}{\pi}\int_0^\infty\frac{dp}{p}\sin(px^0)\cos(px^1)f^2(p^2). \tag{2.4}$$

This integral is finite without the test function and the limiting procedure where $f^2(p^2)\equiv f(p^2)=1$ refers to important mathematical properties of metric spaces (whether Minskowskian or Euclidean) [18].

2.2. The ET-LFT consistency problem

Going to light-cone (LC) variables $x^0\pm x^1=x^\pm$ is motivated by Dirac's early observation that the LC-stability group is maximal: LC-dynamics has much to share with gallilean dynamics (*e.g.*relative motion of LC-interacting particles decouples from global center of mass motion...). However in the LC-variables the nature of the initial Klein-Gordon equation in Eq.(2.1) is changed to a characteristic initial value problem (CIVP) relative to the partial-differential equation

$$\partial_+\partial_-\Phi(x^+,x^-)=0 \tag{2.5}$$

with initial data on characteristic surfaces

$$\Phi(x^+,x_0^-)=\mathfrak{f}(x^+),\quad \Phi(x_0^+,x^-)=\mathfrak{g}(x^-), \tag{2.6}$$

and the continuity condition

$$\Phi(x_0^+,x_0^-)=\mathfrak{f}(x_0^+)=\mathfrak{g}(x_0^-). \tag{2.7}$$

At first sight the LC-Lagrangian is singular[1]: $W(x,y)=\frac{\delta^2L}{\delta[\partial^-\Phi(x)]\delta[\partial^-\Phi(y)]}=0$, but the appearence of a primary contrainst is known to be of no physical significance [21].

Nevertheless the consistency of the solutions in the two reference frames cannot be established without further insight. This is just the content of Ref. [18], with two main conclusions:

-On the one hand, full consistency of EQT and LFT quantizations can only be achieved when fields are considered as OPVD with partition of unity test-functions $f(p^{+2})$ such that, for the light-cone momentum p^+ , $\lim_{p^+\to 0^+}\frac{f(p^{+2})}{p^+}=0$.
-On the other hand operator series in the Discretized-LC-Quantization (DLCQ) find their natural handling of divergences in the substraction scheme embedded in the OPVD formulation. The net effect of the PU-test function is the appearence of its inherent RG-scale parameter (η).

[1] The Hessian is indentically null

Then the LF-formulation and CFT analysis of $2d$-massless models are in complete agreement in their representation of the energy-impulsion tensor in term of infinite dimensional Virasoro Lie-algebras.

III. THE QUANTUM BOSONIC STRING [19, 23_27]

3.1. Equations of motion of the scalar bosonic string in the LC-gauge

The motion under consideration here is taking place on a $2d$-worksheet embedded in a D-dimensionnal space. The initial field variables are then $x_a(\sigma,\tau), p_a(\sigma,\tau)$ elevated to OPVD. A well-defined Lagrangian is then obtained in terms these regular field variables $X_a(\sigma,\tau), P_a(\sigma,\tau)$. After dealing with the LC-gauge conditions the equation of motion for $X_a(\sigma,\tau)$ is just that of Eq.(2.1) with appropriate position and time variables. Accordingly the sum of the zero-point energies of the first quantized string is just $\frac{(D-2)}{2}\sum_{n=0}^{\infty} n$. The well-known conventional evaluation of this sum is given by the Zeta-function $\zeta(s)=\sum_{n=0}^{\infty}\frac{1}{n^s}$ with $\zeta(-1)=-\frac{1}{12}$. The critical dimension for the absence of the overall conformal anomaly must then be such as to suppress that one with the cental charge $c=1$ coming from the $2d$ worksheet analysis and thus obeys $\frac{(D-2)}{2}\zeta(-1)=-1$, that is $D=26$! However, even though at the same time this reasoning based on Zeta-function was already under scruteny [24], this critical value survived the long haul!

3.2. TLRS and the Renormalization Group

In the advocated $2d$ QFT treatment the key role is in the pseudo-function distribution extension $\mathcal{P}f(\frac{1}{p^2})$ of $\frac{1}{p^2}$ at the origin. It is defined by the integral

$$I_N=\int_0^{\infty} d(p^2)\mathcal{P}f(\frac{1}{p^2})f(p^2)\overset{\text{def}}{=}\lim_{\epsilon\to 0}\Big[\int_{\xi\epsilon}^{\Lambda}\frac{d(p^2)}{p^2}+\int_{\frac{\epsilon}{\eta^2}}^{\frac{1}{\Lambda}}\frac{d(p^2)}{p^2}+2\ln(\epsilon)\Big]=\ln(\frac{\eta^2}{\xi}) \qquad (3.1)$$

where η is the dilatation-scale inherent to the construction of the test function $f(p^2)$ [7, 14]. The term in $\ln(\epsilon)$ corresponds to the general Hadamard substraction procedure to generate a Finite part (F.p.).

The factor ξ is arbitrary[2] with no physical meaning unless explicit symmetry violations need enforcement. Consider now the identity

$$\begin{aligned} IPf(\eta) &= \int \frac{d^2(p)}{(2\pi)^2)} \frac{f(p^2)}{p^2} \equiv \int \frac{d^2(p)}{(2\pi)^2} \frac{(p+q)^2}{p^2(p+q)^2} f(p^2), \\ &= \int_0^1 dx \int \frac{d^2(\mathbf{p})}{(2\pi)^2} \frac{(\mathbf{p^2}+q^2(1-x)^2)}{[\mathbf{p^2}+q^2x(1-x)]^2} f(\mathbf{p^2}), \\ &= \frac{1}{4\pi}(\ln(\frac{\eta^2}{\xi}) - 1). \end{aligned} \tag{3.2}$$

This is easy to understand due to the identity in the UV limit of the $\mathbf{p}$-integration where $f[(\mathbf{p}+\mathbf{q})^2]\mathbf{f}(\mathbf{p^2}) \equiv \mathbf{f^2}(\mathbf{p^2}) \equiv \mathbf{f}(\mathbf{p^2})$. Moreover the overall $\mathcal{O}(2)$ $\mathbf{p}$-invariance implies that terms linear in $\mathbf{p}$ do not contribute to the integral.
Consider then the one loop Feynman diagram in relation to the energy-momentum tensor of the X-field and in the same UV limit[3]

$$\begin{aligned} \Pi_{ab|cd}(q) &= \frac{\mathcal{D}}{8}\int \frac{d^2p}{(2\pi)^2} \frac{t_{a,b}(p,q)t_{c,d}(p,q)}{p^2(p+q)^2} f[p^2]f[(p+q)^2], \\ &= \frac{\mathcal{D}}{8}\int_0^1 dx \int \frac{d^2\mathbf{p}}{(2\pi)^2} \frac{t_{a,b}(\mathbf{p},q,x)t_{c,d}(\mathbf{p},q,x)}{[\mathbf{p^2}+q^2x(1-x)]^2} f[\mathbf{p^2}], \end{aligned} \tag{3.3}$$

with

$$\begin{aligned} t_{a,b}(p,q) &= p_a(p+q)_b + p_b(p+q)_a - \delta_{a,b}(p.(p+q)), \\ t_{a,b}(\mathbf{p},q,x) &= (\mathbf{p}-q(1-x))_a(\mathbf{p}+qx)_b + (\mathbf{p}+qx)_a(\mathbf{p}-q(1-x))_b \\ &\quad -\delta_{a,b}[\mathbf{p^2} - \mathbf{p}q(1-2x) - q^2x(1-x)]. \end{aligned}$$

The presence of the test-function $f[\mathbf{p^2}]$ ensures the existence of this phase-space integral, which otherwise would exibit divergences when $\mathbf{p} \to \infty$. The common pratice in the far past was to consider their cancelations by appropriate counter terms. In that case the only surviving regular contribution to $\Pi_{ab|cd}(q)$ is[4]

$$\begin{aligned} \Pi^{reg}_{ab|cd}(q) &= \frac{\mathcal{D}}{8}(2q_aq_b - q^2\delta_{a,b})(2q_cq_d - q^2\delta_{c,d})\int_0^1 dx x^2(1-x)^2 \int \frac{d^2\mathbf{p}}{(2\pi)^2[\mathbf{p^2}+q^2x(1-x)]^2} \\ &= -\frac{\mathcal{D}q_M^2}{192\pi}(\delta_{a,b} - 2\frac{q_aq_b}{q^2})(\delta_{c,d} - 2\frac{q_cq_d}{q^2}) \end{aligned} \tag{3.4}$$

---

[2] For Gauge Theories ξ is related to the gauge fixing parameter [12].
[3] This is the 2-points-function, eq.(9.158), of Poliakov's monograph. A coupling vertex factor would be $\imath\frac{g^2}{2}f^{acd}f^{bcd} = \imath\frac{g^2}{2}\mathbf{C}_A\delta^{ad}$.
[4] Here q_M is with Minkowski's signature opposite to Euclid's one.

Here, from the embedding of the $2-d$ worksheet, $\mathcal{D}$ does stand for $\mathcal{D}-2$. Follwing *sect*(3.1) what is at sake is the sum (e.g. Trace) of the eigen-modes of this matrix. It can be diagonalized by a unitary transformation with a preserved Trace equal to 4. The result [5] is then just the same critical dimension for the absence of the conformal anomaly obtained in the first quantization framework, that is $\mathcal{D}_{cr} = 26$. It is clear then that the elimination of diverging contributions by counter-terms just leaves the evaluation of (3.4) in keeping with the findings of [19].

However our TLRS formalism shows that this is not the end of the story.Indeed from examples (3.1,3.2) we observe that diverging integrals in $\mathbf{p^2}$ and $\mathbf{p^4}$ carry essential dependencies on the RG-parameter η. Then the complete η-dependence governing the RG-analysis of the critical equation is concerned with the behaviour of the central charge under the flow of the renormalization group (RG). Zamolodchikov realized this as early as 1986 with his c-theorem [29]:

"There is a function C on the space of unitary 2d-field theories that monotonically decreaes along the RG-flows and which coincides with the Virasoro central charge c at fixed points."

It takes the form

$$\mu\frac{d}{d\mu}C(\mu,\Lambda) \equiv \frac{\mu}{\Lambda}\frac{d}{d(\frac{\mu}{\Lambda})}C(\frac{\mu}{\Lambda},1) = \eta\frac{d}{d\eta}C(\eta,1) = -\beta(i,\eta)g(i,j)\beta(j,\eta)$$

where the Calan-Symanzik β-function at fixed point is independent of η and takes the primitive value [30] $\frac{6}{LambertW(6)}$.

With the stress energy-tensors $\Theta(z) \equiv T_{z,z}$ and $\bar{\Theta}(\bar{z}) \equiv T_{\bar{z},\bar{z}}$ the C-function and the metric write [31, 33]

$$C = -\frac{1}{2\imath}\int_{\text{real surface}} dz\wedge d\bar{z} < \Theta(z)\bar{\Theta}(\bar{z}) >_c |_{IR(TLRS\ limit)} \tag{3.5}$$

and

$$g_{(z,\bar{z})} = \frac{6\pi^2}{\mu^4} < \phi(z)\bar{\phi}(\bar{z}) >_c |_{IR(TLRS\ limit)},$$

[5] In the perpective of the analytic continuation of *sect.*(3.1) it is instructive to note how here this decomposes as $-\frac{q_M^2}{4\pi}\frac{(\mathcal{D}-2)}{2*8}\frac{4}{6}$,4 from the trace itself and $\frac{1}{6}$ from the final x-integration $\int_0^1 dxx(1-x) = \frac{1}{6}$ *cf* Appendix B

London Journal of Research in Science: Natural and Formal

where the subscript c at the bracket indicates connected collerator contributions. μ is an arbitrary inverse distance inherent to the construction of the TLRS test function as a partition of unity with a dimensionless argument (*cf* footnote 5). The fields $\phi^i(x)$ originate from local coupling sources $\lambda^i(x)$.

Let us consider the correlator of two stress tensors on the plane in the TLRS context [31]

$$< T_{\alpha,\beta}(x)T_{\rho,\sigma}(0) >= \frac{\pi}{3}\int_0^\infty d\mu C(\mu)\int \frac{d^2p f(p^2)}{(2\pi)^2}\exp(\imath px)\frac{(g_{\alpha\beta}p^2 - p_\alpha p_\beta)(g_{\rho\sigma}p^2 - p_\rho p_\sigma)}{p^2+\mu^2}.$$

We are only left with the unknown scalar function of the mass scale μ, the spectral density [32] $C(\mu)$. Its properties have to comply to the following requirements:

(i) Reflexion positivity of the euclidean field theory, i.e. unitarity of the Hibert space, implies $C(\mu) \geq 0$,
(ii) Due to $\dim(T_{\alpha\beta}) = 2$ the spectral density is a dimensionless measure of degrees of freedoom,
(iii)The form of $C(\mu)$ in a scale invariant field theory is completely fixed by it dimensionality. Since $d\mu C(\mu)$ is dimensionless one may not exclude $C(\mu) \sim \frac{c}{\mu}$.
This IR divergence at $\mu = 0$ is fully understood in the TLRS context [7, 12] as long as the scaling limit to 1 of the test fuctions is not taken too early.

Indeed the correlator is[6]

$$\begin{aligned} < \Theta(x)\Theta(0) > &= \frac{c\pi}{3}\partial^4{}_{|x|}\int_0^\infty \frac{d\mu}{\mu}f(\mu^2)\int \frac{d^2p f(p^2)}{(2\pi)^2}\frac{\exp(\imath p.x)}{p^2+\mu^2}, \\ &= -\frac{c}{12\pi}\ln(\eta^2)\partial^4{}_{|x|}[\gamma_E + \ln(\frac{\Lambda|x|}{2})], \\ &= \frac{1}{4\pi}\ln(\eta^2)\frac{2c}{|x|^4} \end{aligned}$$

(iv) Conformity with conformal invariance is exibited through the $\frac{1}{|x|^4}$ dependence in agreement with the results of [18](Eq.(56)) for $< 0|T(z)T(w)|0 >$. The study of the central charge C from Eq.(3.5) on a $2d-$curved manifold [34] has established the general validity of Zamolodchikov c-theorem. It is sufficent, for our purpose, to consider only a flat real surface with coordinate parametrization $\{z, \bar{z}\} = \rho\exp(\pm\imath\theta)$ which leads to[7,8]

[6] It is always possible to write the initial PU-test function regulating the p-integral as $f^2(p^2) \sim f(p^2)f(p^2+\mu^2) \sim f(p^2)f(\mu^2)$, for, in the UV-limit, $f(p^2)f(p^2+\mu^2) \equiv f^2(p^2) \sim f(p^2)$, whereas in the IR-limit the remaining $f(\mu^2)$ function just validates the corresponding integral.

[7] Note that in the initial $\{z, \bar{z}\}$-integrals the factor is $\frac{1}{|z-\bar{z}|^4}$ so that the ρ-integral is on the variable $v = \rho^2\sin^2(\theta)$, hence the independent factorization of the remaining θ-integrals with the appearance the ubiquitous $\frac{1}{12}$ factor [18]($eq.56$).

[8] The TLRS analytic evaluation of $g(v^2)$ is proportional to the difference of step-functions $[\theta(v - x11) - \theta(v - x12)]$, with $x11 = (\eta^2)^{(\frac{1}{\epsilon})}$, $x12 = (2\eta^2)^{(\frac{1}{\epsilon})}$ [16, 32].The final v-integration is then trivial, after Hadamard substractions of diverging contributions in $\ln(\epsilon)$, leaving the $\ln(\eta^2)$ factor.

$$
\begin{aligned}
C(\eta) = & -\frac{1}{32}\int_0^{2\pi}\frac{d(\theta)}{\sin^2(\theta)}\int_0^{\infty} d(v)\frac{f(v^2)}{v^2} = \frac{1}{32}\int_0^{2\pi}\frac{d(\theta)}{\sin^2(\theta)}\int_0^{\infty} d(v)\frac{d}{dv}(\frac{1}{v})f(v^2) \\
= & -\frac{1}{32}\int_0^{2\pi}\frac{d(\theta)}{\sin^2(\theta)}\int_0^{\infty}\frac{dv}{v}g(v^2) \quad \text{with } g(v^2)=\frac{d}{dv}f(v^2) \\
= & -\frac{1}{32}\ln(\eta^2)\lim_{\epsilon\to 0}\{\frac{1}{\epsilon}\int_{\epsilon}^{\frac{\pi}{2}-\epsilon} d(\theta)[\frac{1}{\sin^2(\theta)}+\frac{1}{\cos^2(\theta)}]\} \\
= & \quad \frac{1}{12}\ln(\eta^2) \qquad (3.6)
\end{aligned}
$$

It is plain to see that this result is in agreement with the observation about the unicity of the solution, up to to an arbitrary constant (here $\ln(\eta^2)$), of "Cayley's identity" known as the "Schwarz derivative" [18].

Recently J.F. Mathiot established that, within general arguments valid in the TLRS framework, the trace of the energy-momentum tensor in 4-dimensions does not show any anomalous contribution even though quantum corrections are considered [35]. It is then our concern to turn now to the determination of the critical dimension $\mathcal{D}_{cr}$ for the absence of the overall conformal anomaly with $\mathbf{p^2}$ and $\mathbf{p^4}$ divergences of the Poliakov-tensor treated in the TLRS formalism(*cf* Appendix A). As mentioned after Eq.(3.4) the elimination of diverging contributions by counter-terms just leads to the evaluation in keeping with the findings of [19], that is $\mathcal{D}_{cr} = 26$. However with TLRS the situation is different as shown in Appendix A. The surviving initial Poliakov-term comes with extra TLRS η-independent components. The immediate issue is then the fate of the $\mathcal{D}_{cr} = 26$ value under these additional TLRS terms[9].Following Poliakov's analysis [19] a direct calculation of $\Pi^{(4)}_{--|--}(q,\eta)$ shows explicitly the critical value $\mathcal{D}_{cr} = 4$, as detailed in Appendix B. Consider now the diagonalization of the normalized matrix $\Pi_{ab|cd}(q)$ with a Lagrange parameter ξ in relation to the stress-energy constraint $T_{ab} = 0$. At the value $\mathcal{D}_{cr} = 4$ ξ is completely fixed, indicating that reparametrizations of the world-sheet and conformal rescaling allow to fully fix g_{ab} to anything wanted.

IV. FINAL REMARKS

As a final additional observation it is instructive to consider the string description for the VVA-anomaly [22] versus its direct calculation with TLRS [16, 17]. In the string treatment of the massless case (*cf* *Eq.*(6.44) of [22]) "explicit divergences are made of a difference of two tadepoles type and hence do not contribute in dimensional regularization, whereas for the remaining terms integrations are elementary, and the result is, using Γ-function identities, easily identified to the standard result for the massless QED vacuum polarization". In TLRS the calculation is directly in dimension $D = 4$ with the usual γ_5 and all contributions are either null or finite: a simple bookeeping leads then to the standard VVA-anomaly without further ado. The TLRS procedure does provide

[9] given by Eq.(A.9) of Appendix A.

a very clear and coherent picture. All known invariance properties, besides those of the VVA-anomaly, are preserved [13–15]. It is a direct consequence of the fundamental properties of TLRS. As an "a-priori" regularization procedure, it provides a well defined mathematical meaning to the local Lagrangian we start from in terms of products of OPVD at the same space-time point. It also yields a well defined unambiguous strategy for the calculation of elementary amplitudes, which are all finite in strictly 4-dimensional space-time and with no new non-physical degrees of freedom nor any cut-off in momentum space.

In summary the strategy developped here was based on the passage from first-quantization to second quantization of the bososnic string. It is characterized by the introduction of the notion of L.Schwartz's Pseudo-Functions [8](*cf* Eq.(3.1)) with their dilatation scale dependences. This result is at variance wih the usual dilatation-scale independant Zeta-fuction evaluation of the discrete sum on inverse quantum n of first-quantized space-time objects. Actually it is easy to see that the standard evaluation of the Zeta-function through normal Eulers'integral in the integration interval $(0, \infty)$ should be considered as the limit $\epsilon \to 0$ of the same integral in the interval $(\xi\epsilon, \frac{\eta^2}{\epsilon})$, thereby collecting first from the logarithmic term the contribution $\ln(\frac{\eta^2}{\xi})$ and not the value $\zeta(-1) = -\frac{1}{12}$.

The main conclusion is then that String Theory in the OPVD picture reduces to Finite Quantum Field Theory, *directly in 4-dimensions with no trace anomaly of the energy-momentum tensor* , and in the limit where the tension along the string becomes infinite.

ACKNOWLEDGEMENTS

This study finds its origin through numerous discussions with Professor Ernst Werner from the Theoretical Physics section of Regensburg University. The first outcomes were publications [17, 18]. In the early 2021 we undertook the present work. Up to April 2021 Ernst Werner contributed activly and continuously to its developments. He departed unexpectedly on May 12th 2021.

This publication is then dedicated to his memory. Our collaborations and constant friendship lasted ever since the Thesis of A. Lacroix-Borderie submitted on September 9,1994 at the Université de Strasbourg.

We are grateful to André Neveu for sharing his past experience on the subject and his quest for clarifying comments along this presentation.

We acknowlege constant support from Denis Puy, Head of the "Laboratoire Univers et Particules" UMR-5299 of IN2P3-CNRS and Université de Montpellier and from Dominique Pallin, Head of the "Laboratoire de Physique Corpusculaire" UMR-6533 of IN2P3-CNRS and Université de Clermont Auvergne.

BIBLIOGRAPHY

1. N.N. Bogoliubov and O.S. Parasiuk: Acta. Math. 97 227 (1957); N.N. Bogoliubov and D.V.Shirkov 1980 "Introduction to the Theory of Quantized Fields", J. Wiley & Sons, Publishers, Inc., 3rd edition (1990).
2. H. Epstein and V. Glaser: Ann. Inst. Henri Poincaré XIXA 211 (1973).
3. G. Scharf: "Finite Quantum Electrodynamics: the Causal Approach", Springer Verlag (1995).
4. R. Stora : "Lagrangian Field Theory", Proceedings of Les Houches, C. DeWitt-Morette and C. Itzykson eds., Gordon and Breach (1973).
5. A.N. Kuznetsov, A.V. Tkachov and V.V. Vlasov: "Techniques of Distributions in Perturbative Quantum Field Theory": hep-th/9612037 (1996).
6. (a) J.M. Gracia-Bondia: Math. Phys. Annal. Geom. 6 59 (2003); (b) J.M. Garcia-Bondia and S. Lazzarini, J. Math. Phys. 44 3863 (2003).
7. P. Grangé and E. Werner: Nucl. Phys. (Proc. Suppl.) B161 75 (2006).
8. L. Schwartz: "Théorie des Distributions" (Paris: Hermann) (1966).
9. S.S. Schweber: "An Introduction to Relativistic Quantum Field Theory", New-York: Harper and Row (1964).
10. G. 't Hooft and M. Veltman : Nucl. Phys. B44 189 and B50 318 (1972); J. Collins "Renormalization", Gambridge University Press (1987).
11. P. Grangé and E. Werner: J. Phys.A 44 385402 (2011).
12. B. Mutet, P. Grangé and E. Werner: J. Phys.A 45 315401 (2012).
13. P. Grangé, J.-F. Mathiot, B. Mutet, E. Werner: Phys. Rev. D 80 105012 (2009).
14. P. Grangé, J.-F. Mathiot, B. Mutet, E. Werner: Phys. Rev. D 82 025012 (2010).
15. P. Grangé J.F. Mathiot B. Mutet and E. Werner: Phys. Rev. D 88 125015 (2013].
16. P. Grangé and E. Werner: "Fields on Paracompact Manifolds and Anomalies", Proceedings of "Light Cone meeting:Hadrons and beyond", 5th-9th August 2003, Durhan (UK), S. Dalley Editor, [e-print: math-ph/0310052v2 (2003)]
17. P. Grangé, J.-F. Mathiot and E. Werner: Int. J. Mod. Phys. A35,5 2050025 (2020).
18. P. Grangé and E. Werner: Mod. Phys. Lett. A33 No 22 1850119 (2018).
19. A.M. Polyakov: Phys.Lett. B103 207 (1981); "Gauge Fields and Strings", Contemporary Concepts in Physics Vol 3, Harwwod academic publishers, London-Paris-New-York (1987).
20. B. Hat_eld: "Quantum Field Theory of Particules and Strings", Frontiers in physics v. 75, Addison- Wesley Publishing Company (1992).
21. L. Faddeev and R. Jackiw: Phys. Rev. Lett. 60, 1692 (1988); R. Jackiw: "(Constrained) Quantization Without Tears" MIT preprint CTP 2215 arXiv:hep-th/9306075 (1993).
22. C. Schubert: "Perturbative Quantum Field Theory in the String-Inspired Formalism" Phys.Rept. 355 73-234 (2001).
23. O. Alvarez: Nucl.Phys. B 216, 125 (1983).
24. T.S. Bunch: "General Relativity and Gravitation" 15,3,27 (1983).
25. B. Zwiebach: "A _rst course in string theory", Cambridge University Press, (2004);
26. J. Polchinski: "String theory vol.(1,2), Cambridge University Press, (2001); K. Becker, M. Becker, J.H. Schwartz: String Theory and M-theory", Cambridge University Press, (2007); E. Kiritsis "String Theory in a nutshell", Princetown University Press, (2007); P. Ginsparg: "Applied Conformal Field Theory", Les Houches, Session XLIX (1988).
27. "MIT Spring Lecture 19 (2007) " https://ocw.mit.edu/courses/physics/8-251-string-theory-forundergraduates-spring-2007/lecture-notes/lec19.pdf
28. C. Itzykson and J.M. Drou_e: "Théorie Statistique des Champs, Vol.2", Savoirs Actuels, Inter Editions du CNRS,(1989); Y. Grandati: "Éléments d'introduction á l'invariance conforme",

Ann. Phys. Fr. 17,159 (1992); Ph. Di Francesco, P. Mathieu, D. Sénéchal: "Conformal Field Theory", Springer-Verlag New-York (1997). Finite QFT, Bosonic String. 12
29. A.B. Zamolodchikov: JETP Lett. 43,730 (1986) [Pisma ZH. Eksp. Teor. Fiz. 43, 565 (1986)]; J Polchinski: Nucl.Phys. B 303,2, 226 (1988).
30. S. Salmons, P. Grangé, E. Werner: Phys.Rev.D65, 125014 (2002).
31. A. Cappelli, D. Friedan, J.L. Latorre: Nucl.Phys.B 352, 616 (1991).
32. E. Kneur and A. Neveu: Phys.Rev.D101, 074009 (2020).
33. D. Freidman and A. Konechny: J. Phys.A43, 215401 (2010) [e-Print:hep-th/0910.3109].
34. H. Osborn , G.M. Shore: Nucl.Phys.B 571, 287 (2000)[e-Print:hep-th/9909043].
35. J.-F. Mathiot: Int. J. Mod. Phys. A36,33, 2150265 (2021). Finite QFT, Bosonic String.

This page is intentionally left blank

Novel Improvement of the Van Der Waals Forces Characterization from Published Vaporization Enthalpies

Paul Laffort

ABSTRACT

It has been proposed in 2020 to characterize the intermolecular Van der Waals and hydrogen bonding forces of volatile organic compounds (VOCs) by means of four molecular descriptors (or parameters) established from known and easily obtained molecular properties. These properties are: refractive index at 25°C, intrinsic molecular volume, molecular polar surface area, normal boiling point, number of hydroxyl radicals and number of pentavalent nitrogens. The sum of the four molecular parameters thus defined was found to equal the normal boiling enthalpy with a high correlation coefficient (r = 0.95) for a first dataset of 445 VOCs, and confirmed in a second one of 180 compounds including liquids, solids and gases. The normal boiling enthalpy values for these two datasets being between 20 and 55 kJ/mol, the first purpose of the present study has been to test the validity of the proposed 2020 model for a total of 616 compounds whose boiling enthalpy range is between 20 and 75 kJ/mol. Since the 2020 model was inaccurate for normal boiling enthalpy values above 55kJ/mol, the second objective of this study has been to overcome this limitation.

Keywords: enthalpies of vaporization at 25°c and at normal boiling points, van der waals intermolecular forces, molecular polarity, polar surface area, chemo-informatics, olfaction.

Classification: LCC Code: QD1-QD999

Language: English

Great Britain Journals Press

LJP Copyright ID: 925661
Print ISSN: 2631-8490
Online ISSN: 2631-8504

London Journal of Research in Science: Natural and Formal

Volume 22 | Issue 8 | Compilation 1.0

Novel Improvement of the Van Der Waals Forces Characterization from Published Vaporization Enthalpies

Paul Laffort

ABSTRACT

It has been proposed in 2020 to characterize the intermolecular Van der Waals and hydrogen bonding forces of volatile organic compounds (VOCs) by means of four molecular descriptors (or parameters) established from known and easily obtained molecular properties. These properties are: refractive index at 25°C, intrinsic molecular volume, molecular polar surface area, normal boiling point, number of hydroxyl radicals and number of pentavalent nitrogens. The sum of the four molecular parameters thus defined was found to equal the normal boiling enthalpy with a high correlation coefficient (r = 0.95) for a first dataset of 445 VOCs, and confirmed in a second one of 180 compounds including liquids, solids and gases. The normal boiling enthalpy values for these two datasets being between 20 and 55 kJ/mol, the first purpose of the present study has been to test the validity of the proposed 2020 model for a total of 616 compounds whose boiling enthalpy range is between 20 and 75 kJ/mol. Since the 2020 model was inaccurate for normal boiling enthalpy values above 55kJ/mol, the second objective of this study has been to overcome this limitation.

Keywords: enthalpies of vaporization at 25°c and at normal boiling points, van der waals intermolecular forces, molecular polarity, polar surface area, chemo-informatics, olfaction.

Author: Honorary Director of Research at CNRS 541 rue Burdin Bidea, 64310 Ascain, France.
email: paul.laffort@sfr.fr

I. INTRODUCTION

Acronyms used in this article are detailed at the end of the paper.

It has been published in 2020 a study on the *Interest of splitting the enthalpies of vaporization in four distinct parts reflecting the Van der Waals and the hydrogen bonding forces* [1]. The results can be summarized by four empirical equations as shown below. This has been optimized to obtain the best prediction of the enthalpies of vaporization values from ChemSpider [2], for a set of 445 organic compounds in liquid state at room temperature. It must be specified that these data from ChemSpider are enthalpies of vaporization at normal boiling point, also briefly called *boiling enthalpies,* that we will abbreviate here H_{BPCS}:

H_{BPCS} =

- 0.4840 fn Vw + 17.23 [F = 2554] (δ_{2020} + 17.23) (1)
- + 0.3713 fn Vw – 0.1048 Vw + 2.25 [F = 194] (ε_{2020}) (2)
- + 22.50 PSA1/GSS [F = 905] (ω_{2020}) (3)
- + (2671 O1 – 2064 N122)/TBP [F = 589] ($S_{vap\ 2020}$) (4)

in which δ_{2020}, ε_{2020} and ω_{2020} respectively stand up-to-now for the intermolecular descriptors of dispersion, induction-polarizability and orientation or polarity strictly speaking, reflecting the forces of London, Debye and Keesom. Furthermore, Svap 2020 stands for the entropy of vaporization due to the hydrogen bonding forces. The acronyms in the first column stand for classical molecular properties widely accessible, which will be specified in the present Material and Methods section. The F values between square brackets stand for the partial statistical test F ratios in the global prediction of H_{BPCS}, which depends on the correlation coefficient r, the number of independent variables and the number of compounds (see Abdi [3] for more details). Their values are expected to be as high as possible, and this is the case for the four equations above.

The predictive regressions of enthalpy values as the sum of equations (1-4) applied to the all 445 compounds of the database under study in the previous publication and to the 116 hydrocarbons taken alone from this database are visualized in figure 1.

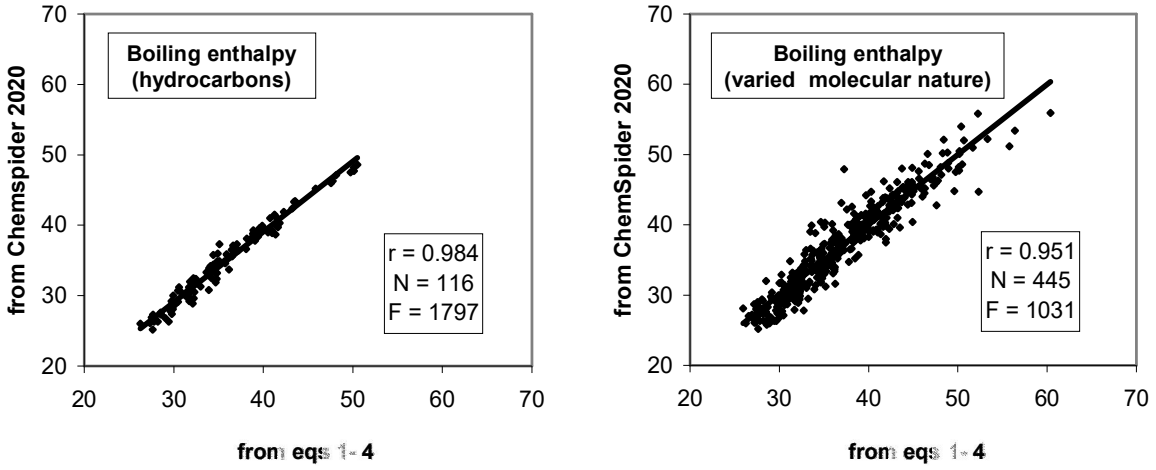

Fig. 1: Comparison of the normal boiling enthalpy prediction for two sets of VOCs (Volatile Organic Compounds) in liquid state at room temperature, expressed in kilojoules.mol^{-1} (from [1]). See text.

It clearly appears from figure 1 that the intermolecular forces are better characterized for the pure hydrocarbons, for which the equations 3 and 4 equal zero, than for the global set of 445 compounds. Let us however note the high partial F ratios already mentioned for the four equations involved in this case and the strong mutual independence of the four retained molecular characteristics in their 2020 version, as shown in figure 2.

	δ_{2020}	ω_{2020}	ε_{2020}
ω_{2020}	-0.28		
ε_{2020}	0.23	-0.11	
$S_{vap\ 2020}$	-0.08	0.20	-0.04

Fig. 2: Correlation matrix of the three molecular descriptors reflecting the intermolecular Van der Waals forces and the entropy of vaporization due to the hydrogen bonding forces according to [1], showing their high degree of mutual independence.

In another diagram reproduced hereafter (figure 3), it has also been shown in [1] with another data set of 180 compounds including some gases and solids at room temperature, that the equations (1-4) remain relatively valid in all cases. However, the purpose of the present study is to verify and possibly refine all these recent results.

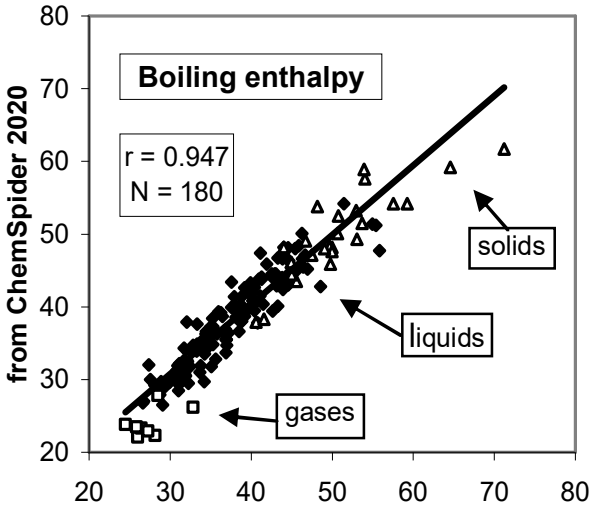

Fig. 3: Prediction of the boiling enthalpy vs enthalpy published by ChemSpider [2] for 180 compounds (145 liquids, 27 solids and 8 gases), both expressed in kilojoules.mol^{-1} (from [1]).

Comment on this 2020 publication

One of the objectives of the author of this study since the beginning of his research activity in 1960, as well as of his team, has been oriented towards quantitative structure-activity relationships (QSAR) in olfaction, including in parallel measurements or calculations of molecular properties and biological properties in humans and in bees. A synthesis of the state-of-the-art in 1991 (translated into English and updated in 1994) on this subject can be read in chapter 6 of *Odors and Deodorization in the Environment* [4].

Without going into details, it can be said that for Corwin Hansch, considered as one of the pioneers in the more general field of QSAR in biology, the response of a biological system to a biologically active agent is mainly a function of three properties of the latter: a hydrophobic factor, a steric factor and an electronic factor [5]. Of course, the final validation of the parameters or molecular descriptors likely to be the most relevant depends on a satisfactory prediction of the biological properties. However, it turns out that biological experimental data are most often obtained with a margin of uncertainty greater than those obtained in physical chemistry, hence the approach often followed of choosing a so-called global physicochemical property based on several so-called contributing physicochemical properties. Progressively, the number of contributing factors (or descriptors) has increased to 4, then to 5 by several authors while refining. This was the case in 1973 for the author of the present study in cooperation with Andrew Dravnieks, of the IIT-Research Institute of Chicago [6]. We were left with 4 contributing descriptors for solutes and 4 for stationary phases (solvents), with the global properties assumed to be the retention (or Kováts) indices in gas-liquid chromatography (GLC). Later, our team followed the approach of Karger, Snyder and Eon [7,8] by moving to five descriptors: two for the proton donor and acceptor properties and three for the three

Van der Waals forces. The rest of this pathway is detailed in the Introduction of our 2020 paper, which it does not seem necessary to repeat here in full.

II. MATERIALS AND METHODS

2.1. Statistical tools

In addition to the Microsoft Excel facilities for drawing diagrams and handling data sets, the SYSTAT 12 ® for Windows has been applied for stepwise MLRA (Multidimensional Linear Regression Analysis).

2.2. SMT terminology

A tool named *Simplified Molecular Topology* (SMT) has been defined and applied in various previous studies and recently in [1]. It consists of considering, for each atom of a molecule, its nature and the nature of its bonds, leaving aside the nature of its first neighbors (with sometimes few limited exceptions). Each atom is provided with an index comprising a series of digits. Their sum is at most equal to its valence. The value of the digits defines the type of bonds (1 for a single, 2 for a double bond, etc.), but the bonds with hydrogen are excluded. The SMT has been applied to the present study for characterizing the hydroxyl term (O1), the monovalent nitrogen (N1), the pentavalent nitrogen (N122), the sulphur in thiols and sulphides (respectively S1 and S11) and the halogenated compounds (F1, Cl1, Br1 and I1).

2.3. Intrinsic molecular volume

The various expressions which reflect the *intrinsic molecular volume* or the *Van der Waals molecular volume* ($\mathbf{V_w}$), are all additive properties (which is not the case for V_{20}, the ratio molar mass/density at 20°C). We have selected, among those of various studies, the values of molecular volumes (expressed in cubic angstroms) proposed by the freely interactive calculator of Molinspiration [9]. The authors of this calculator have used, in a first step, a semi-empirical quantum chemistry method to build 3D molecular geometries for a training set of about 12 000 molecules. In a second step, they have fitted the sum of fragment contributions to the supposed real volumes of the training set. We name this expression V_w (as Van der Waals volume).

A predictive tool of V_w has been proposed in [10], which appears satisfactory as shown in figure 4 and alternatively applicable in some particular cases (e.g. for polymers), but we have preferred to keep the original values of Molinspiration in the present study.

molecular features	SMT coefficients	partial F ratios
C	10.692	207 958
H	3.050	72 030
O	8.539	71 564
N	9.306	21 917
F	7.995	38 403
Cl	16.700	108 463
Br	21.080	87 110
I	27.265	33 119
S	17.946	33 037
P	17.874	2 275
SSSR	-0.767	4 116
constant	6.080	

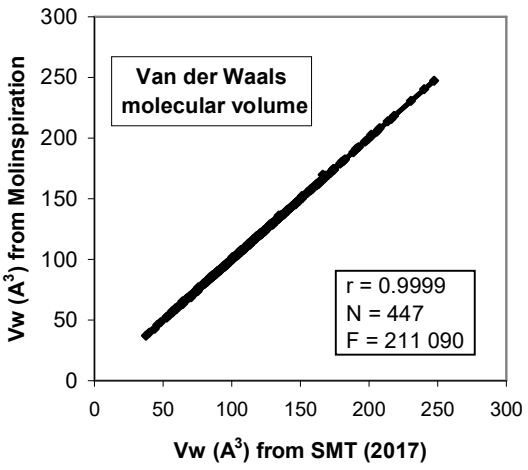

Fig. 4: Correlogram between Van der Waals molecular volumes obtained using figure 1 of [10], and Molinspiration [9]. An erratum on the F value in the original publication has been corrected

2.4. Global Spherical Surface (GSS)

Another property we call *Global Spherical Surface* (GSS) has been used. It is derived from the intrinsic molecular volume as follows:

$$GSS = (36\ \pi)^{1/3}\ Vw^{2/3} \equiv 4.836\ Vw^{2/3} \quad \text{(in Å}^2 \text{ when } V_W \text{ is expressed in cubic angstroms)} \quad (6)$$
(π or Pi standing for the constant 3.14159...)

This GSS expression reflects in some way the molecular surface on the condition that molecules are considered as spheres. As specified in 2.5, the ratio PSA/GSS could therefore reflect a fraction of polarity without dimension.

2.5. Polar Surface Area (PSA)

We have considered until now three variants of PSA:

- The most classical, only including the polar atoms N and O. We have selected the values named TPSA (T as topological) established by Molinspiration [9]. We name this expression PSA1.
- The variant including the same polar atoms N and O as in TPSA, but also the divalent sulfur atoms S1 and S11 according to Ertl et al. [11]. This expression has been adopted by ChemSpider [2], without decimal. We name it PSA3.
- In 2013 [12] we have named PSA2 a third variant initially identical to PSA3, but diminished of the pentavalent nitrogen contribution according to [11]. Indeed, this molecular feature cannot be considered as polar as it is visualized in figure 5 from [12]. PSA2, as specified in the equation (9) of [12], has been selected by the MLRA processing as the most suitable variant in a QSAR (Quantitative Structure-Activity Relationship) olfactory application.

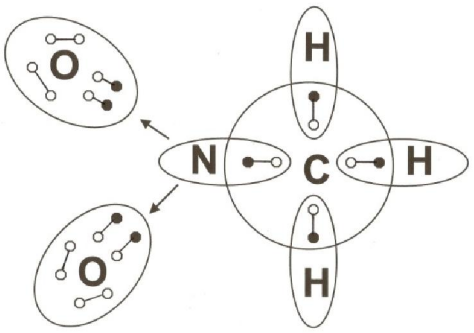

Fig. 5: Graphical representation from [12], of the four dative (or semi-polar) bonds and the four covalent bonds of nitromethane, according to the Lewis theory [13], clearly showing that the pentavalent nitrogen is not polar (absence of pairs of peripheral electrons not included in the bonding whereas each oxygen atom has two pairs).

We propose here a fourth variant named PSA4, also without nitro contributions as in PSA2, but including thiols and sulphides with different coefficients, as in addition fluorinated, chlorinated, brominated and iodinated compounds. These seven modifications, specified hereafter, have been obtained by an empirical approach that it didn't seem necessary to detail. A competition using the stepwise MLRA between the four PSA expressions divided by GSS has been applied in the present study, in order to optimize the polarity characterization.

PSA4 = PSA1 – 11.68*N122 (like in PSA2)

- + 11.47*S1 (instead of 38.80 in PSA2 and PSA3)
- + 7.48*S11 (instead of 25.30 in PSA2 and PSA3)
- + 4.79*F1 (no considered in any of the three other variants)
- + 8.69*Cl1 (no considered in any of the three other variants)
- + 19.73*Br1 (no considered in any of the three other variants)
- + 27.24*I1 (no considered in any of the three other variants)
- + 9.69

2.7. The Data Sets Selected in this Study

Our previous publication on boiling enthalpy [1] was initially based on a set of 445 organic compounds in liquid state at room temperature. We keep it here under the name C445.

Also in [1] as mentioned in the *Introduction* at the figure 3, we applied a second data set of 180 organic compounds including 147 liquids, 25 solids and 8 gases at room temperature to test a possible extension to solid and gaseous VOCs at room temperature of the interesting results obtained with C445. This dataset, we name A180 and already used in [12], is added in the present study.

It is also added a database for 200 compounds according to Goss and Schwarzenbach [14]. The first advantage of adding this third data set, which we call B200, is that its boiling enthalpy range covers values 20-75 kJ/mol, instead of 20-60 for A180 and 25-55 for C445. That could test a possible curvilinear inflection of the regression, suspected in figure 3 for values above 55 kJ/mol. The second advantage of considering these 200 compounds, is to test as a global molecular property, the enthalpy of vaporization at 25°C, applied by these authors, instead of the boiling enthalpy in an environment of 1 atmosphere. It should be underlined that the only difference between these three groups comes from the substances considered, as detailed above. Together, the three datasets total a database of 616 organic compounds, grouped as 616N in Appendix A as *Supplementary Information*.

2.8. Recapitulation of the molecular property sources used in this study

- ChemSpider [2]. This compilation of properties consists primarily of three sites: "Experimental Data", "Predicted ACD/Labs", "Predicted EPISuite". The second of these sites is the most complete both in number of compounds and in number of properties. Therefore, it is the one we have chosen in this study for the properties of refractive index (RI) and boiling point (BP)
- Molinspiration [9]. We used according to this calculator, the polar surface area (TPSA) and the intrinsic molecular volume (V_w).
- Ertl P, Rohde B, Selzer P [11]. We used the coefficients recommended by these authors to define the polar surface areas variants PSA2 and PSA3 from PSA1, as mentioned and specified in 2.5.
- Goss, KU and Schwarzenbach, RP. [14]. We have taken their published values of enthalpy of vaporization at 25°C (H_{25GS}) and saturating vapor pressure at 25°C for 200 substances.

In a very few cases, these sources proved insufficient and were supplemented by the Handbook of Chemistry and Physics [15] or simple interpolations.

2.8. Assistance in writing the text

The Linguee Dictionary [16] and the DeepL translator [17], both available free of charge, have been used to write this publication in English.

III. RESULTS

3.1. Testing the 2020 model for the 616N dataset

In the previous study summarized in the *Introduction*, the chosen global property was boiling enthalpy, which could be predicted as the sum of four molecular descriptors reflecting Van der Waals and hydrogen bonding forces for 445 organic compounds in the liquid state at room temperature. The statistical tests r and F shown in figure 1 are high and the descriptors δ_{2020}, ε_{2020}, ω_{2020} and $S_{vap2020}$ relatively independent of each other as shown in figure 2. The pleasant surprise was, with another data set of 180 organic compounds including liquids, solids and gases, that the previous equations remain valid, with however some suspicion for boiling enthalpy values greater than 55 kJ.mol^{-1}, as suggested by the top of Figure 3 (for at least 1 compound). It is clear that if this curvilinear shape of boiling enthalpies vs a predicting model is confirmed for values greater than 55 kJ.mol^{-1}, the model cannot be considered as totally valid. And this is however the result observed with the 2020 model applied to the data set of 616 compounds, as it can be observed in figure 6.

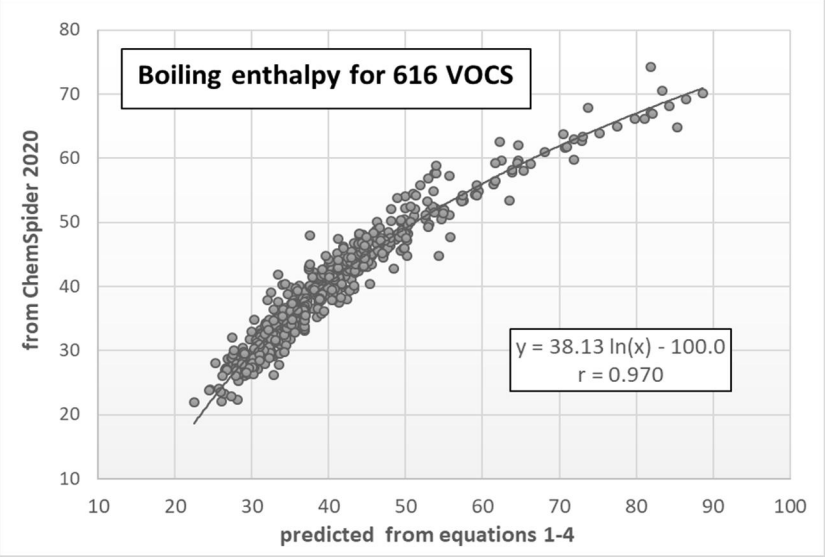

Fig. 6: Confirmation of the validity model published in 2020 [1] for the range of enthalpy values 20-55 kJ/mol, but needing a logarithmic model to be suitable for extended range values (dataset of 616 compounds). See consequences in text

One possible solution to overcome this difficulty is to consider that the molecular property that reflects the sum of the four intermolecular forces is not the boiling enthalpy, but an exponential function of this boiling enthalpy. Although this solution has been found to be partially satisfactory, it has the disadvantage that the units of the descriptors obtained can no longer be expressed in recognized thermodynamic units, in this case kilojoules.mol^{-1}. In addition, use of non-linear equations lead to a model less robust and readable.

In doing so, as mentioned in *Material and Methods*, we found it interesting to test the feasibility of considering the enthalpy of vaporization at 25°C instead of the boiling enthalpy at normal pressure,

as a global property that best reflects the four intermolecular forces under investigation in the present study. However, since experimental values of enthalpy of vaporization at 25°C are few, this option requires the prior development of a robust predictive method for this property. Subsection 3.2 describes one such method of particular relevance.

3.2. A first prediction of the enthalpy of vaporization at 25°C

In their study of 1999 [14], Goss and Schwarzenbach provide experimental values of enthalpy of vaporization at 25°C (H_{25GS}) for about 200 organic compounds of very different natures. But above all, Goss and Schwarzenbach provide an excellent QSPR (Quantitative Structure Property Relationship) between these experimental H_{25GS} and the saturated vapor pressures at 25°C. This result is summarized in figure 7, largely provided by the authors.

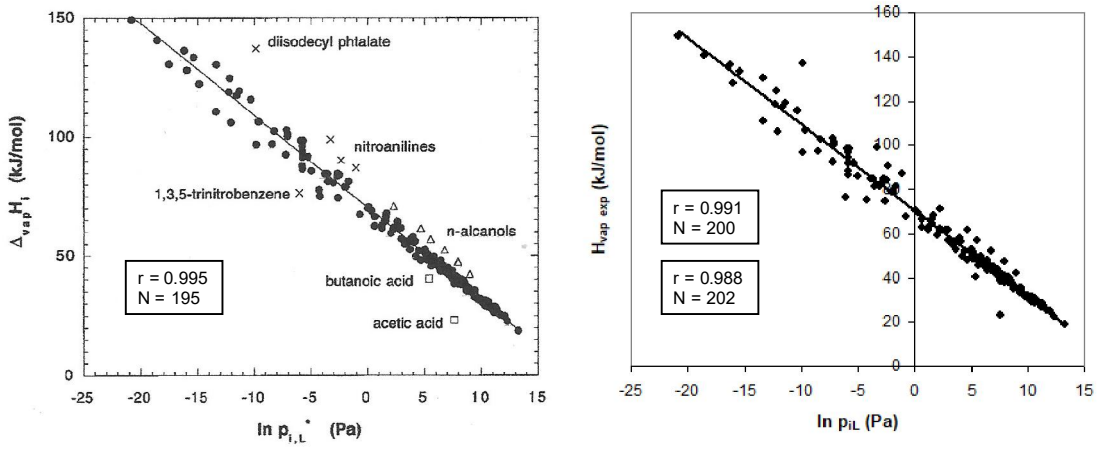

Fig 7: On the left, plot of the enthalpy of vaporization against the logarithm of the saturated liquid vapor pressures at 25°C for compounds that cover a wide range of different chemical classes (original diagram from Goss and Schwarzenbach [14]). A correlation coefficient r = 0.995 has been obtained by the authors after exclusion of the 13 outliers indicated by their names.

On the right, similar diagram for the 202 retained compounds in the present study including the 13 outliers of the left side. Two specifications of statistical tests are mentioned, respectively for 202 and 200 compounds. See comments in text. In order to simplify its expression, we use H_{vap} for enthalpy of vaporization, without Δ.

In the right side of figure 7 the 13 compounds considered as outliers by Goss and Schwarzenbach [14] have been included in the global regression equation, which becomes:

$$H_{vap25°C} = -3.886 \ln svp + 70.67 \quad H_{vap25°C} = -3.886 \ln svp + 70.67 \qquad (7)$$

(r = 0.988; N = 202; F = 8040)

where $H_{vap25°C}$ is expressed in kJ/mol and *svp* stands for the saturated vapor pressure at 25°C in Pa, in other words p_{iL}* *(Pa, 25 °C)*

Two principal outliers can be easily seen in the right side of figure 7: the diisoethylphthalate and the acetic acid. The first one is the highest and it is very probably due to a wrong value of the saturated vapor pressure for this substance (comparison with the values for the other phthalates in the present study). The additional removing of acetic acid from this dataset has been supported by the

conjunction of its outlier status and the uncertainty in the following steps on its molecular volume due to the formation of stable cyclic dimmers.

The equation (7) has therefore been revised slightly in the equation (8) to consider the discarding of these two outliers:

$$H_{vap25°C} = -3.842 \ln svp + 70.46 \; H_{vap25°C} = -3.842 \ln svp + 70.46$$
$$(r = 0.991; \quad N = 200; \quad F = 10702) \qquad (8)$$

where $H_{vap25°C}$ and *svp* are expressed in the same units as in equation (7)

We have appreciated in various previous studies (e.g. reference [18]) the expression of the saturated vapor pressure as its colog values of atmospheres at 25°C. This expression, named ICE (as Internal Cohesive Energy), has for example the advantage to be homogeneous with the molar fraction of a solute in solution in an environment of one atmosphere. The equation (9) allows the transformation of the expression of the saturated vapor pressure applied by Goss and Schwarzenbach [14] into ICE. It should be noted that, unlike the majority of equations proposed in this study, equation (9) is not the result of a regression, but of a strict equivalence between two expressions of the same property: the saturation vapor pressure.

$$ICE = 5.005717 - 0.4342945 \ln p_{iL}^{*} \text{ (Pa, 25 °C)} \qquad (9)$$

Therefore, the equation (10) is an alternative expression of the equation (8) with the saturated vapor pressure expressed in ICE:

$$H_{vap25°C} = 8.847 \; ICE_{eq9} + 26.17 \; H_{vap25°C} = 8.847 \; ICE_{eq9} + 26.17$$
$$(r = 0.991; \quad N = 200; \quad F = 10702) \qquad (10)$$

The satisfactory result described here is not fundamentally surprising in terms of substance, since it appears in several equations derived from Emile Clapeyron's general and simplified formulas published in 1834 [19] and recovered by Rudolf Clausius in 1850 [20]. The nice surprise is the high degree of correlation observed here for 200 substances of very different natures. We have however to underline that the application of equations 8 or 10 based on saturated vapor pressure of a given component is not always easily and accurately accessible. Indeed, it can be obtained on required temperature using formulas such as Antoine equation based on various empirical parameters but only for some ranges of value. Therefore, an alternative prediction is described in the subsection 3.3.

3.3. An alternative prediction of the enthalpy of vaporization at 25°C

Equation (11) below is the best performing one we have obtained in a first stage, using a purely empirical approach based on multiple linear regression analysis (MLRA) applied to 199 out of the initial B200 dataset, squalane having been excluded because of its strong outlier behavior, as can be seen in Figure 8. This compound is a highly branched substance, unlike all others in the present study, and this molecular characteristic could perhaps account for the observed exception.

$$H25_{\text{pred eq 11 2023}} = \underset{[202]}{10.949*(BP_{CS}-25)/100} + \underset{[264]}{21.884*M*T_{BPCS}/100\,000} + \underset{[81]}{9.391*(O1 + N1)} + 20.509 \quad (11)$$

where: BP_{CS} stand for boiling point in °C from ChemSpider (ACD/Labs)
M stand for molecular weight
T_{BPCS} stand for boiling point in kelvin
O1 stand for oxhydric molecular element
N1 stand for primary amine element

The proportionality coefficients of O1 and N1, initially separated and unexpectedly found to be identical, were brought together. Furthermore, these two molecular characteristics being considered as the main ones involved in hydrogen bonding, we propose to call provisionally HB_{2023} (as Hydrogen Bonding) the third term of equation 11.

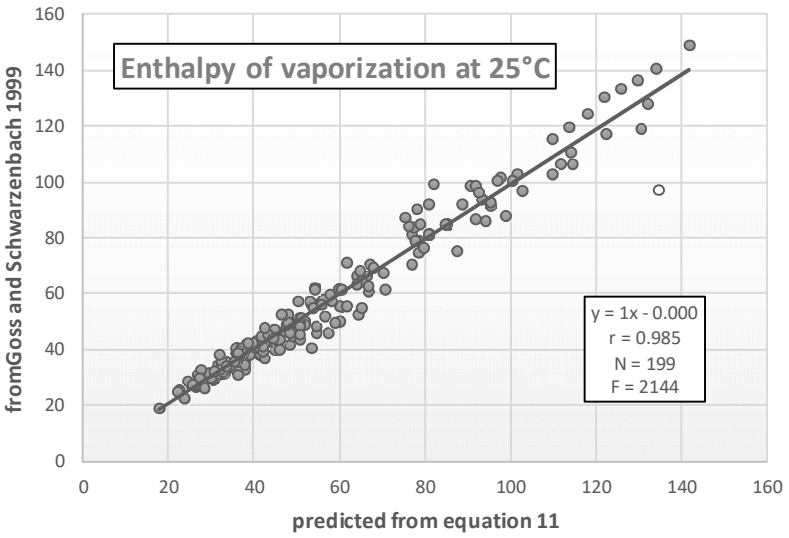

Fig 8: Application of the equation 11 to 199 compounds out of the 200 initially retained from the study of Goss and Schwarzenbach [9]. The compound not kept in consideration in the equation 11 nor in the statistical tests here reported is squalane (open circle).

Whatever the case of equation 11, which at the present stage of the inquiry appears to be the most efficient for representing a general estimate of the enthalpy of vaporization at 25 °C, let us recall that the main goal of this study is the characterization of each of the four molecular descriptors reflecting the three Van der Waals forces and the hydrogen bonding forces of compounds in a condensed phase at 25 °C. Therefore, a first important step remains to be performed now: the splitting $H25_{\text{pred eq11 2023}}$ in four suitable descriptors for 616 organic compounds, similarly to those published in 2020 for 445 compounds on the basis of the boiling enthalpy in the environment of one atmosphere, as recalled in the present Introduction (equations 1–4).

Of course, a second step is also needed to be performed: the verification that the molecular descriptors remain constant when the size and nature of the component samples vary.

These two topics are the subject of subsection 3.4.

3.4. The optimal model to date

This new step to be crossed implies that the enthalpy of vaporization obtained by the application of equation 11 to the 616N dataset can be expressed as the sum of four molecular descriptors in agreement with the previous developments summarized in the Introduction of the present article, possibly improved. The updated definitions are given by the four equations 12, 13, 14 and 15 , obtained using MLRA :

$H25_{\text{pred eqs 12-15/2023}}$ =

0.9353 fn Vw	[F = 20110]	(δ_{2023})	(12)
+ 0.3192 fn Vw – 0.08917 Vw + 1.70	[F = 159]	(ε_{2023})	(13)
+ 31.86 PSA4/GSS	[F = 1011]	(ω_{2023})	(14)
+ 9.437 (O1 +N1)	[F = 724]	(HB_{2023})	(15)
+ 7.949			

in which δ_{2023}, ε_{2023} and ω_{2023}, similarly to equations 1-4, respectively stand for the update molecular descriptors values reflecting the forces of London, Debye and Keesom. Furthermore, HB_{2023} stands for the descriptor reflecting the hydrogen bonding forces involved in pure organic compounds in condensed phases at 25°C. The acronyms in the first column stand for the classical molecular properties widely accessible, which have been specified in the present Material and Methods section. The F values between square brackets stand for the partial statistical tests F ratios.

- The descriptor of Dispersion δ_{2023}, as in our previous papers on GLC since 2005 [18] and in that of 2020 using boiling enthalpy, is based on the product fn*Vw.
- The descriptor of Induction-Polarizability ε_{2023} is also based as previously on a bilinear regression of fnVw and Vw, but slightly modified, characterized by negative values for fluorinated and branching compounds and by strongly positive values for polycyclic compounds and compounds with multiple bonds. Most of normal paraffines have values near of zero. (Let us underline that the initial data set of 200 substances do not include fluorinated compounds).
- The descriptor of orientation or polarity strictly speaking ω_{2023} is similar to that of 2020, but including an expression of polar surface area in its version of PSA4, as selected by the MLRA processing. This is not surprising since is not easy to understand, from a strictly physicochemical point of view, a definition of a polarity not including values for divalent sulfur compounds and halogenated compounds.
- Concerning the descriptor reflecting the hydrogen bonds HB_{2023}, its definition is very different of that in the 2020 paper, but its consideration in the present one seems to be pragmatically acceptable. In this respect, one can note the very strong resemblance of the coefficient of the third term of equation 11 (9.391) with that of equation 15 (9.437). One could very well separate, as soon as equation 11 was obtained, the third term of this equation as the definitive definition of HB_{2023} (instead of provisional) and called the sum of the other terms “Global Property reflecting the Van der Waals forces” (GWP). Not only could this be done, but we did it, and the resulting values of δ_{2023}, ε_{2023} and ω_{2023} turned out to be practically identical to those in equations 12-15. The reason we did not keep this procedure as a pathway is in order to keep the reference to the H25 enthalpy all the way through.

In order to base the reference values of the three descriptors reflecting the Van der Waals forces on the largest number of compounds studied so far, the 616N dataset has of course been chosen. The results given by equations 12, 13, 14 and 15 are applied in figure 9.

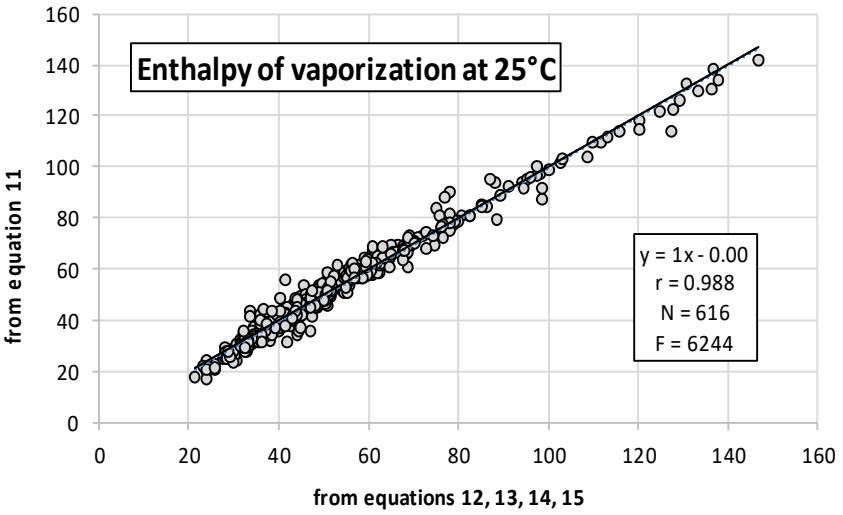

Fig 9: Application of the four equations 12-15 to the 616N dataset, showing a good proximity between equation 11 (without squalane) on one side and the equations 12-15 on another side, as both validated predicting tools of H25. The second option presenting the additional interest to be reflect the four molecular intermolecular forces, has been selected to be kept for both purposes.

It now remains to test that the four molecular descriptors defined by equations 12-15 remain valid in their nature when the sample of substances to be studied is changed. Figure 10 is directly deduced from Figure 9 in which only the initial 200 substances were retained. There is a clear improvement in the correlation observed in this figure 10 compared to figure 8, which reinforces the aforementioned choice in favor of the predictive model of H25 via equations 12-15, rather than via equation 11. There is also a more Gaussian distribution of points in figure 10 in a comparison of figures 8 and 9, making the high value of the correlation coefficient more convincing.

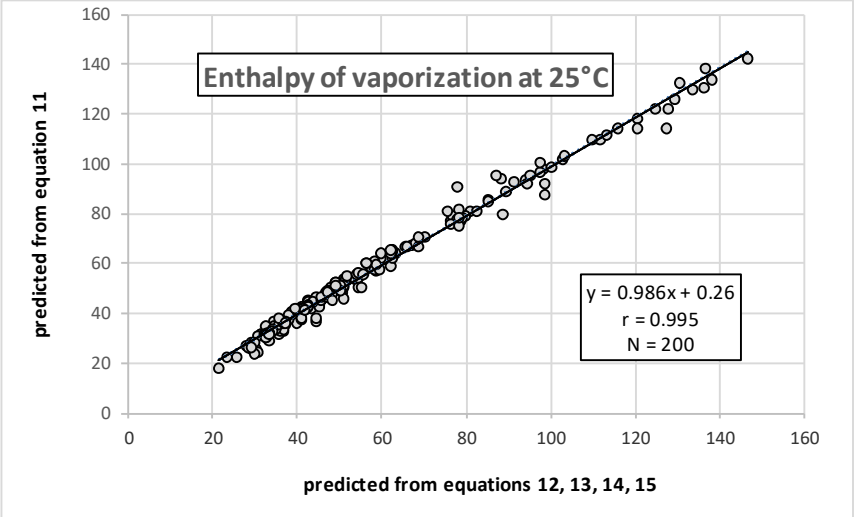

Figure 10: The comparison of Figures 8, 9 and 10 would seem to be interpreted as a validation of equations 12-15 rather than equation 11, whatever are the sample of substances considered, in order to characterize a suitable predicted H25. See text.

To complete the comparisons between the 2020 study and the present one, the correlation matrix in Figure 11 shows that for the 616 selected compounds, the relative independence of the molecular descriptors reflecting the four intermolecular forces is comparable to that observed in Figure 2.

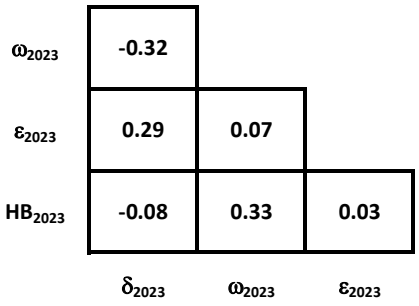

Fig. 11: Correlation matrix of the four molecular descriptors in their 2023 version, showing mutual independence comparable to that of figure 2.

3.5. Supplementary Information

An abridged version of the dataset for the 616 VOCs used in the present study is reproduced in Appendix A. This database is limited to organic compounds including C, H, O, N, S, P, F, Cl, Br, I. Therefore, compounds including Se, Pb or Si, for example, are excluded.

The main information reported in this Appendix are the values of the four contributing molecular descriptors defined in equations 12, 13, 14, and 15, as well as their sum characterizing the predicted values of enthalpy of vaporization at 25°C (H25). All these data are expressed in kilojoules/mol.

IV. DISCUSSION AND COMMENTS

Generally speaking, the present publication represents the most recent step of a long investigation of our team in Physical Chemistry, pursued since the 1970's in parallel with other less risky themes and more centered on the olfactory physiology in Man and in Honeybee. This physicochemical thematic initially privileged the Kováts retention indices in gas-liquid chromatography (GLC), associated with a data processing that we now call MMA (Multiplicative Matrix Analysis). This MMA algorithm seems to have been poorly understood in the publications involved in this subject. However, it allowed us to characterize since 1976 [21], a polarizability parameter reflecting the Debye forces in a relatively satisfactory way, with an optimization in 2005 still valid today [18]. In this 2005 paper, we also refined the characterization of dispersion or London forces. In fact, the content of this 2005 publication was already present in Françoise Chauvin's 1998 thesis [22], of which chapter 2 is a translation into French of a multi-author manuscript submitted to a well-known Chromatography journal and twice rejected (see page 26 of this thesis for the presentation of the chapter in question)...

There remained the polarity, whose characterization turned out to be different according to the GLC-MMA tandem and according to a SMT molecular topology procedure [23]. A first solution, suggested by a QSAR publication in olfaction in 2013 [12], was obtained in our 2020 publication by using normal boiling enthalpy as a global property in place of GLC retention indices, as well as the PSA1/GSS fraction to characterize a polarity independent of the polarizability. The latter approach has been refined in the present study with the PSA4/GSS fraction.

an important advance. The PSA4/GSS fraction that we propose remains to be verified and possibly improved, for example with an evaluation of the molecular surface more in line with a general reality than GSS, and less complicated than those proposed so far in the literature.

The third and final suggestion for possible improvement of this study concerns the polarizability descriptor that we have called ε_{2023}. As we saw in subsection 3.4 and as can be verified in Appendix A, this descriptor is characterized by negative values for fluorinated compounds as well as for squalane, the substance that caused us some difficulties mentioned in the Results section. The hypothesis that this singularity characterizes a highly branched molecular structure seems to be confirmed, but our present definition of ε_{2023} proves to be inadequate to account for partial branching. However, it is possible that a more general branching index established by molecular topology, such as the one proposed by Randic [32], would allow an improvement of the definition of ε_{2023}. Unfortunately, we did not succeed in applying this Randic index, which seemed to us rather complex. This is not the case for a similar topological index such as the one proposed by Zamora in 1976 under the name of SSSR (Smallest Set of Smallest Rings) [33] to characterize the connectivity of polycyclic substances. We have used it successfully on several occasions, but in the present study it was not necessary as the fn and Vw properties proved sufficient.

4.3 Estimates in the literature of the energies of the diverse intermolecular forces

Although they are not always an agreement among colleagues in this scientific discipline, figure 12 reflects quite well a certain consensus, namely that the Van der Waals forces are relatively clustered and distinct from the hydrogen bonding forces, and that among the former the London forces are the most important and the Debye forces the weakest. One may note that this last observation is reminiscent of the order of the F ratios in equations 12-15. Finally, the intramolecular covalent forces are really very far from all the intermolecular forces (up to 1100 kJ.mol^{-1}).

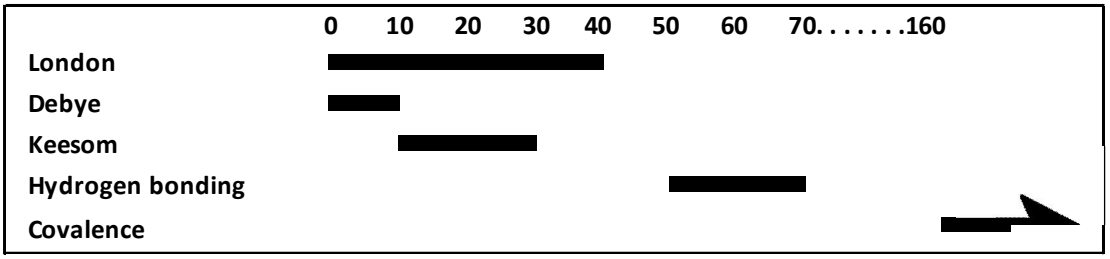

Fig. 12: Order of magnitude of the energies usually encountered, expressed in kJ.mol^{-1}, in the intermolecular forces of VOC compared to the intramolecular covalent forces.

4.4. Other alternatives for getting predicted values of enthalpies of vaporization at 25°C (H25)

Several equations for predicting the enthalpy of vaporization at a given temperature are proposed in the physicochemical literature. One of the simplest and most popular is the one proposed by Watson in 1943 [34], reproduced below in the particular case of 25°C :

$$H_{25pred} = H_{BP} * \left[\frac{1 - 298.2/Tc}{1 - T_{BP}/Tc} \right]^{0.38}$$

Where H_{BP} stands for the enthalpy at boiling point
T_{BP} stands for the boiling point expressed in kelvins
Tc stands for the critical temperature expressed in kelvins

Although relatively simplified, this equation has the disadvantage of depending on the critical temperature Tc, which is not well represented in the physicochemical property banks. As an example, out of the 616 substances studied in this study, we could obtain Tc values from the Handbook of Chemistry and Physics (1995) [28] for only 206 of them. The second drawback is that the exponent of 0.38 is totally empirical, valid in many cases, but must be modulated for some compounds (for the 206 compounds tested, methanol and ethanol). All this does not correspond to the objective we had set ourselves, namely to provide the reader with a simple and generalizable tool.

4.5. Can Van der Waals forces be relevant for odorant recognition by olfactory receptors?

This has been the hypothesis that has guided us for many years, but we have to recognize that it is very little shared. Before debating it and trying to demonstrate it, let us make a small but general incursion into the animal world on individual recognition, without which many observed behaviors could not occur. For example, the recognition of the leader of a deer herd won in a yearly fight, or a perennial couple life in whales. The principal sensory modality for this can be song coupled with hearing, as for example in whales for their pair life, but also in many species of diurnal birds for the duration of a nest. However, undoubtedly the most widespread individual recognition in the animal world is done via olfaction, vision remaining the prerogative of the human species and of some other Primates. Let us take the example of vision which is familiar to us. Without underestimating the richness of the visual information brought by color, stereoscopic vision and the appreciation of movement, individual recognition can be using only a two-dimensional black and white photography. In other words, using only three physical properties: X and Y coordinates and luminance. Only three physical properties, but a very large number of points (let us call them pixels) that differ from each other in their modulation of these three properties. This is only possible if these points are very numerous and if we have a powerful information processing system, which is indeed the case with the voluminous human visual cortex located in the occipital part of the brain. Why would it not be the same with olfaction, with, for example, the three Van der Waals forces? This does not exclude additional refinements such as, for example, those due to the individuals themselves using memory, and those due to additional molecular details such as optical isomerism.

In 1993 [35], a planar representation was published showing a fairly good superposition, on one hand of odorant clusters obtained experimentally using electrophysiological responses from frog olfactory mucosa by the group of André Holley in Lyon, and on the other hand of their X and Y coordinates equal to expressions of the molecular descriptors that we now call δ (dispersion) and ε (polarizability). A satisfactory characterization of the descriptor ω (orientation-polarity) has been long to obtain in order to complete this three-dimensional space, but it has been curiously suggested by a publication of QSAR in olfaction [12]. Let us note, however, that this publication [12] was not about olfactory quality (and thus about recognition of odorants by olfactory receptors), but about a relationship between threshold values and odorant intensities perceived at the supraliminal level.

V. CONCLUSION

We can presently state that the results presented above represent a clear improvement of those presented in 2020. Firstly by an improvement of the correlation between a global molecular property and the sum of four contributing molecular descriptors, from 0.95 to 0.99 in round numbers, and moreover based on a more numerous and more diversified sample of substances, for which the 2020 model proved to be insufficient and partially deficient (outside the window of r = 0.95).

One can certainly object that in 2020 the chosen global property, the enthalpy of vaporization at the boiling point in a pressure environment of 1 atmosphere, is a widely published and accessible physicochemical property, and that this is not the case for the enthalpy of vaporization at 25°C (H25) in a constant volume and variable pressure environment (the saturation vapor pressure). We therefore had to go through an intermediate step of predicting H25 via equation 11.

We can already add, however, that the four contributing molecular descriptors defined in equations 12, 13, 14 and 15 follow a long progressive improvement in gas-liquid chromatography (GLC) from 1976 to 2018, as well as on the basis of the boiling enthalpy of vaporization in 2020. The small changes to the 2020 version have already been specified in Section 3.4, after their actual definitions. The important difference of our approaches compared to those reported in the very interesting Poole review of 2002, is that the descriptors reflecting the Debye and Keesom forces can very well be separated according to us, contrary to what is claimed by many authors.

In spite of a possible improvement in the future, highlighted in 4.2, of the polarizability index ε_{2023}, the author of the present study, started in 2020, cannot help but feel enthusiastic about the results reported in subsections 3.3 and 3.4 and summarized in figures 8, 9 and 10, which are better than those initially expected. Perhaps, the future will tell, they close a long investigation in physical chemistry of our team, pursued since the 1970s. The optimum we thought possible regarding the characterization of molecular parameters reflecting the three Van der Waals forces for solutes in solutions using GLC was published in 2016, the approach using the normal boiling enthalpy of pure organic compounds developed in 2020 performed better, and finally the present study via the enthalpy of vaporization at 25°C together with the modified characterization of the polar surface area seems to result in a clear improvement. As for using it, readers now have here all the details for establish the corresponding values of δ_{2023}, ω_{2023} and ε_{2023} and try to apply them to olfaction or to other pharmacological properties. The author will also try to work in this direction.

ACKNOWLEDGEMENTS

The author reiterates its gratitude to ChemSpider for having inspired the new approach of the Van der Waals forces characterization described here. He also warmly thanks David Laffort for his strongly needed writing assistance and Régis Bolling for his strongly help in overcoming some computing difficulties.

This research did not receive any specific grant from funding agencies in the public, commercial, or not-for-profit sectors.

Summary of the Acronyms Applied in Equations

- **δ**, **ω** and **ε** stand for the molecular descriptors reflecting the Van der Waals forces (**δ** for dispersion, **ω** for orientation or polarity strictly speaking and **ε** as reminiscent of electronic for polarizability)
- **O1** stands for an oxygen atom in a hydroxyl group
- **N122** stands for a nitrogen in nitrates
- $\mathbf{S_{VAP}}$ stands for the boiling entropy due to the hydrogen bonding forces involved in pure organic compounds in condensed phases (2020 version).
- **HB** stands for the same meaning in the 2023 version
- $\mathbf{H_{BPCS}}$ stands for normal Boiling Enthalpy from ChemSpider [2]
- $\mathbf{V_w}$ stands for Van der Waals molecular volume according to Molinspiration [4]
- **GSS** stands for Global Spherical Surface
- $\mathbf{T_{BP}}$ stands for boiling point expressed in kelvins

- **PSA** stands for Polar Surface Area
- **SMT** stands for Simplified Molecular Topology
- **SSSR** stands for Smallest Set of Smallest Rings according to [33]
- **MLRA** stands for Multiple Linear Regression Analysis
- **IR** stands for the index of refraction at 25°C according to ChemSpider [2]
- **fn** stands for a function of the index of refraction at 25°C
- **r** stands for correlation coefficient
- **F** stands for the F ratio statistical test
- **N** in statistical results stands for the number of observations
- **VOC** stands for volatile organic compound
- **QSAR** stands for Quantitative Structure-Activity Relationship
- **QSPR** stands for Quantitative Structure-Property Relationship

REFERENCES

1. Laffort P. (2020) Interest of Splitting the Enthalpies of Vaporization in Four Distinct Parts Reflecting the Van der Waals and the Hydrogen Bonding Forces, *Open Journal of Physical Chemistry,* 10, 117-137.https://doi.org/10.4236/ojpc.2020.102007.
2. ChemSpider, Search and Share Chemistry. http://www.chemspider.com/Search.aspx.
3. Abdi H. (2007) Multiple correlation coefficient, In: N. J. Salkind, Ed, Encyclopedia of Measurement and Statistics, Sage, Thousand Oaks (CA), USA, pp. 648-651 http://dx.doi.org/ 10.4135/ 9781412952644.n91
4. Laffort P. (1994). Relationships between molecular structure and olfactory activity, in G. Martin and P. Laffort eds., *Odors and deodorization in the environment*, VCH publ., New York, 143-183 (translated in English and updated from French, 1991, Tec-Doc Lavoisier, Paris, 131-168)
5. Hansch C. (1969) Quantitative approach to biochemical structure-activity relationships, *Accounts of Chemical Research,* 2, 8, 232–239 https://doi.org/10.1021/ar50020a002
6. Dravnieks A, Laffort P. (1972), Physicochemical basis of quantitative and qualitative odor discrimination in Humans. In D. Schneider ed., Olfaction and Taste IV, Wissens-Verlag-MBH, Stuttgart, Germany, 142-148
7. Karger BL, Snyder LR, Eon C. (1976), An expanded solubility parameter treatment for classification and use of chromatographic solvents and adsorbents: Parameters for dispersion, dipole and hydrogen bonding interactions, *Journal of Chromatography A*, 125, 71-88 https://doi.org/10.1016/ S0021-9673(00)93812-3
8. Karger BL, Snyder LR, Eon C. (1978), Expanded solubility parameter treatment for classification and use of chromatographic solvents and adsorbents, *Analytical Chemistry*, 50, 2126-2136 https://doi.org/ 10.1021/ac50036a044
9. Molinspiration (2020) Calculation of Molecular Properties and Bioactivity Score http://www.molinspiration.com/cgi-bin/properties
10. Laffort P. (2018) Updated Definition of the Three Solvent Descriptors Related to the Van der Waals Forces in Solutions. *Open Journal of Physical Chemistry, 8, 1-14* https://doi.org/10.4236/ojpc.2018.81001
11. Ertl P, Rohde B, Selzer P (2000) Fast calculation of molecular polar surface area as a sum of fragment-based contributions and its application to the prediction of drug transport properties, *Journal of Medicinal Chemistry*, 43, 3714-3717 http://dx.doi.org/10.1021/jm000942e
12. Laffort, P. (2013) A Slightly Modified Expression of the Polar Surface Area Applied to an Olfactory Study. *Open Journal of Physical Chemistry* , 3, 150-156. https://doi.org/ 10.4236/ojpc.2013.34018

13. Lewis, GN (1916) The atom and the molecule, *Journal of the American Chemical Society*, 38, 762-785 https://doi.org/10.1021/ja02261a002
14. [Goss KU, Schwarzenbach RP. (1999) Empirical Prediction of Heats of Vaporization and Heats of Adsorption of Organic Compounds, *Environmental Science and Technology*, 33 (19), 3390-3393 https://pubs.acs.org/doi/abs/10.1021/es980812j
15. [CRC Handbook of Chemistry and Physics (1969) 50th Edition, RC Weast (Ed), The Chemical Rubber Company (Publisher), Cleveland, Ohio, USA
16. Linguee Dictionary (2021) https://www.linguee.fr/francais-anglais
17. DeepL (2023) https://www.deepl.com/translator (free version)
18. Laffort, P. Chauvin, F., Dallos, A., Callegari, P. and Valentin, D. (2005) Solvation Parameters. Part 1: Mutual Improvements of Several Approaches and Determination of Two First Sets of Optimized Values. *Journal of Chromatography A*, 1100, 90-107 https://doi.org/10.1016/j.chroma.2005.09.022
19. Clapeyron E (1834) Memoir on the Motive Power of Heat (*in French*). *Journal de l'École Polytechnique (Paris),* 23 (14), 153-191 .
20. Clausius R. (1850) About the Moving Power of Heat, and the Laws which can be Derived for Thermodynamics Itself (*in German*). *Annalen der Physik*, 155, 500-524. https://doi.org/10.1002/andp.18501550403
21. [21] Laffort P, Patte F (1976) Solubility factors in gas-liquid chromatography: Comparison between two approaches and application to some biological studies. *Journal of Chromatography A*, 126, 625-639 https://doi.org/10.1016/S0021-9673(01)84107-8
22. Chauvin F. (1998) Improvement of the definition and determination of solubility parameters. Application to olfaction (*in French*). Thesis of the Bourgogne University, 149 pp
23. Laffort P. (2016) A revisited definition of the Three Solute Descriptors Related to the Van der Waals Forces in Solutions. *Open Journal of Physical Chemistry*, 6, 86-100 https://doi.org/10.4236/ ojpc.2016.64009
24. Tijssen R, Billiet HAH, Schoenmakers PJ. (1976) Use of the solubility parameter for predicting selectivity and retention in chromatography, *Journal of Chromatography A*, 122, 185-203 https://doi.org/10.1016/S0021-9673(00)82244-X
25. Abraham MH. (1993) Scales of solute hydrogen-bonding: Their construction and application to physicochemical and biochemical processes, *Chemical Society Reviews*, 22, 73-83 https://doi.org/10.1039/cs9932200073
26. Zissimos AM, *Abraham MH, Klamt A, Eckert F, Wood J. (2002) A comparison between the two general sets of linear energy descriptors of Abraham and Klamt, Journal of Chemical Information and Computer Sciences, 42, 1320-1331 http://dx.doi.org/10.1021/ci0255300*
27. Daubert TE, Danner RP. (1997) Physical and thermodynamic properties of pure chemicals: data compilation, Washington, DC : Taylor & Francis, ©1989-
28. CRC Handbook of Chemistry and Physics (1995) 76th Edition, CRC Press: Boca Raton, FL, USA
29. Palm K, Luthman K, Ungell AL, Strandlund G, Artursson P. (1996) Correlation of drug absorption with molecule surface properties, *Journal of Pharmaceutical Sciences*, 85, 32-39 http://dx.doi.org/10.1021/js950285r
30. Palm K, Stenberg P, Luthman K, Artursson P. (1997) Polar molecular surface properties predict the intestinal absorption of drugs in humans, *Pharmaceutical Research,* 14, 568-571 http://dx.doi.org/10.1023/A:1012188625088
31. Poole CF, Atapattu SN, Poole SK, Bell AK. (2009) Determination of solute descriptors by chromatographic methods, *Analytica Chimica Acta*, 652, 32-53 http://dx DOI: 10.1016/j.aca.2009.04.038
32. Randic M., (1975) Characterization of molecular branching, *Journal of the American Chemical Society*, 97, 23, 6609-6615 https://doi.org/10.1021/ja00856a001.

33. Zamora A. (1976) An Algorithm for Finding the Smallest Set of Smallest Rings, *Journal of Chemical Information and Computer Sciences*, 16, 40-43. https://doi.org/10.1021/ci60005a013
34. Watson KM. (1943) Thermodynamics of the Liquid State, *Industrial Engineering Chemistry*, 35, 4, 398-406 https://doi.org/10.1021/ie50400a004
35. Laffort P. (1993) Graphical structuring of olfactory quality based on molecular parameters applied to experimental data from the André Holley group (partially bilingual French-English), *Comptes Rendus de l'Académie des Sciences Paris*, 316 (series III), 105-111
36. Devos M., Patte F., Rouault J., Laffort P., Van Gemert L.J. (1990)xvvcgf. Standardized human olfactory thresholds in air, IRL Press, Oxford, 165 pp
37. Devos M., Rouault J., Laffort P., 2002. Standardized olfactory power law exponents in Man, Editions Universitaires de Dijon, 4 boulevard Gabriel,.21000 Dijon, France, 128 pp

APPENDIX A: SUPPLEMENTARY INFORMATION

An abridged version of the dataset for the 616 VOCs used in the present study is reproduced hereafter. This database is limited to organic compounds including C, H, O, N, S, P, F, Cl, Br, I. Therefore, compounds including Se, Pb or Si, for example, are excluded.

Some column headings explanations:

- A stand for data used in figure 3 for 180 VOCs in liquid, solid and gaseous phases at room temperature and involved in olfactory studies [1, 36, 37]
- B stand for data from Goss KU and Schwarzenbach RP [9] for 200VOCs in liquid, solid and gaseous phases at room temperature
- C stand for data from 445 VOCs in liquid phase at room temperature applied in our 2020 study on boiling enthalpy [1]
- 616N stand for the global ranking of the 616 VOCs applied in the present study and resulting of the union of A + B + C
- ID_{ChSpd} stand for the identification number of ChemSpider[2]
- d_{2023}, e_{2023}, $w_{2023}$and HB_{2023}stand respectively for the molecular descriptors reflecting the intermolecular forces, expressed in kJ/mol,of London, Debye, Keesom and of hydrogen bonding, according to equations 12, 13, 14 and 15 of the present study.
- $H25_{pred\ 2023}$ stand for predicted enthalpy of vaporization at 25°C,expressed in kJ/mol, as the sum of the four molecular descriptors d_{2023}, e_{2023}, HB_{2023}+ the constant 7.949

A	B	C	616N	Compounds	ID_{ChSpd}	$H25_{pred\ 2023}$	δ_{2023}	ε_{2023}	ω_{2023}	HB_{2023}
		C001	1	Methanol	864	36.748	6.726	0.678	11.958	9.437
A063	B190	C002	2	Ethanol	682	38.327	10.983	0.631	9.327	9.437
		C003	3	1,2-Ethanediol	13835235	59.788	14.800	1.198	16.967	18.874
A154	B191	C004	4	1-Propanol	1004	41.136	15.343	0.621	7.786	9.437
A155		C005	5	2-Propanol (isopropylalcohol)	3644	40.916	15.152	0.576	7.802	9.437
A017	B192	C006	6	1-Butanol	258	44.440	19.691	0.607	6.756	9.437
A018		C007	7	2-Butanol (sec.butylalcohol)	6320	44.228	19.510	0.565	6.767	9.437
A136	B193	C008	8	1-Pentanol	6040	48.032	24.041	0.594	6.010	9.437
		C009	9	2-Pentanol	21011	47.854	23.889	0.560	6.018	9.437
		C010	10	2-Methyl-2-butanol	6165	47.890	23.862	0.602	6.040	9.437
		C011	11	3-Methyl-2-butanol	11239	47.675	23.735	0.527	6.027	9.437
A079	B194	C012	12	1-Hexanol	7812	51.880	28.452	0.601	5.441	9.437

		C013	13	2-Hexanol	11794	51.678	28.282	0.562	5.448	9.437
		C014	14	2-Methyl-1-pentanol	7459	51.680	28.285	0.562	5.447	9.437
		C015	15	2-Methyl-2-pentanol	11056	51.647	28.209	0.588	5.465	9.437
		C016	16	4-Methyl-2-pentanol	7622	51.474	28.111	0.523	5.454	9.437
A075		C017	17	1-Heptanol	7837	55.771	32.806	0.588	4.990	9.437
		C018	18	2-Heptanol	10511	55.634	32.686	0.567	4.995	9.437
		C019	19	3-Heptanol	11036	55.634	32.686	0.567	4.995	9.437
		C020	20	2-Methyl-2-hexanol	11739	55.610	32.621	0.594	5.009	9.437
A125	B195	C021	21	1-Octanol	932	59.874	37.257	0.609	4.622	9.437
		C022	22	1-Nonanol	8574	63.943	41.636	0.605	4.315	9.437
		C023	23	2-Nonanol	11861	64.232	41.834	0.693	4.319	9.437
		C024	24	1-Decanol	7882	68.022	45.988	0.593	4.055	9.437
		C025	25	1-Undecanol	7892	72.202	50.389	0.596	3.831	9.437
A039		C026	26	Cyclopentanol	7026	51.033	25.246	1.947	6.454	9.437
A035	B150	C027	27	Cyclohexanol	7678	54.294	29.295	1.831	5.783	9.437
		C028	28	Cycloheptanol	9970	57.674	33.319	1.706	5.263	9.437
A159		C029	29	2-Propen-1-ol (allylalcohol)	13872989	41.414	14.846	0.954	8.228	9.437
		C030	30	trans-2-Buten-1-ol	13871721	45.362	19.714	1.167	7.094	9.437
		C031	31	2-Propyn-1-ol (Propargylalcohol)	21106466	41.836	14.427	1.299	8.724	9.437
	B160	C032	32	m-Cresol	21105871	58.402	32.169	2.993	5.854	9.437
		C033	33	Benzylalcohol(α-Hydroxytoluene)	13860335	58.468	32.240	2.996	5.846	9.437
A146		C034	34	2-Phenylethanol (phenethylalcohol)	5830	62.351	36.651	3.002	5.312	9.437
A059	B128	C035	35	Acetaldehyde	172	25.665	8.812	0.411	8.493	0.000
	B129	C036	36	Propionaldehyde	512	28.262	13.010	0.346	6.958	0.000
A012	B130	C037	37	Butyraldehyde	256	31.531	17.301	0.312	5.969	0.000
		C038	38	Isobutyraldehyde	6313	31.332	17.131	0.273	5.979	0.000
A132	B131	C039	39	Pentanal	7772	35.110	21.607	0.284	5.270	0.000
A077	B132	C040	40	Hexanal	5949	38.886	25.932	0.261	4.745	0.000
		C041	41	2-Ethylbutanal	7081	38.690	25.767	0.224	4.751	0.000
A073		C042	42	Heptanal	7838	42.840	30.303	0.255	4.334	0.000
A123	B133	C043	43	Octanal	441	46.872	34.674	0.248	4.001	0.000
A120	B134	C044	44	Nonanal	29029	51.005	39.077	0.253	3.726	0.000
A157		C045	45	2-Propenal (acrolein)	7559	28.507	12.495	0.672	7.391	0.000
A020		C046	46	trans-2-Butenal (Crotonaldehyde)	394562	32.291	17.217	0.835	6.290	0.000
		C047	47	2-Methylpropenal	6314	31.470	16.638	0.609	6.273	0.000
A081		C048	48	trans-2-Hexenal (leafaldehyde)	4444608	39.646	25.954	0.820	4.922	0.000
		C049	49	2-Ethyl-2-Hexenal	4510484	47.351	34.514	0.767	4.121	0.000
A004	B135	C050	50	Benzaldehyde	235	47.802	31.480	3.256	5.117	0.000
A071		C051	51	2-Furaldehyde (Furfural)	13863629	44.434	23.858	2.299	10.328	0.000
		C052	52	2-Hydroxybenzaldehyde (Salicylaldehyde)	13863618	68.629	36.390	4.217	10.636	9.437
		C053	53	Paraldehyde	21106173	43.291	28.320	-0.130	7.151	0.000
A156	B112	C054	54	Propanone	175	28.101	12.861	0.316	6.975	0.000
A019	B113	C055	55	2-Butanone	6321	31.328	17.125	0.273	5.981	0.000
	B114	C056	56	2-Pentanone	7607	34.936	21.455	0.253	5.278	0.000

		C057	57	3-Methyl-2-Butanone	10777	34.767	21.310	0.222	5.286	0.000
A137		C058	58	3-Pentanone (diethylketone)	7016	34.936	21.455	0.253	5.278	0.000
A080	B115	C059	59	2-Hexanone	11095	38.764	25.820	0.244	4.751	0.000
A106		C060	60	4-Methyl-2-Pentanone	7621	38.569	25.655	0.207	4.757	0.000
		C061	61	3-Hexanone	11025	38.764	25.820	0.244	4.751	0.000
	B116	C062	62	2-Heptanone	7760	42.705	30.182	0.235	4.339	0.000
		C063	63	3-Heptanone	7514	42.705	30.182	0.235	4.339	0.000
		C064	64	2,4-Dimethyl-3-Pentanone	10797	42.268	29.821	0.150	4.348	0.000
A126		C065	65	2-Octanone	7802	46.724	34.544	0.225	4.006	0.000
		C066	66	3-Octanone	215929	46.724	34.544	0.225	4.006	0.000
		C067	67	5-Methyl-3-Heptanone	7534	46.481	34.345	0.177	4.010	0.000
	B117	C068	68	2-Nonanone	12632	50.834	38.927	0.227	3.731	0.000
		C069	69	5-Nonanone	9976	50.844	38.938	0.227	3.730	0.000
		C070	70	2,6-Dimethyl-4-Heptanone	7670	50.424	38.592	0.147	3.736	0.000
		C071	71	2-Decanone	12218	54.897	43.250	0.200	3.497	0.000
		C072	72	2-Undecanone	7871	59.073	47.630	0.196	3.298	0.000
		C073	73	2-Dodecanone	21153	63.360	52.072	0.214	3.124	0.000
A040		C074	74	Cyclopentanone	8141	37.548	22.411	1.503	5.685	0.000
A036		C075	75	Cyclohexanone	7679	40.896	26.491	1.397	5.060	0.000
		C076	76	Cycloheptanone	9971	44.381	30.562	1.288	4.582	0.000
		C077	77	2-Methylcyclohexanone	10939	43.700	30.036	1.128	4.588	0.000
		C078	78	3-Butene-2-one	6322	31.470	16.638	0.609	6.273	0.000
A002		C079	79	Acetophenone	7132	48.636	33.564	2.491	4.633	0.000
		C080	80	Phenylethylketone	6881	52.651	37.963	2.494	4.244	0.000
		C081	81	Isophorone (3,5,5-Trimethyl-2-cyclohexene-1-one)	6296	50.841	37.552	1.320	4.020	0.000
A064	B097	C082	82	Diethylether	3168	29.357	18.281	0.062	3.066	0.000
		C083	83	1-Methoxypropane	10709	29.357	18.281	0.062	3.066	0.000
	B105	C084	84	2-Methoxypropane (Isopropylmethtylether)	11228	29.200	18.146	0.034	3.071	0.000
		C085	85	1-Methoxybutane	11833	33.271	22.567	0.025	2.730	0.000
		C086	86	Methyl isobutyl ether (1-Methoxy-2-methylpropane)	11749	33.087	22.413	-0.008	2.733	0.000
	B102	C087	87	Methyltert-butylether	14672	33.058	22.346	0.020	2.743	0.000
	B100	C088	88	Dipropylether	7823	37.347	26.915	0.011	2.473	0.000
	B101	C089	89	Di-isopropylether	7626	36.935	26.574	-0.067	2.479	0.000
A024	B103	C090	90	Dibutylether	8569	45.605	35.581	-0.027	2.102	0.000
	B106	C091	91	Divinylether	7733	29.263	17.245	0.712	3.357	0.000
		C092	92	Vinylbutylether	7817	37.282	26.433	0.349	2.552	0.000
		C093	93	Dimethoxymethane	13837190	30.619	16.123	0.022	6.525	0.000
	B173	C094	94	Furan	7738	30.253	15.755	1.227	5.322	0.000
		C095	95	2-Methylfuran	10340	34.123	20.295	1.299	4.580	0.000
	B163	C096	96	Tetrahydrofuran	7737	30.628	18.341	1.006	3.331	0.000
		C097	97	2-Methyltetrahydrofuran	7028	33.603	21.962	0.762	2.929	0.000
		C098	98	Tetrahydropyran	8554	34.214	22.436	0.904	2.925	0.000

A182		C099	99	1,8-Cineole (Eucalyptol)	2656	54.166	42.773	1.437	2.008	0.000
	B090	C100	100	Anisole (Methoxybenzene)	7238	42.418	29.737	2.077	2.655	0.000
	B089	C101	101	Benzofuran (Coumarone)	8868	50.693	35.069	3.895	3.780	0.000
	B108	C102	102	Ethylphenylether	7391	46.634	34.177	2.094	2.414	0.000
		C103	103	β-Propiolactone	2275	36.057	15.775	1.433	10.901	0.000
		C104	104	1,3-Dioxolane	12066	31.743	15.805	0.837	7.153	0.000
A056	B164	C105	105	1,4-Dioxane	29015	34.776	19.894	0.734	6.199	0.000
		C106	106	2-Methoxyethanol	7728	45.956	17.531	0.567	10.471	9.437
		C107	107	2-Propoxyethanol	16778	52.507	26.281	0.556	8.284	9.437
		C108	108	3-Methoxyphenol	8657	62.618	34.247	2.900	8.085	9.437
		C109	109	2-Phenoxyethanol	13848467	66.316	38.656	2.886	7.388	9.437
A003		C110	110	Eugenol (4-Allyl-2-methoxy phenol)	13876103	74.580	47.287	3.380	6.527	9.437
	B138	C111	111	Nitromethane	6135	35.472	10.789	0.698	16.036	0.000
	B139	C112	112	Nitroethane	6338	37.082	15.126	0.680	13.327	0.000
A117		C113	113	1-Nitropropane	7615	39.637	19.486	0.670	11.532	0.000
		C114	114	2-Nitropropane	387	39.438	19.309	0.628	11.551	0.000
		C115	115	1-Nitrobutane	11799	42.705	23.854	0.662	10.240	0.000
		C116	116	1-Nitropentane	191367	46.085	28.223	0.655	9.258	0.000
		C117	117	1-Nitrohexane	12069	49.755	32.654	0.669	8.482	0.000
		C118	118	Nitrocyclohexane	13647	51.052	32.569	1.583	8.951	0.000
A116	B137	C119	119	Nitrobenzene	7138	53.652	32.523	3.224	9.956	0.000
		C120	120	2-Nitrotoluene	21106144	57.401	37.096	3.308	9.048	0.000
	B141	C121	121	3-Nitrotoluene	21106146	57.401	37.096	3.308	9.048	0.000
A061	B118	C122	122	Cyanomethane (Acetonitrile)	6102	29.560	8.811	0.601	12.199	0.000
		C123	123	Cyanoethane (Proprionitrile)	7566	31.448	13.040	0.545	9.914	0.000
	B162	C124	124	1-Cyanopropane (Butyronitrile)	7717	34.322	17.380	0.528	8.466	0.000
		C125	125	1-Cyanobutane (Valeronitrile)	7770	37.640	21.726	0.513	7.452	0.000
		C126	126	1-Cyanopentane (Hexanenitrile)	11846	41.221	26.077	0.500	6.695	0.000
		C127	127	1.Cyanohexane (Heptanenitrile)	11866	45.015	30.462	0.499	6.106	0.000
		C128	128	1-Cyanoheptane (Caprylonitrile)	29026	48.907	34.835	0.492	5.630	0.000
		C129	129	1-Cyanooctane (Nonanenitrile)	15846	52.902	39.223	0.492	5.238	0.000
		C130	130	1-Cyanononane (Decanenitrile)	67360	57.036	43.700	0.486	4.901	0.000
		C131	131	Acrylonitrile (Vinyl cyanide)	7567	31.924	12.544	0.878	10.554	0.000
	B136	C132	132	Phenyl cyanide (Benzonitrile)	7224	47.536	29.564	2.792	7.231	0.000
	B169	C133	133	n-Propylamine	7564	44.330	16.501	0.725	9.718	9.437
		C134	134	iso-Propylamine	6123	44.153	16.341	0.690	9.737	9.437
A026		C135	135	n-Butylamine	7716	47.468	20.881	0.722	8.480	9.437
	B171	C136	136	n-Pentylamine	7769	50.887	25.223	0.705	7.573	9.437
	B170	C137	137	n-Hexylamine	7811	54.547	29.588	0.697	6.876	9.437
		C138	138	n-Octylamine	7851	62.294	38.354	0.692	5.863	9.437
A046		C139	139	Diethylamine	7730	32.426	20.177	0.404	3.896	0.000
		C140	140	Di-n-propylamine	8562	40.182	28.740	0.329	3.164	0.000
A044	B168	C141	141	Di-n-butylamine	7856	48.431	37.469	0.312	2.701	0.000

		C142	142	Di-n-pentylamine	15482	56.880	46.243	0.311	2.377	0.000
A177		C143	143	Triethylamine	8158	38.487	29.209	0.477	0.852	0.000
		C144	144	Pyrrolidine (Tetrahydropyrrole)	29008	32.882	19.587	1.126	4.220	0.000
		C145	145	Piperidine (Hexahydropyridine)	7791	36.375	23.678	1.024	3.723	0.000
		C146	146	N-Methylpiperidine	11788	38.805	28.720	1.234	0.902	0.000
		C147	147	N-Ethylpiperidine	12466	42.763	32.846	1.144	0.824	0.000
		C148	148	Pyrrole	7736	36.129	19.723	2.276	6.182	0.000
		C149	149	N-Methylpyrrole	7031	34.506	23.004	1.885	1.667	0.000
A168	B143	C150	150	Pyridine	1020	36.630	22.014	2.089	4.578	0.000
	B146	C151	151	2-Methylpyridine (2-Picoline)	13839199	40.734	26.577	2.170	4.038	0.000
	B147	C152	152	3-Methylpyridine (3-Picoline)	21106520	40.734	26.577	2.170	4.038	0.000
		C153	153	4-Methylpyridine (4-Picoline)	13874733	40.734	26.577	2.170	4.038	0.000
	B144	C154	154	Aniline	5889	58.544	29.631	3.312	8.214	9.437
		C155	155	N-Methylaniline (Methylphenylamine)	7234	49.677	34.828	3.509	3.391	0.000
		C156	156	2,3-Dimethylpyridine (2,3-Lutidine)	10940	45.043	31.193	2.268	3.633	0.000
		C157	157	2,4-Dimethylpyridine (2,4-Lutidine)	21132380	45.043	31.193	2.268	3.633	0.000
		C158	158	2,5-Dimethylpyridine (2,5-Lutidine)	11042	45.043	31.193	2.268	3.633	0.000
	B148	C159	159	2,6-Dimethylpyridine (2,6-Lutidine)	13842613	45.043	31.193	2.268	3.633	0.000
		C160	160	3,4-Dimethylpyridine (3,4-Lutidine)	10937	45.043	31.193	2.268	3.633	0.000
		C161	161	3,5-Dimethylpyridine (3,5-Lutidine)	11077	45.043	31.193	2.268	3.633	0.000
		C162	162	3-Vinylpyridine	13634	47.654	32.691	3.260	3.753	0.000
		C163	163	Benzylamine (α-Aminotoluene)	7223	61.069	33.259	3.052	7.372	9.437
	B176	C164	164	Quinoline	6780	58.150	41.848	4.936	3.417	0.000
		C165	165	1,2-Ethanediamine	13835550	46.954	17.165	1.421	20.419	0.000
		C166	166	Pyridazine	8902	40.469	20.938	2.093	9.488	0.000
		C167	167	Pyrimidine	8903	40.469	20.938	2.093	9.488	0.000
		C168	168	2-Methylpyrazine	7688	43.961	25.517	2.179	8.316	0.000
		C169	169	Nicotine	80863	63.492	48.527	3.493	3.524	0.000
		C170	170	3-Chloropyridine	11784	41.645	26.990	2.581	4.125	0.000
		C171	171	Formamide	693	50.597	9.078	0.972	23.161	9.437
		C172	172	N-Methylformamide	28994	33.616	12.629	0.608	12.429	0.000
		C173	173	N,N-Dimethylformamide	5993	33.463	17.421	0.733	7.360	0.000
		C174	174	N.N-Dimethylacetamide	29107	36.782	21.661	0.703	6.469	0.000
		C175	175	1,1,3,3-Tetraethylurea	13811	62.221	48.378	1.211	4.684	0.000
		C176	176	N-Methyl urethane (Ethyl methylcarbamate)	7466	43.341	23.390	0.504	11.498	0.000
		C177	177	Morpholine	13837537	36.939	21.171	0.865	6.954	0.000
		C178	178	N-Methylmorpholine	7684	38.851	26.195	1.069	3.638	0.000
A153		C179	179	Propanoicacid (propionicacid)	1005	48.699	16.442	0.802	14.069	9.437
A016	B196	C180	180	Butanoicacid	259	51.304	20.854	0.810	12.254	9.437
A135		C181	181	Pentanoicacid	7701	54.423	25.284	0.823	10.930	9.437
		C182	182	2-Methylbutanoic acid	8012	54.178	25.076	0.771	10.945	9.437

A099		C183	183	3-Methylbutanoic acid (isovalericacid)	10001	54.178	25.076	0.771	10.945	9.437
A078		C184	184	Hexanoicacid (caproicacid)	8552	57.824	29.694	0.830	9.914	9.437
		C185	185	2-Ethylbutanoic acid	6649	57.543	29.461	0.770	9.925	9.437
		C186	186	Heptanoicacid	7803	61.403	34.082	0.829	9.105	9.437
		C187	187	Octanoicacid	370	65.132	38.473	0.830	8.443	9.437
		C188	188	Nonanoicacid	7866	69.057	42.929	0.852	7.890	9.437
	B109	C189	189	Methyl formate	7577	30.777	10.847	0.305	11.677	0.000
	B110	C190	190	Ethyl formate	7734	33.161	15.116	0.263	9.833	0.000
	B111	C191	191	n-Propyl formate	7782	36.201	19.434	0.239	8.579	0.000
		C192	192	n-Butyl formate	11125	39.634	23.795	0.229	7.660	0.000
		C193	193	iso-Butyl formate	10492	39.454	23.640	0.195	7.670	0.000
		C194	194	n-Pentyl formate	12012	43.253	28.137	0.213	6.954	0.000
		C195	195	Methylacetate	6335	33.035	14.989	0.242	9.855	0.000
A065	B119	C196	196	Ethylacetate	8525	36.044	19.291	0.211	8.594	0.000
	B120	C197	197	n-Propylacetate	7706	39.450	23.634	0.195	7.672	0.000
A025	B121	C198	198	n-Butylacetate	29012	43.127	28.021	0.194	6.963	0.000
		C199	199	sec-butylacetate	7472	42.923	27.849	0.154	6.971	0.000
		C200	200	tert-Butylacetate	10446	42.907	27.783	0.183	6.992	0.000
		C201	201	Methyltrimethylacetate (Methylpivalate)	62249	42.907	27.783	0.183	6.992	0.000
A138	B122	C202	202	n-Pentylacetate	11843	46.907	32.377	0.183	6.398	0.000
A082	B123	C203	203	Hexylacetate	8568	50.860	36.786	0.190	5.935	0.000
		C204	204	1,3-Dimethylbutyl acetate	7671	50.460	36.451	0.114	5.946	0.000
		C205	205	n-Heptylacetate	7867	54.812	41.139	0.176	5.548	0.000
		C206	206	n-Octylacetate	7872	58.929	45.571	0.191	5.218	0.000
		C207	207	Vinylacetate	7616	36.294	18.821	0.554	8.970	0.000
		C208	208	Allylacetate	13862665	39.599	23.161	0.536	7.952	0.000
		C209	209	Phenylacetate	28969	52.746	35.607	2.388	6.802	0.000
		C210	210	Butyl propionate	11045	46.907	32.377	0.183	6.398	0.000
		C211	211	Methylhexanoate	7536	46.907	32.377	0.183	6.398	0.000
		C212	212	Methyloctanoate	7800	54.812	41.139	0.176	5.548	0.000
A007		C213	213	Methyl benzoate	6883	53.146	35.906	2.489	6.802	0.000
		C214	214	Ethyl benzoate	6897	57.044	40.328	2.500	6.267	0.000
		C215	215	n-Propyl benzoate	15965	61.056	44.765	2.516	5.826	0.000
		C216	216	n-Butyl benzoate	8374	65.071	49.152	2.515	5.456	0.000
		C217	217	Dimethylphthalate	13837329	70.963	48.901	2.954	11.159	0.000
	B091	C218	218	Diethylphthalate	13837303	78.431	57.632	2.936	9.914	0.000
		C219	219	Dipropylphthalate	8241	86.305	66.442	2.947	8.967	0.000
		C220	220	Methylmethacrylate	6406	39.423	23.005	0.504	7.965	0.000
		C221	221	Isobutylmethacrylate	7074	50.464	35.969	0.453	6.093	0.000
		C222	222	Dimethyl carbonate	11526	37.564	17.116	0.166	12.334	0.000
		C223	223	Diethyl carbonate	7478	43.771	25.846	0.149	9.827	0.000
		C224	224	Propylene carbonate (4-Methyl-1,3-dioxolan-2-one)	7636	41.469	20.875	0.894	11.751	0.000

		C225	225	Ethylacetoacetate	13865426	48.829	29.144	0.383	11.352	0.000
		C226	226	Dimethyl succinate	13848341	52.879	31.421	0.359	13.151	0.000
		C227	227	Diethyl succinate	13865630	59.887	40.227	0.368	11.343	0.000
		C228	228	Trimethyl phosphate	10101	45.546	25.423	-0.112	12.286	0.000
		C229	229	Triethyl phosphate	6287	56.128	38.601	-0.109	9.687	0.000
		C230	230	1-Fluorohexane	9377	33.866	24.932	-0.326	1.311	0.000
		C231	231	1-Fluorooctane	9633	42.249	33.566	-0.375	1.109	0.000
		C232	232	1,1,1-Trifluorooctane	458989	43.675	33.710	-1.179	3.195	0.000
	B079	C233	233	Fluorobenzene	9614	34.610	23.344	1.733	1.583	0.000
		C234	234	Hexafluorobenzene	13836549	40.141	24.271	-0.149	8.071	0.000
		C235	235	α,α,α-Trifluorotoluene	7090	40.129	27.414	0.771	3.995	0.000
		C236	236	2,2,2-Trifluoroethanol	21106169	41.771	11.357	-0.554	13.583	9.437
		C237	237	Hexafluoro-2-propanol	12941	46.354	15.825	-1.823	14.967	9.437
		C238	238	2-Fluorophenol	9326	55.415	27.712	2.509	7.808	9.437
		C239	239	3-Fluorophenol	9360	55.415	27.712	2.509	7.808	9.437
		C240	240	Methoxyflurane (Ethane,2,2-dichloro-1,1-difluoro-1-methoxy-)	3973	42.198	23.661	0.104	10.484	0.000
		C241	241	Isoflurane (Ethane, 2-chloro-2-(difluoromethoxy)-1,1,1-trifluoro-)	3631	37.736	19.292	-1.522	12.017	0.000
		C242	242	Fluoroxene (2,2,2-Trifluoroethoxyethane)	9461	32.760	18.235	-0.766	7.342	0.000
		C243	243	Enflurane(Ethane,2chloro-1-(difluoromehoxy)-1,1,2-trifluoro-)	3113	37.736	19.292	-1.522	12.017	0.000
		C244	244	Halothane (2-Bromo-2-chloro-1,1,1-trifluoroethane)	3441	42.594	20.391	0.439	13.815	0.000
		C245	245	1-Chloropropane	10437	28.309	16.614	0.564	3.182	0.000
		C246	246	2-Chloropropane	6121	28.116	16.453	0.527	3.187	0.000
		C247	247	1-Chlorobutane	7714	32.205	20.932	0.538	2.786	0.000
		C248	248	1-Chloropentane	10512	36.218	25.258	0.517	2.495	0.000
		C249	249	1-Chlorohexane	10526	40.347	29.622	0.508	2.269	0.000
		C250	250	Chlorocyclohexane	10487	40.935	29.256	1.326	2.405	0.000
		C251	251	1-Chloroheptane	11865	44.507	33.974	0.495	2.088	0.000
		C252	252	1-Chlorooctane	7850	48.724	38.346	0.489	1.940	0.000
		C253	253	3-Chloro-1-propyne	21112738	28.203	15.536	1.186	3.533	0.000
	B051	C254	254	Dichloromethane	6104	29.495	12.756	1.015	7.775	0.000
A176	B052	C255	255	Trichloromethane	5977	36.901	17.442	1.405	10.105	0.000
A170	B053	C256	256	Tetrachloromethane	5730	44.279	22.402	1.919	12.008	0.000
	B056	C257	257	1,1-Dichloroethane	6125	32.399	16.937	0.963	6.550	0.000
A045	B055	C258	258	1,2-Dichloroethane	13837650	32.581	17.098	0.998	6.537	0.000
	B062	C259	259	1,1,1-Trichloroethane	6042	39.957	21.778	1.436	8.794	0.000
	B057	C260	260	1,1,2-Trichloroethane	6326	39.946	21.835	1.406	8.756	0.000
	B059	C261	261	Pentachloroethane	6179	54.284	31.736	2.398	12.201	0.000
		C262	262	1,1-Dichloroethene	13835316	32.534	16.393	1.281	6.911	0.000
		C263	263	cis-1,2-Dichloroethene	558928	33.355	16.968	1.506	6.933	0.000

		C264	264	trans-1,2-Dichloroethene	553742	33.355	16.968	1.506	6.933	0.000
	B060	C265	265	Trichlorethylene	13837280	40.912	21.811	1.951	9.200	0.000
	B081	C266	266	Chlorobenzene	7676	41.283	28.059	2.575	2.701	0.000
A009		C267	267	Benzylchloride (α-Chlorotoluene)	13840690	45.993	32.889	2.725	2.430	0.000
	B083	C268	268	1,2-Dichlorobenzene	13837988	49.033	33.056	3.074	4.954	0.000
	B084	C269	269	1,3-Dichlorobenzene	13857694	49.033	33.056	3.074	4.954	0.000
		C270	270	Chloroiodomethane	11154	45.395	20.399	2.691	14.355	0.000
		C271	271	2-Chloroethanol	21106015	45.887	15.945	1.097	11.460	9.437
		C272	272	2,2,2-Trichloroethanol	7961	60.183	25.971	2.131	14.695	9.437
A032	B156	C273	273	2-Chlorophenol	13837686	62.037	32.684	3.438	8.528	9.437
		C274	274	Chloroacetonitrile	7568	36.498	13.566	0.995	13.988	0.000
	B048	C275	275	Dibromomethane	2916	45.270	18.929	2.345	16.046	0.000
	B049	C276	276	Tribromomethane	13838404	59.339	27.308	3.608	20.474	0.000
		C277	277	Bromo(chloro)methane	6093	37.469	15.765	1.654	12.101	0.000
		C278	278	Bromodichloromethane	6119	44.430	20.576	2.086	13.818	0.000
		C279	279	Bromoethane (Ethylbromide)	6092	32.494	15.214	1.196	8.134	0.000
	B054	C280	280	1,2-Dibromoethane	7551	47.436	23.356	2.358	13.772	0.000
		C281	281	1,1,2,2-Tetrabromoethane	6339	74.952	40.392	4.978	21.633	0.000
		C282	282	cis-1,2-Dibromoethene	558875	48.697	23.333	2.902	14.512	0.000
		C283	283	1-Bromopropane	7552	35.670	19.575	1.185	6.961	0.000
		C284	284	2-Bromopropane	6118	35.472	19.403	1.146	6.974	0.000
		C285	285	1-Bromobutane	7711	39.261	23.984	1.192	6.136	0.000
		C286	286	2-Bromo-2-Methylpropane	10053	39.043	23.745	1.180	6.169	0.000
		C287	287	1-Bromopentane	7766	42.988	28.339	1.180	5.519	0.000
		C288	288	Bromocyclohexane	7672	48.623	33.097	2.249	5.327	0.000
		C289	289	1-Bromohexane	7810	46.936	32.759	1.191	5.037	0.000
		C290	290	1-Bromoheptane	11863	50.872	37.101	1.174	4.648	0.000
		C291	291	1-Bromooctane	7848	55.026	41.554	1.196	4.326	0.000
		C292	292	1-Bromononane	12219	59.062	45.883	1.175	4.055	0.000
	B080	C293	293	Bromobenzene	7673	47.620	30.645	3.069	5.957	0.000
		C294	294	Benzylbromide	13851576	53.170	36.329	3.511	5.381	0.000
	B088	C295	295	3-Bromotoluene	13875392	51.754	35.252	3.165	5.388	0.000
		C296	296	1,2-Dibromobenzene	13875212	61.012	38.284	4.082	10.697	0.000
		C297	297	1,3-Dibromobenzene	13875356	61.012	38.284	4.082	10.697	0.000
		C298	298	2-Bromophenol	6974	68.258	35.418	3.983	11.471	9.437
		C299	299	Iodomethane	6088	38.141	15.319	2.185	12.689	0.000
		C300	300	Diiodomethane	6106	60.824	28.569	4.547	19.759	0.000
		C301	301	Iodoethane	6100	40.495	19.772	2.207	10.567	0.000
		C302	302	1-Iodopropane	31029	43.574	24.238	2.233	9.155	0.000
		C303	303	2-Iodopropane	6122	43.368	24.059	2.190	9.170	0.000
A086		C304	304	1-Iodobutane	10497	47.028	28.689	2.254	8.136	0.000
		C305	305	1-Iodopentane	11830	50.695	33.118	2.267	7.360	0.000
		C306	306	1-Iodohexane	12010	54.524	37.547	2.281	6.747	0.000

		C307	307	Iodobenzene	11087	55.533	35.492	4.180	7.912	0.000
A062		C308	308	Ethanethiol	6103	29.006	15.130	1.187	4.740	0.000
A151		C309	309	1-Propanethiol (propyl mercaptan)	7560	32.656	19.480	1.173	4.054	0.000
A158		C310	310	2-Propene-1-thiol (allyl mercaptan)	13836713	32.605	18.917	1.483	4.255	0.000
A014		C311	311	1-Butanethiol (butyl mercaptan)	7721	36.515	23.832	1.161	3.573	0.000
A134		C312	312	1-Pentanethiol (amyl mercaptan)	7776	40.551	28.227	1.162	3.213	0.000
		C313	313	1-Hexanethiol	7815	44.691	32.641	1.170	2.932	0.000
		C314	314	1-Heptanethiol	14680	48.875	37.046	1.175	2.705	0.000
		C315	315	1-Octanethiol	7852	53.055	41.419	1.170	2.517	0.000
		C316	316	1-Nonanethiol	14349	57.309	45.825	1.175	2.359	0.000
		C317	317	1-Decanethiol	8577	61.500	50.168	1.159	2.224	0.000
A172	B161	C318	318	Thiophene	7739	35.046	21.834	2.486	2.777	0.000
		C319	319	3-Methylthiophene	21111820	39.380	26.425	2.575	2.430	0.000
A006		C320	320	Benzenethiol (thiophenol)	7681	47.104	32.100	3.587	3.468	0.000
A115		C321	321	Dimethyl sulfide (Methylthiomethane)	1039	27.528	15.277	1.218	3.084	0.000
A070	B165	C322	322	Diethyl sulfide	9233	35.605	24.130	1.206	2.320	0.000
		C323	323	Carbon disulfide	6108	28.226	17.308	2.969	0.000	0.000
A101		C324	324	Dimethyldisulfide	11731	38.935	23.394	2.371	5.221	0.000
		C325	325	Diethyldisulfide	7786	46.801	32.289	2.410	4.153	0.000
A166	B166	C326	326	Di-n-propyl sulfide	7827	43.809	32.759	1.191	1.910	0.000
A030		C327	327	n-Dibutyl sulfide	10536	52.342	41.557	1.196	1.640	0.000
		C328	328	Thiazole	8899	39.126	20.813	2.508	7.856	0.000
A147		C329	329	Phenyl isothiocyanate	7390	51.399	36.514	3.566	3.369	0.000
		C330	330	1-Pentene	7713	28.253	19.889	0.415	0.000	0.000
		C331	331	2-Methyl-2-Butene	10113	28.695	20.165	0.581	0.000	0.000
	B040	C332	332	1-Hexene	11109	32.503	24.174	0.380	0.000	0.000
	B041	C333	333	1-Heptene	11121	36.830	28.518	0.364	0.000	0.000
		C334	334	trans-2-Heptene	555074	37.534	29.006	0.579	0.000	0.000
A128	B042	C335	335	1-Octene	7833	41.170	32.870	0.350	0.000	0.000
	B043	C336	336	1-Nonene	29025	45.556	37.257	0.350	0.000	0.000
		C337	337	1-Decene	12809	49.958	41.656	0.353	0.000	0.000
		C338	338	1-Undecene	12635	54.217	45.948	0.319	0.000	0.000
		C339	339	1-Dodecene	7891	58.678	50.391	0.338	0.000	0.000
		C340	340	Cyclopentene	8544	30.159	20.584	1.626	0.000	0.000
A037	B037	C341	341	Cyclohexene	7788	34.118	24.653	1.516	0.000	0.000
		C342	342	1-Methylcyclopentene	12222	34.119	24.638	1.532	0.000	0.000
		C343	343	Cycloheptene	11857	38.090	28.731	1.410	0.000	0.000
		C344	344	1-Methylcyclohexene	11086	38.102	28.725	1.429	0.000	0.000
		C345	345	1-Methylcycloheptene	66448	42.082	32.808	1.324	0.000	0.000
		C346	346	1,4-Pentadiene	11099	28.012	19.335	0.728	0.000	0.000
		C347	347	2-Methylbuta-1,3-diene	6309	27.847	19.196	0.702	0.000	0.000
		C348	348	1,5-Hexadiene	11110	32.326	23.668	0.709	0.000	0.000
		C349	349	2,3-Dimethylbuta-1,3-diene	10124	31.949	23.355	0.645	0.000	0.000
		C350	350	Cyclopentadiene	7330	30.332	20.302	2.081	0.000	0.000

		C351	351	1,3 Cyclohexadiene	11117	34.329	24.399	1.981	0.000	0.000
		C352	352	1,4 Cyclohexadiene	11838	34.329	24.399	1.981	0.000	0.000
		C353	353	2-Butyne	9990	23.924	15.157	0.818	0.000	0.000
		C354	354	1-Pentyne	11806	27.990	19.329	0.712	0.000	0.000
	B046	C355	355	1-Hexyne	12209	32.294	23.655	0.690	0.000	0.000
		C356	356	2-Hexyne	31016	32.552	23.823	0.780	0.000	0.000
		C357	357	3-Hexyne	12979	32.552	23.823	0.780	0.000	0.000
		C358	358	1-Heptyne	11845	36.660	28.027	0.684	0.000	0.000
		C359	359	1-Octyne	11864	41.022	32.396	0.677	0.000	0.000
A131		C360	360	2-Octyne	16791	41.297	32.578	0.770	0.000	0.000
		C361	361	4-Octyne	15221	41.297	32.578	0.770	0.000	0.000
		C362	362	1-Nonyne	17880	45.415	36.788	0.678	0.000	0.000
		C363	363	1-Decyne	12456	49.808	41.181	0.678	0.000	0.000
		C364	364	1-Dodecyne	63019	58.585	49.958	0.678	0.000	0.000
A005	B064	C365	365	Benzene	236	33.111	23.079	2.083	0.000	0.000
A173	B065	C366	366	Toluene	1108	37.797	27.674	2.174	0.000	0.000
	B066	C367	367	Ethylbenzene	7219	42.280	32.134	2.197	0.000	0.000
A047	B074	C368	368	o-Xylene (1,2-Dimethylbenzene)	6967	42.433	32.232	2.252	0.000	0.000
	B075	C369	369	m-Xylene	7641	42.433	32.232	2.252	0.000	0.000
	B076	C370	370	p-Xylene	7521	42.433	32.232	2.252	0.000	0.000
	B067	C371	371	n-Propylbenzene	7385	46.781	36.606	2.226	0.000	0.000
A179	B027	C372	372	1,3,5-Trimethylbenzene	7659	47.150	36.850	2.351	0.000	0.000
	B068	C373	373	Butylbenzene	7419	51.144	40.976	2.219	0.000	0.000
		C374	374	1,2-Diethylbenzene	8335	51.551	41.264	2.338	0.000	0.000
		C375	375	1,3-Diethylbenzene	8531	51.551	41.264	2.338	0.000	0.000
		C376	376	1,4-Diethylbenzene	7448	51.551	41.264	2.338	0.000	0.000
		C377	377	o-cymene (2-Methyl-1-isopropylbenzene)	10253	51.113	40.922	2.241	0.000	0.000
		C378	378	p-cymene (4-Methyl-1-isopropylbenzene)	7183	51.113	40.922	2.241	0.000	0.000
		C379	379	β-Myrcene	28993	49.878	40.779	1.150	0.000	0.000
		C380	380	Pentylbenzene	10404	55.549	45.378	2.223	0.000	0.000
		C381	381	Heptylbenzene	13492	64.486	54.274	2.263	0.000	0.000
		C382	382	Octylbenzene	15747	68.925	58.701	2.275	0.000	0.000
		C383	383	1-Methylnaphthalene	6736	60.227	47.322	4.956	0.000	0.000
		C384	384	1-Ethylnaphthalene	13677	64.712	51.783	4.980	0.000	0.000
		C385	385	2-Ethylnaphthalene	13063	64.712	51.783	4.980	0.000	0.000
		C386	386	1,4-Dimethylnaphthalene	10829	64.909	51.914	5.047	0.000	0.000
		C387	387	1-Ethyl-2-Methylbenzene	11409	46.966	36.729	2.289	0.000	0.000
		C388	388	1-Ethyl-4-Methylbenzene	11660	46.966	36.729	2.289	0.000	0.000
	B077	C389	389	1,2,3-Trimethylbenzene	10236	47.150	36.850	2.351	0.000	0.000
	B078	C390	390	1,2,4-Trimethylbenzene	6977	47.150	36.850	2.351	0.000	0.000
A185		C391	391	Styrene (Vinylbenzene)	7220	44.891	33.706	3.236	0.000	0.000
		C392	392	3-Methylstyrene	7248	49.573	38.297	3.326	0.000	0.000
		C393	393	4-Methylstyrene	11661	49.573	38.297	3.326	0.000	0.000

		C394	394	Indane (2,3-Dihydroindene)	9903	48.916	37.493	3.473	0.000	0.000
		C395	395	Phenylethyne (Ethynylbenzene)	10364	42.139	31.290	2.900	0.000	0.000
		C396	396	Allylbenzene	8950	46.586	36.087	2.550	0.000	0.000
	B001	C397	397	Pentane	7712	28.426	20.392	0.085	0.000	0.000
		C398	398	2-Methylbutane	6308	28.253	20.249	0.055	0.000	0.000
	B002	C399	399	Hexane	7767	32.709	24.702	0.058	0.000	0.000
	B028	C400	400	2-Methylpentane	7604	32.512	24.542	0.022	0.000	0.000
	B029	C401	401	3-Methylpentane	7010	32.512	24.542	0.022	0.000	0.000
		C402	402	2,2-Dimethylbutane	6163	32.549	24.531	0.069	0.000	0.000
	B026	C403	403	2,3-Dimethylbutane	6340	32.391	24.437	0.005	0.000	0.000
A074	B003	C404	404	Heptane	8560	37.019	29.033	0.037	0.000	0.000
		C405	405	2-Methylhexane	11094	36.798	28.853	-0.005	0.000	0.000
		C406	406	2,2-Dimethylpentane	11055	36.854	28.859	0.047	0.000	0.000
		C407	407	2,3-Dimethylpentane	10786	36.666	28.741	-0.024	0.000	0.000
A054		C408	408	2,4-Dimethylpentane	7619	36.666	28.741	-0.024	0.000	0.000
		C409	409	3,3-Dimethylpentane	10755	36.854	28.859	0.047	0.000	0.000
		C410	410	2,2,3-Trimethylbutane	9649	36.634	28.680	0.005	0.000	0.000
A124	B004	C411	411	Octane	349	41.351	33.380	0.022	0.000	0.000
		C412	412	3-Methylheptane	11035	41.205	33.257	0.000	0.000	0.000
		C413	413	2,3-Dimethylhexane	10963	40.964	33.062	-0.048	0.000	0.000
		C414	414	2,4-Dimethylhexane	11027	40.964	33.062	-0.048	0.000	0.000
		C415	415	3,4-Dimethylhexane	10932	40.964	33.062	-0.048	0.000	0.000
		C416	416	2,2,3-Trimethylpentane	10781	40.939	33.006	-0.016	0.000	0.000
	B025	C417	417	2,2,4-Trimethylpentane	10445	40.939	33.006	-0.016	0.000	0.000
		C418	418	2,3,4-Trimethylpentane	10795	40.720	32.866	-0.095	0.000	0.000
A121	B005	C419	419	Nonane	7849	45.751	37.777	0.025	0.000	0.000
		C420	420	2-Methyloctane	17558	45.486	37.566	-0.029	0.000	0.000
		C421	421	4-Methyloctane	15802	45.486	37.566	-0.029	0.000	0.000
		C422	422	3,3-Diethylpentane	13402	45.470	37.515	0.005	0.000	0.000
		C423	423	2,2,5-Trimethylhexane	17976	45.315	37.386	-0.020	0.000	0.000
	B006	C424	424	Decane	14840	50.063	42.109	0.005	0.000	0.000
	B007	C425	425	Undecane	13619	53.950	46.124	-0.123	0.000	0.000
	B008	C426	426	Dodecane	7890	58.737	50.810	-0.022	0.000	0.000
	B009	C427	427	Tridecane	11882	63.204	55.258	-0.002	0.000	0.000
		C428	428	Tetradecane	11883	67.596	59.649	-0.002	0.000	0.000
	B030	C429	429	Cyclopentane	8896	29.972	20.856	1.167	0.000	0.000
A034	B035	C430	430	Cyclohexane	7787	33.952	24.940	1.063	0.000	0.000
	B031	C431	431	Methylcyclopentane	7024	33.295	24.437	0.910	0.000	0.000
	B036	C432	432	Cycloheptane	8908	37.934	29.026	0.958	0.000	0.000
	B032	C433	433	Methylcyclohexane	7674	37.333	28.564	0.820	0.000	0.000
A038		C434	434	Cyclooctane	8909	41.913	33.110	0.854	0.000	0.000
		C435	435	Methylcycloheptane	18919	41.324	32.656	0.719	0.000	0.000
		C436	436	cis-1,2-Dimethylcyclohexane	15765	40.510	31.996	0.566	0.000	0.000

		C437	437	trans-1,2-Dimethyl cyclohexane	221117	40.647	32.138	0.560	0.000	0.000
		C438	438	cis-1,4-Dimethylcyc lohexane	10179173	40.647	32.138	0.560	0.000	0.000
		C439	439	trans-1,4-Dimethyl cyclohexane	10265264	40.647	32.138	0.560	0.000	0.000
		C440	440	Cyclodecane	8910	49.872	41.278	0.645	0.000	0.000
		C441	441	Pentylcyclopentane	18410	50.489	41.724	0.816	0.000	0.000
		C442	442	cis-Hydrindane (*cis*-Octahydroinde ne)	558720	47.108	37.383	1.776	0.000	0.000
		C443	443	trans-Hydrindane	558721	47.108	37.383	1.776	0.000	0.000
		C444	444	cis-Decalin	10179239	51.127	41.496	1.682	0.000	0.000
		C445	445	trans-Decalin	10265270	51.127	41.496	1.682	0.000	0.000
	B200		446	1,3, 5-Trinitrobenzene	13873689	88.502	51.523	5.547	23.483	0.000
	B010		447	Hexadecane	10540	76.389	68.439	0.002	0.000	0.000
	B011		448	Heptadecane	11892	80.770	72.822	0.000	0.000	0.000
	B012		449	Octadecane	11145	85.197	77.239	0.008	0.000	0.000
	B013		450	Eicosane	7929	93.948	85.998	0.001	0.000	0.000
	B014		451	Heneicosane	11897	98.254	90.325	-0.020	0.000	0.000
	B015		452	Docosane	11899	102.830	94.853	0.027	0.000	0.000
	B016		453	Tetracosane	12072	111.574	103.607	0.018	0.000	0.000
	B017		454	Pentacosane	11900	115.977	108.006	0.021	0.000	0.000
	B018		455	Hexacosane	11901	120.401	112.422	0.030	0.000	0.000
	B019		456	Heptacosane	11146	124.848	116.854	0.045	0.000	0.000
	B020		457	Octacosane	11902	129.316	121.302	0.065	0.000	0.000
	B021		458	Nonacosane	11903	133.481	125.525	0.008	0.000	0.000
	B022		459	Triacontane	12018	137.984	129.999	0.036	0.000	0.000
	B023		460	Dotriacontane	10542	146.694	138.727	0.018	0.000	0.000
	B024		461	Squalane (Spinacane)	7798	136.661	128.927	-0.215	0.000	0.000
	B033		462	Ethylcyclohexane	14751	41.324	32.656	0.719	0.000	0.000
	B034		463	n-Decylcyclohexane	14942	76.525	67.837	0.739	0.000	0.000
	B038		464	cis-2-Octene	4512361	41.883	33.365	0.569	0.000	0.000
	B039		465	trans-2-Octene	4516601	41.883	33.365	0.569	0.000	0.000
	B044		466	1-Octadecene,	7925	85.052	76.757	0.347	0.000	0.000
	B045		467	1-Nonadecene	27049	89.367	81.091	0.327	0.000	0.000
	B047		468	Bromomethane	6083	30.053	10.910	1.225	9.969	0.000
	B050		469	Chloromethane	6087	21.489	8.176	0.680	4.684	0.000
A169	B058		470	1,1,2,2-Tetrachloro ethane	6342	47.083	26.684	1.851	10.599	0.000
	B061		471	Tetrachlorethylene	13837281	48.176	26.739	2.426	11.062	0.000
	B063		472	1,2-Dichlorobutane	11522	39.592	25.623	0.930	5.090	0.000
	B069		473	Octadecylbenzene	70563	113.099	102.806	2.345	0.000	0.000
	B070		474	Decylbenzene	7430	77.734	67.503	2.283	0.000	0.000
	B071		475	Tetradecylbenzene	14358	95.300	85.067	2.284	0.000	0.000
A057	B072		476	Diphenylmethane	7299	65.390	53.010	4.432	0.000	0.000
	B073		477	tert-Butylbenzene	7088	50.172	40.200	2.023	0.000	0.000
	B082		478	1,4-Dichlorobenzene	13866817	49.033	33.056	3.074	4.954	0.000
	B085		479	1,2,4-Trichlorobenz ene	13862559	56.500	38.085	3.583	6.883	0.000

	B086		480	1,3,5-Trichlorobenzene	7662	56.500	38.085	3.583	6.883	0.000
	B087		481	Hexachlorobenzene	8067	77.912	53.377	5.180	11.406	0.000
	B092		482	Dibutylphthalate	13837319	94.336	75.222	2.947	8.218	0.000
	B093		483	Dioctylphthalate	8043	127.635	110.417	2.972	6.297	0.000
	B094		484	Dinonylphthalate	6529	136.224	119.295	3.006	5.974	0.000
	B095		485	Methyloleate	4516661	97.510	85.197	0.782	3.582	0.000
	B096		486	α-Epichlorohydrin	13837112	35.771	18.571	1.373	7.878	0.000
	B098		487	Butylethylether	11849	37.347	26.915	0.011	2.473	0.000
	B099		488	1-Ethoxypropane	11835	33.271	22.567	0.025	2.730	0.000
	B104		489	Ethylvinylether (1-Ethoxyethene)	7732	29.286	17.751	0.383	3.203	0.000
	B107		490	Dioctylether	11893	79.913	70.628	-0.053	1.388	0.000
	B124		491	Decylacetate	7875	67.172	54.348	0.190	4.685	0.000
	B125		492	Butylstearate	29018	109.808	98.391	0.239	3.230	0.000
	B126		493	Methyl 2-octadecenoate	23254956	97.510	85.197	0.782	3.582	0.000
	B127		494	Dibutylmaleate	4436356	76.194	58.013	0.997	9.235	0.000
	B140		495	1,2-Dichloro-4-nitrobenzene	21106095	67.983	42.788	4.314	12.933	0.000
	B142		496	3,4-Dinitrotoluene	11390	75.683	46.995	4.606	16.133	0.000
	B145		497	4-Chloroaniline	13869339	66.005	34.741	3.849	10.029	9.437
	B149		498	1,2-Butadiene	11051	23.206	14.628	0.629	0.000	0.000
A143	B151		499	Phenol	971	54.371	27.554	2.895	6.537	9.437
	B152		500	3,4-Dimethylphenol (3,4-xylenol)	13839105	62.521	36.734	3.074	5.326	9.437
	B153		501	3,5-Dimethylphenol	13839110	62.521	36.734	3.074	5.326	9.437
	B154		502	2,6-Dimethylphenol	13839174	62.521	36.734	3.074	5.326	9.437
	B155		503	3-Chlorophenol	13875432	62.037	32.684	3.438	8.528	9.437
	B157		504	4-Chlorophenol	13875219	62.037	32.684	3.438	8.528	9.437
	B158		505	4-Nonylphenol	1688	91.269	67.423	3.038	3.422	9.437
	B159		506	2,4-Dinonylphenol	8406	130.576	107.468	3.243	2.480	9.437
	B167		507	Cyclohexylamine	7677	55.365	29.183	1.501	7.295	9.437
	B172		508	Dodecylamine (Laurylamine)	12994	78.703	55.974	0.713	4.630	9.437
	B174		509	Diethylene glycol dibutylether	13881964	70.119	57.572	-0.118	4.716	0.000
	B175		510	Biphenyl	6828	59.862	47.771	4.142	0.000	0.000
	B177		511	Naphthalene	906	55.523	42.713	4.861	0.000	0.000
	B178		512	Acenaphthene	6478	68.673	54.031	6.693	0.000	0.000
	B179		513	Fluorene	6592	68.662	54.728	5.985	0.000	0.000
	B180		514	Fluoranthene	8800	98.710	78.939	11.823	0.000	0.000
	B181		515	Phenanthrene	970	79.094	63.212	7.933	0.000	0.000
	B182		516	Pyrene	29153	98.710	78.939	11.823	0.000	0.000
	B183		517	Chrysene	8817	103.104	84.038	11.118	0.000	0.000
	B184		518	1-Nonylnaphthalene	105267	88.026	75.349	4.729	0.000	0.000
	B185		519	1-Decylnaphthalene	3721664	100.062	87.074	5.039	0.000	0.000
	B186		520	1-Hexylnaphthalene	148477	82.404	69.440	5.014	0.000	0.000
	B187		521	Tetraphenylmethane	11917	120.289	103.415	8.925	0.000	0.000
	B188		522	1,4-Diphenylbenzene (p-Terphenyl)	6848	87.044	72.784	6.311	0.000	0.000
	B189		523	Tetraphenylethylene	62645	127.263	109.340	9.974	0.000	0.000

	B197		524	2-Nitroaniline	13853943	78.155	39.690	4.664	16.415	9.437
	B198		525	4-Nitroaniline	13846959	78.155	39.690	4.664	16.415	9.437
	B199		526	3-Nitroaniline	7145	78.155	39.690	4.664	16.415	9.437
A008			527	Benzylacetate	13850405	57.044	40.328	2.500	6.267	0.000
A010			528	Dibenzyl sulfide	10407	82.693	67.183	6.154	1.407	0.000
A011			529	Bromine	22817	44.280	14.446	2.313	19.572	0.000
A013			530	2,3-Butanedione (diacetyl)	630	38.321	18.180	0.439	11.753	0.000
A015			531	2-Butanethiol (sec.butyl mercaptan)	10120	36.406	23.733	1.146	3.578	0.000
A021			532	1-Butene	7556	24.046	15.635	0.462	0.000	0.000
A022			533	2-Butene	11719	24.586	16.001	0.636	0.000	0.000
A023			534	2-Butene-1-thiol (crotyl mercaptan)	4938601	37.139	23.767	1.690	3.733	0.000
A027			535	p-tert.Butyl-cycloh exylacetate (oryclon)	33188	67.548	53.734	1.012	4.852	0.000
A028			536	1-tert.Butyl-3,5-di methyl-2,4,6-trinitr obenzene (muskxylene)	56123	108.639	78.080	5.756	16.854	0.000
A029			537	6-tert.Butyl-3-meth yl-2,4-dinitroanisol e (musk ambrette)	6496	95.959	70.351	4.398	13.261	0.000
A031			538	Dichlorodiethyl sulfide	21106142	50.794	34.105	2.190	6.550	0.000
A033			539	Coumarin	13848793	60.809	40.867	4.181	7.812	0.000
A041			540	trans,trans-2,4-Dec adienal	4446470	56.509	43.523	1.375	3.661	0.000
A042			541	Decanal	7883	55.070	43.397	0.229	3.494	0.000
A044			542	trans-2-Decenal	4446466	55.819	43.485	0.810	3.575	0.000
A048			543	7-Hydroxy-3,7-dim ethyloctanal (hydroxycitronellal)	1363703	72.739	47.077	0.837	7.439	9.437
A049			544	(2E)-3,7-Dimethyl-2,6-octadienal (citral a, geranial)	553578	56.175	43.237	1.320	3.668	0.000
A050			545	(2Z)-3,7-Dimethyl-2,6-octadienal (citral b, neral)	558878	56.175	43.237	1.320	3.668	0.000
A051			546	trans-3,7-Dimethyl octa-2,6-dien-1-ol (geraniol)	13849989	69.244	45.899	1.709	4.251	9.437
A052			547	3,7-Dimethyloctan-1-ol (tetrahydrogeraniol)	7504	67.679	45.699	0.532	4.061	9.437
A053			548	3,7-Dimethyl-6-oct enal (citronellal)	7506	55.369	43.114	0.725	3.582	0.000
A055			549	Dimethyltrithiocar bonate	15959	52.880	36.333	4.302	4.296	0.000
A058			550	1-Dodecanol	7901	76.476	54.838	0.617	3.635	9.437
A060			551	1,2-Ethanediol	13865015	41.367	23.078	2.303	8.036	0.000
A066			552	Ethylamine	6101	41.886	12.208	0.758	11.535	9.437
A067			553	EthylButanoate (ethyl butyrate)	7475	43.127	28.021	0.194	6.963	0.000
A068			554	Ethyl isothiocyanate	10501	35.898	21.692	1.900	4.358	0.000
A069			555	Ethyl 2-methylpropanoat e (ethylisobutyrate)	7065	42.923	27.849	0.154	6.971	0.000
A072			556	trans-2-trans-4-He ptadienal	4446442	44.218	30.288	1.353	4.627	0.000
A076			557	trans,trans-2,4-Hex adienal (Sorbaldehyde)	553167	40.309	25.892	1.351	5.118	0.000
A083			558	4-Hydroxy-3-meth oxybenzaldehyde (vanillin)	13860434	76.131	42.994	4.193	11.558	9.437

A084			559	15-Hydroxypentadecanoic acidlactone (exaltolide, pentadecanolide)	205386	77.138	64.803	0.187	4.200	0.000
A085			560	Indole	776	57.663	39.993	5.271	4.450	0.000
A087			561	Isopentylacetate (isoamylacetate)	29016	46.679	32.188	0.137	6.404	0.000
A088			562	Isopentyl 3-methylbutanoate (isoamylisovalerate)	12093	58.459	45.186	0.098	5.226	0.000
A089			563	(d)-4-Isopropenyl-1-methylcyclohex-1-ene ((d)-limonene)	20939	50.478	40.898	1.631	0.000	0.000
A090			564	5-Isopropenyl-2-methyl-2-cyclohexen-1-one (carvone)	21106424	56.188	42.449	1.966	3.824	0.000
A091			565	2-Isopropyl-5-methylcyclohexanol (menthol)	1216	68.054	45.140	1.304	4.224	9.437
A092			566	Methanal (formaldehyde)	692	23.943	4.449	0.371	11.174	0.000
A093			567	Methanethiol (methyl mercaptan)	855	25.787	10.812	1.212	5.814	0.000
A094			568	2-Methoxyphenol (guaiacol)	447	62.618	34.247	2.900	8.085	9.437
A095			569	1-Methoxy-4-propenylbenzene (Anethole)	553166	58.986	45.412	3.504	2.120	0.000
A096			570	Methyl 2-aminobenzoate (methylanthranylate)	13858096	76.643	42.670	3.791	12.795	9.437
A097			571	4-Methylbenzenethiol (p-thiocresol)	21111822	51.477	36.710	3.682	3.136	0.000
A098			572	3-Methylbutane-1-thiol (isoamyl mercaptan)	10462	40.355	28.064	1.126	3.217	0.000
A100			573	Diisopenthyl sulfide	10525	60.549	50.022	1.127	1.451	0.000
A102			574	3,4-Methylenedioxybenzaldehyde (piperonal, heliotropine)	13859497	63.181	41.441	4.522	9.269	0.000
A103			575	3-Methylindole (skatole)	6480	61.809	44.474	5.323	4.062	0.000
A104			576	Methyl isothiocyanate	10694	32.157	17.238	1.879	5.091	0.000
A105			577	Methyl 3-methylbutanoate (methylisovalerate)	10687	42.923	27.849	0.154	6.971	0.000
A107			578	2-Methylpropane-1-thiol (isobutyl mercaptan)	10118	36.343	23.686	1.130	3.578	0.000
A108			579	2-Methylpropane-2-thiol (tert.butyl mercaptan)	6147	36.347	23.641	1.165	3.592	0.000
A109			580	2-Methylpropan-1-ol (isobutylalcohol)	6312	44.228	19.510	0.565	6.767	9.437
A110			581	2-Methylpropan-2-ol (tert.butyl alcohol)	6146	44.256	19.472	0.602	6.796	9.437
A111			582	2-Methylpropene (isobutylene)	7957	23.848	15.472	0.427	0.000	0.000
A112			583	Methyl salicylate	13848808	72.805	40.514	3.347	11.558	9.437
A113			584	Methylthiocyanate	10695	39.241	16.748	1.693	12.852	0.000
A114			585	Methylthioethane (methylethyl sulfide)	11729	31.454	19.654	1.212	2.639	0.000
A118			586	Nitrosobenzene	10989	48.154	28.520	2.617	9.068	0.000
A119			587	trans-2-trans-4-Nonadienal	4446460	52.310	39.080	1.357	3.924	0.000
A122			588	trans-2-Nonenal	4446456	51.694	39.108	0.815	3.822	0.000
A127			589	trans-2-Octenal	4446445	47.590	34.712	0.813	4.116	0.000
A130			590	1-Octen-3-ol	17778	59.606	36.578	0.899	4.742	9.437
A133			591	2,3-Pentanedione	11254	41.323	22.542	0.429	10.403	0.000

A139			592	Pentyl 3-methylbutanoate (amylisovalerate)	86646	58.630	45.330	0.128	5.222	0.000
A140			593	Pentylthiopentane (diamyl sulfide)	12810	61.039	50.417	1.224	1.449	0.000
A141			594	Phenacylbromide (α-bromoacetophenone)	6023	63.141	42.258	3.842	9.091	0.000
A142			595	Phenacylchloride (α-chloroacetophenone)	10303	56.266	38.775	3.041	6.501	0.000
A144			596	Phenoxybenzene (diphenylether)	7302	64.986	50.679	4.333	2.026	0.000
A145			597	2-Phenylacetic acid	10181341	68.617	38.209	3.339	9.683	9.437
A148			598	3-Phenylpropenal (cinnamaldehyde)	553117	56.618	40.430	3.867	4.372	0.000
A149			599	3-Phenylprop-2-en-1-ol (cinnamicalcohol)	21105870	70.375	43.547	4.410	5.033	9.437
A150			600	Phenylthiobenzene (diphenyl sulfide)	8436	74.404	58.637	6.234	1.584	0.000
A152			601	2-Propanethiol (isopropyl mercaptan)	6124	32.456	19.311	1.134	4.062	0.000
A160			602	2-Propenylamine (allylamine)	13835977	44.686	16.000	1.056	10.243	9.437
A161			603	2-Propenyl disulfide (diallyldisulfide)	15730	54.837	40.110	3.087	3.691	0.000
A162			604	2-Propenyl isothiocyanate (allyl isothiocyanate)	21105854	38.504	24.645	1.913	3.997	0.000
A163			605	Diallyl sulfide	11128	43.544	31.725	1.842	2.027	0.000
A164			606	Propylbutanoate	7482	46.907	32.377	0.183	6.398	0.000
A165			607	Propylpropanoate	7515	43.127	28.021	0.194	6.963	0.000
A167			608	2-Propynal (propargylaldehyde)	11721	28.678	11.891	0.954	7.883	0.000
A171			609	Tetrahydrothiophene (thiophane)	1095	37.348	24.574	2.317	2.507	0.000
A174			610	α-Toluenethiol (benzyl mercaptan)	13851383	50.710	36.157	3.472	3.132	0.000
A175			611	Tributylamine	7340	64.574	55.567	0.483	0.575	0.000
A178			612	Trimethylamine	1114	25.872	16.194	0.530	1.199	0.000
A180			613	1,7,7-Trimethylbicyclo[2,2,1]heptan-2-one (camphor)	2441	56.689	42.852	2.070	3.818	0.000
A181			614	2,6,6-Trimethylbicyclo[3,1,1]hept-2-ene (α-pinene)	6402	50.117	40.264	1.904	0.000	0.000
A183			615	Undecanal	7894	59.257	47.786	0.228	3.295	0.000
A184			616	9-Undecenal (undecylenicaldehyde)	7895	59.285	47.384	0.594	3.359	0.000

Electrochemical Obtaining of Thin Tellurium Coatings from Chloride-Sulphate Solutions

E.A. Salakhova, D.B. Tagıyev, P.E.Kalantarova, I.I. Jabbarova, R.E. Huseynova, A. F. Heybatova, N. N. Khankishiyeva & K.F.Ibrahimova

ABSTRACT

The possibility of electrochemical obtaining of thin tellurium coatings from a chloride-sulfate electrolyte has been investigated. The studies have been carried out in solution containing (mol / l): 0.01 - 0.08 TeO_2 + 1.5H_2SO_4 + 1.5HCl + 0.01 - 0.08 $(NH_4)_2SO_4$ +1.0 gelatin. It has been found that with the increase in the concentration of HCl in the electrolyte from 0.5 mol/l to 4 mol/l, the cathodic deposition of tellurium accelerated, the polarization curves shifted in the positive direction. Experiments carried out in solutions containing chloride-sulfate ions show that in the initial stages of the cathodic process, chemical difficulties play the main role, and at negative potentials of the process, they are limited by diffusion polarization. At cathodic potentials up to 0.2 V, the process of tellurium electrodeposition from a chloride sulfate electrolyte is mainly accompanied by chemical polarization and effective activation energy at these potentials reaches up to 40 kJ / mol, and at a potential of 0.30–0.25 V, the process is controlled by mixed kinetics.

Keywords: tellurium, thin coatings, electrodeposition, semiconductor, current density, cathodic process, acidity.

Classification: LCC Code: QA1-QA939

Language: English

Great Britain Journals Press

LJP Copyright ID: 925684
Print ISSN: 2631-8490
Online ISSN: 2631-8504

London Journal of Research in Science: Natural and Formal

Volume 22 | Issue 8 | Compilation 1.0

Electrochemical Obtaining of Thin Tellurium Coatings from Chloride-Sulphate Solutions

E.A. Salakhova[α], D.B. Tagıyev[σ], P.E.Kalantarova[ρ], I.I. Jabbarova[Ↄ], R.E. Huseynova[¥], A. F. Heybatova[§], N. N. Khankishiyeva[χ] & K.F.Ibrahimova[ν]

ABSTRACT

The possibility of electrochemical obtaining of thin tellurium coatings from a chloride-sulfate electrolyte has been investigated. The studies have been carried out in solution containing (mol / l): 0.01 - 0.08 TeO_2 + 1.5H_2SO_4 + 1.5HCl + 0.01 - 0.08 $(NH_4)_2SO_4$ +1.0 gelatin. It has been found that with the increase in the concentration of HCl in the electrolyte from 0.5 mol/l to 4 mol/l, the cathodic deposition of tellurium accelerated, the polarization curves shifted in the positive direction. Experiments carried out in solutions containing chloride-sulfate ions show that in the initial stages of the cathodic process, chemical difficulties play the main role, and at negative potentials of the process, they are limited by diffusion polarization. At cathodic potentials up to 0.2 V, the process of tellurium electrodeposition from a chloride sulfate electrolyte is mainly accompanied by chemical polarization and effective activation energy at these potentials reaches up to 40 kJ / mol, and at a potential of 0.30–0.25 V, the process is controlled by mixed kinetics.

Keywords: tellurium, thin coatings, electrodeposition, semiconductor, current density, cathodic process, acidity.

Author α σ ρ Ↄ ¥ § χ ν: Institute of Catalysis and Inorganic Chemistry named after M.Nagiyev of the Ministry of Science and Education of the Azerbaijan Republic, H.Javid ave. 113, AZ1143, Baku, Azerbaijan.

I. INTRODUCTION

In recent years, with the development of semiconductor technology, the need for tellurium has increased sharply. In this regard, research aimed at studying the electrodeposition of tellurium from various electrolytes is of great scientific and practical interest [1-5]. Tellurium has a number of specific properties. As the purity level increases, new properties are revealed, the scale and specificity of their application are expanded. In expanding the field of application there is a need for intensive research into the chemical and physico-chemical properties as well as the technology for obtaining pure and ultrapure tellurium and its compounds.

Tellurium is mainly used in semiconductor technology, in instrument engineering, in the chemical and metallurgical industries [6-11]. Unlike other semiconductors, tellurium easily melts and evaporates; therefore, semiconductor films which are necessary in modern microelectronics can be obtained from it without any particular difficulties. It should be noted that pure tellurium is rarely used as a semiconductor; metal tellurides are more common. Tellurium is used in the production of lead alloys with increased plasticity and strength (used, for example, in cable production). When introducing 0.05% tellurium, lead losses during dissolution under the influence of sulfuric acid are reduced by 10 times, and this is used in the production of lead-acid batteries. Production of lanthanide tellurides, their alloys and alloys with metal selenides for manufacturing thermoelectric generators with very high (up to 72-78%) efficiency will be very important in the coming years, that will allow to use them in the energy sector and automotive industry.

London Journal of Research in Science: Natural and Formal

As have been well known from the literature [12-14], acidic electrolytes are the best tellurium electrolytes [15-20].During electrolysis from acidic tellurium-containing solutions, depending on the electrolysis condition and electrolyte composition, coarse-crystalline or fine-grained tellurium precipitates are deposited on the cathode. The high positive potential of the Te/Te^{4+} system and good solubility of TeO_2 and $TeC1_4$ in hydrochloric acid solutions are very favorable for the electrolytic extraction of pure tellurium. In this work, chloride-sulfate electrolyte was used to obtain tellurium semiconductor coatings. The choice of chloride-sulfate electrolyte was explained by the fact that high-quality tellurium deposits can be obtained from this electrolyte, while high-quality tellurium films cannot always be obtained from an alkaline electrolyte. In addition, precipitates obtained from chloride baths always contain 2% chlorine in the form of $TeCl_2$, the content of which increases with the increase in the acidity of the solution and in the current density. Also, preliminary experiments have shown that high-quality tellurium films can be obtained from chloride-sulfate electrolyte even at very low concentrations of tellurium in the electrolyte. This is very important when co-deposition tellurium with more electronegative metals such as bismuth, antimony, cadmium, rhenium. At low concentrations of tellurium in the electrolyte, its deposition is accompanied by high polarization, which causes the tellurium deposition potential to shift to the deposition potential of more electronegative metal and thus creates favorable conditions for the co-deposition of these metals.Therefore, in this case, the study of the kinetics and mechanism of tellurium deposition focused on those factors that contribute not only to high-quality precipitation, but also significantly shift the potential of the more noble metal to the negative side (or deposition of the more noble metal is accompanied by high polarization). For this purpose the cathodic reduction of Te(IV) in chloride-sulfate electrolyte on Pt and Te electrode was investigated. The present work was carried out in order to find out the possibility of obtaining by electrochemical method tellurium coatings during electrolysis from chloride-sulfate electrolyte. The investigations were carried out in solutions containing (mol/l): 0.01 - 0.08 TeO_2 + 1.5H_2SO_4 + 1.5HCl + 0.01 - 0.08 $(NH_4)_2SO_4$ + 1.0 gelatin.

II. METHODS

Platinum electrode with a visible surface of 0.07 cm^2 was used as a working electrode. The three-electrode cell contained investigated electrode, an auxiliary platinum electrode with an area of 4 cm^2, and silver-silver chloride reference electrode. All potential values are given relative to this electrode. The working electrodes were washed with alcohol and water. Current-voltage curves were recorded without stirring. The deposition of films for investigation of structure and composition was carried out on Pt, Cu, and Ni substrates with an area of 2.0 cm^2. The working temperature during electrodeposition was 75°C, the deposition time was 30-60 minutes. After deposition, the samples were washed with distilled water. pH value was measured on instrument AZ 86551 and in a solution of the composition (mol/l): 0.01 - 0.08 TeO_2 + 1.5H_2SO_4 + 1.5HCl + 0.01 - 0.08 $(NH_4)_2SO_4$ + 1.0 gelatin.

The study has been carried out from a chloride-sulfate solution containing tellurium oxide. The kinetics of the processes was explored using measurements by the method of cyclic voltammetry on IVIUMSTAT. The films were obtained in galvanostatic mode without electrolyte stirring.

III. EXPERIMENTAL PART

Usually, after immersion of the Te-electrode in a chloride-sulfate solution for 30 minutes, the electrode potential takes the constant value equal to +0.5 ± 0.05 V, which does not change by change in concentration of Te in the solution. However, in the case of a platinum electrode, the stationary

potential has a value of +0.36 V and within 30 minutes takes the value +0.56 V. When establishing a stationary potential, the main role is played not by the equalization of the concentration ratios in the cathode layer, but by the equilibrium between the electrode surface and a solution, which are caused by the presence of a film of oxide and insoluble tellurium compounds on the cathode surface. It is more likely that the insoluble $TeCl_2$ salt plays the main role in the contamination of the cathode surface, because tellurium oxide compounds are readily soluble in these solutions.

As can be seen from fig. 1, the forward and reverse branches of the polarization curves differ significantly. The observed hysteresis on PS can be easily explained if we assume that tellurium oxide compounds existing on the surface are reduced during cathodic polarization and the surface of tellurium electrode is in an active state. The presence of hysteresis on polarization curves in this case may be due to the semiconducting nature of tellurium itself. Usually, the rate of electrode reaction on a semiconductor surface depends not only on the concentration of charge carriers. The more active manifestation of the semiconducting properties of tellurium in the field of relatively high cathodic polarization can be explained as follows. It is known that tellurium oxide compounds are electron donors, i.e. source of electrons generation. Since with increasing cathodic polarization there is a gradual reduction of tellurium oxide compounds, it is easy to see that the donor levels and related electron generation centers also disappear. As a result, the discharge of tellurium ions at the cathode is difficult, the rate of the process drops sharply, and the polarization curve shifts towards negative potentials. Therefore, in this case, when studying the kinetics and mechanism of tellurium deposition, the main attention was paid to those factors that contribute not only to the production of high-quality precipitation, but also significantly shift the potential of a more noble metal to the electronegative side. Therefore, a more detailed study of tellurium electrodeposition patterns from the selected electrolyte was required, knowledge of which would help to choose the optimal conditions for the co-deposition of tellurium with other metals. For this purpose, preliminary experiments were carried out to study the effect of various complexing agents and surfactant additives on the rate of the cathodic process and on the quality of the obtained precipitates from different acid concentrations. The highest quality precipitates were obtained from an electrolyte containing ammonium sulfate and gelatin. Therefore, most of the experiments were carried out with $(NH_4)_2SO_4$, which ensured the stability of the electrolyte and made it possible to create an increased concentration of the complexing agent in the electrolyte. Below are the main results of polarization measurements obtained by using the specified electrolyte. With the increase in the concentration of HCl in the electrolyte from 0.5 mol / l to 4 mol /l, the cathodic deposition of tellurium becomes easier (Fig. 1), the polarization curves shifts to the positive direction. Thus, in this case, it is logical to assume that with an increase in the concentration of HCl in the solution, the dissolution of partially hydrolyzed tellurium ions occurs, and at 2–3 mol/l of HCl, $TeCl_4$ is formed, which dissociates well into ions, which causes the polarization curves to shift in the positive direction. The same pattern with a change in polarization curves in solutions containing up to 3 mol /l HCl was observed in [12-24].

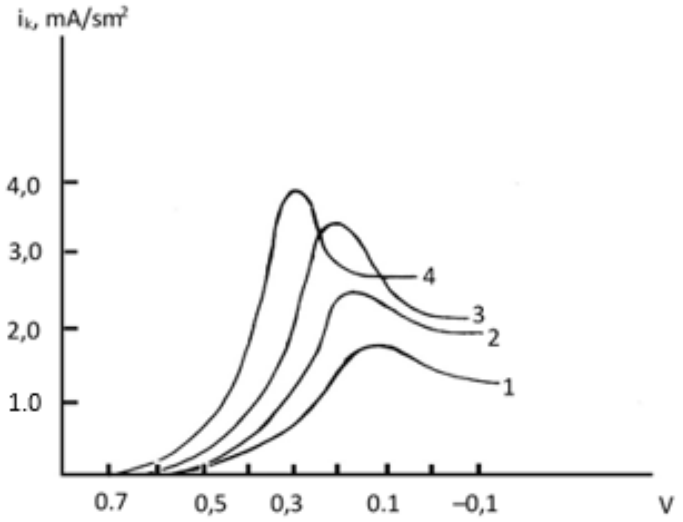

Fig. 1: Cathodic polarization curves obtained from solutions containing 0.05 mol/l TeO_2 + 0.01 mol/l $(NH_4)_2SO_4$ + 1.5 mol/l H_2SO_4 at various HCl concentrations (mol/l): 1 - 0.5 ; 2 - 1; 3 - 2.0; 4 - 4.0. t = 75°C

However, in more acidic solutions (>4 mol /l HCl), with an increase in the concentration of hydrochloric acid, the polarization curves shifts to the negative side. This is probably due to the change in the nature of complex ions of tellurium with chlorine. According to [19], in the concentration range of 0.1- 0.05 mol/l HCl, the potential-determining ion is $Te(OH)Cl_2$, and at HCl<5 mol/l - $Te(OH)_2Cl_2$. Hence, we can conclude that the composition of the solution has a significant effect on the kinetics of tellurium deposition, which is mainly determined by the state of tellurium-containing ions in the solution. With an increase in the concentration of H_2SO_4 in the solution, the equilibrium potential of tellurium slightly shifts to the negative side, and the cathodic deposition of tellurium occurs at a significant negative potentials. Moreover, the increase in polarization with an increase in the current density is much stronger and probably due to the higher strength of the sulfate complex than the tellurium chloride complex. It should be noted that the high polarization during deposition of tellurium from the chloride-sulfate electrolyte is associated with the previous chemical reaction of $Te(OH)_2Cl_4^{2-}$ dissociation:

$$Te(OH)_2Cl_4^{2-} \rightarrow [Te(OH)_2]^{2+} + 4Cl^-$$

In cathodic reduction, the dissociation product $[Te(OH)_2]^{2+}$is directly involved.Figure 2 (a) shows the cathodic polarization curves recorded at different concentrations of tellurium in solution. It can be seen from the curves that with an increase in the concentration of tellurium dioxide in the electrolyte, the rate of tellurium extraction at the cathode increases, the potential shifts towards positive values. At a concentration of 0.01 - 0.07 mol /l TeO_2, the cathodic process is characterized by the occurrence of wave. At a potential of + 0.3V, the wave appears on the polarization curves and the cathode surface is covered with a layer of elementary tellurium. The value of i_{lim} is directly proportional to the concentration of tellurium in the electrolyte (Fig. 2 b). This shows that at the indicated concentration of tellurium in the electrolyte, the nature of the tellurium-containing ions participating in the cathodic process does not change. When i_{lim} is reached, due to a decrease in the surface concentration of

tellurium ions, the electrode potential shifted to the negative side, reaching a value at which hydrogen is released. We assume that initially the electrode process is determined by the reaction:

$$[Te(OH)_2Cl_4]^{2-} \rightarrow [Te(OH)_2]^{2+} + 4Cl^-$$

$$[Te(OH)_2]^{2+} + 4e + 2H^+ \rightarrow Te + 2H_2O$$

According to [8-11], the overall reaction occurs in stages, since the rate-determining stage is the receiving of the last electron:

$$[Te(OH)_2]^{2+} + e = Te(OH)_2^+ \text{ (fast)}$$

$$Te(OH)_2^+ + e = Te(OH)_2 \text{ (fast)}$$

$$Te(OH)_2 + e = Te + 2OH^- \text{ (slowly).}$$

The cathodic polarization curve has three sections.Section I is due to the reduction of tetravalent tellurium to the elementary state. In area where the wave appears, the release of powdery tellurium is observed.

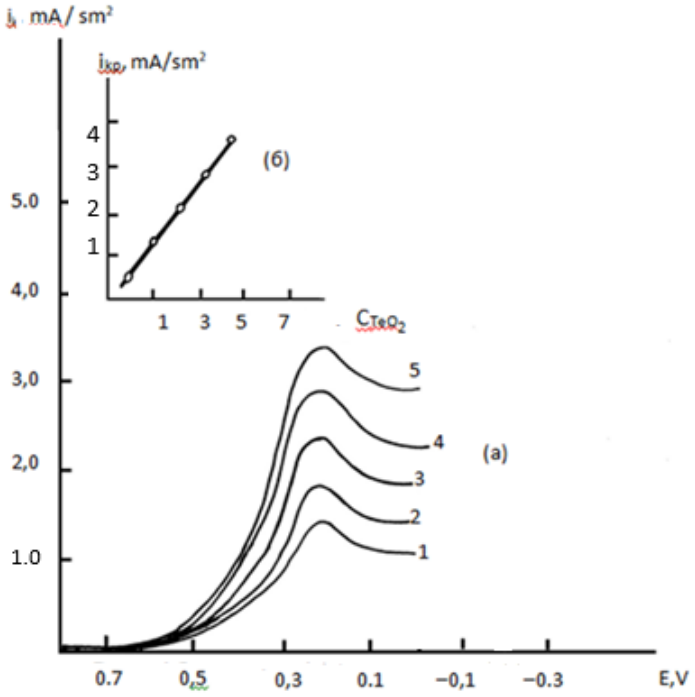

Fig. 2: Cathodic polarization curves obtained from solutions containing 5 mol/l H_2SO_4 + 5 mol/l HCl + 0.01 mol /l $(NH_4)_2SO_4$ and various concentrations of TeO_2 at t = 75°C. The concentration of TeO_2 (mol/l): a) 1 - 0.01; 2 - 0.03; 3 - 0.05; 4 - 0.07; b) Dependence of the wave value on the concentration of tellurium in the electrolyte.

From a potential of +0.28 V, the wave falls, and then rises again (II section). Perhaps, in these potentials, H_2Te is formed on the electrode surface.

$$Te + 2H^+ + 2e \rightarrow H_2Te.$$

Section III of the polarization curve is due to the vigorous evolution of hydrogen, which occurs according to the reaction:

$$H_2Te + 2e \rightarrow Te^{2-} + H_2$$

The resulting Te^{2-} ions diffuse from the cathode surface, meeting with $[Te(OH)_2]^{2-}$ ions, form elementary tellurium, and disproportionation reaction occurs in the solution according to the equation:

$$Te^{4+} + 2Te^{2-} = 3Te$$

since the possibility of a cathodic reaction in concentrated solutions is much greater than in dilute solutions. At more positive potentials (<0.3 V), anodic oxidation of tellurium occurs. The large potential difference between the cathodic reduction and anodic oxidation waves indicates that the tellurium deposition reaction is irreversible.

As it's known, during electrolysis, metal ions, before entering the crystal lattice of the precipitate, go through a number of successive stages, each of which proceeds at a certain rate. The slowest stage limits the rate of the processes in general.

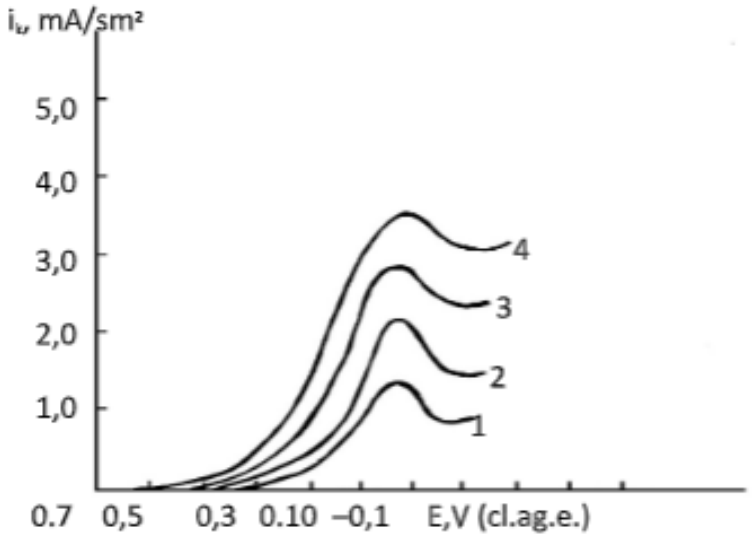

Fig. 3: Cathode polarization curves, obtained from solutions, containing 1,5 mol/l H_2SO_4+1,5 mol/l HCl+0,01 mol/l $(NH_4)_2SO_4$+0,05 mol/l TeO_2 at various temperatures on the Pt electrode. Temperature (°C) 1 – 20; 2 – 40; 3 – 80; 4-90

The electrodeposition of tellurium is significantly affected by the temperature of the electrolyte. As the experiments have shown, the temperature has a significant effect on the rate of the process under study. In the studied temperature range, the polarization curves have waves. As the

temperature rises, the rate of the electroreduction reaction increases, which is accompanied by increase in wave height. It was found that with the increase in temperature, the content of tellurium in the precipitate also increases, and fine-crystalline precipitates are obtained at the cathode. To determine the nature of cathodic polarization during tellurium deposition, on the basis of the data in Fig. 4, the lgi – 1/T graphs were plotted at various constant values of the cathodic potential . From the slope of these curves, we find the effective activation energy.

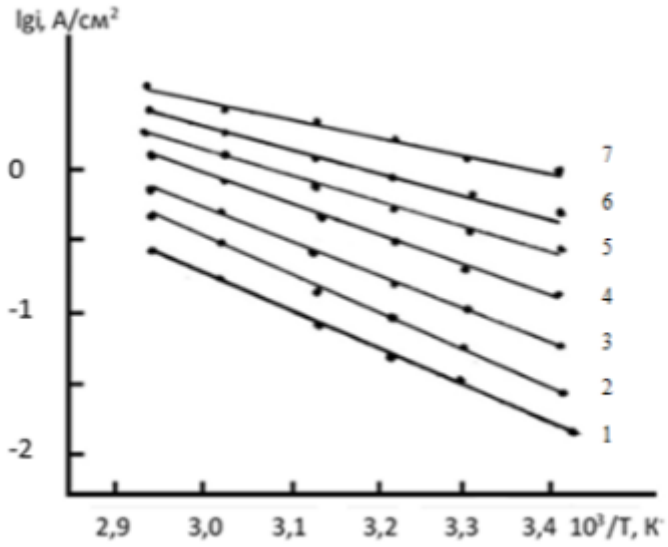

Fig. 4: Temperature dependence of the current density at various potentials of Te electrode Ek. 1–0.5; 2 - 0.45; 3 - 0.40; 4 - 0.35; 5 - 0.30; 6 - 0.25; 7 - 0.20.

Data provided in Fig. 4 show that the logarithmic rate dependence of the electrode process (lgi) on 1 /T in the potential range 0.50 to 0.20 V is linear. With the increase in the cathodic potential, the slope of the curves gradually decreases; in the range of cathodic potentials 0.2 to 0.1 V, it remains almost unchanged.

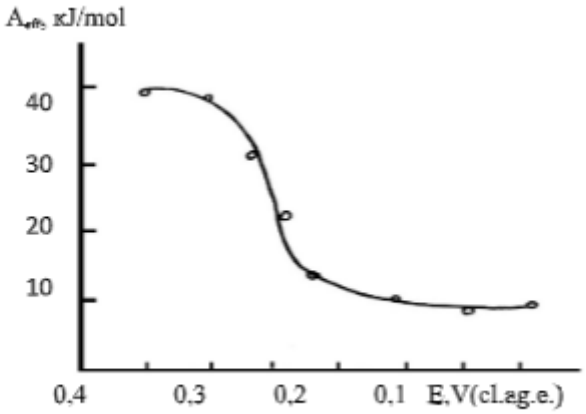

Fig. 5: The dependence of effective activation energy A_{eff} from E_c

Changing of effective energy activation in dependence from cathodic polarization has shown on the fig.5.The small value of the effective activation energy (12 KJ / mol) in the range of cathodic potentials (+0.2) - (+0.1) V and its insignificant independence from the potential show that in this case the rate of the cathodic process is limited only by the diffusion of discharging ions to cathode surface.

Based on the results, it can be concluded that at cathodic potentials up to 0.2 V, the process of tellurium electrodeposition from a chloride-sulfate electrolyte is accompanied mainly by chemical polarization and the effective activation energy at these potentials reaches 40 kJ /mol, and at a potential of 0, 30–0.25 V the process is controlled by mixed kinetics.

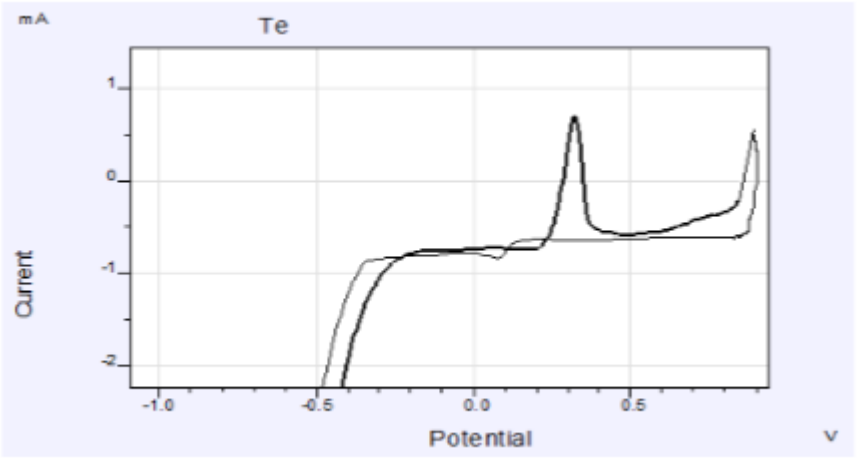

Fig. 6: Cyclic polarization curves of tellurium obtained from solutions containing $1 \cdot 10^{-3}$ TeO_2+1.5 mol /l H_2SO_4 + 1.5 mol/l HCl + 0.01 mol/l $(NH_4)_2SO_4$; PH= 0. 5. Temperature 75°C; (scanrate $V=0.005VS^{-1}$)

Thus, the totality of the obtained results give reason to consider that the rate of the cathodic process at the initial stages is limited by chemical difficulties and determined by diffusion only in the zone of limiting current.

As can be seen from figure 6, one wave is observed on the cyclic polarization curves, which shows the oxidation of tellurium. These data are consistent with the references presented in [9–10].We have also studied the effect of the electrode substrate (Pt, Ni) on the mechanism and quality of tellurium deposition.

On the figure 7 are presented the cyclic polarization curves of cathodic deposition and anodic dissolution of tellurium on various (Ni) electrodes in solutions containing (mol/l): TeO_2 + $2H_2SO_4$ +2HCl. Scan speed , temperature 348 °K.

It can be seen from the figure 7 that the cyclic polarization curves of tellurium on a nickel electrode do not differ significantly from the cyclic polarization curves obtained on a platinum electrode. However, oxidation on the platinum electrode occurs at more positive potentials and the maximum on the nickel electrode is lower than on the platinum one.

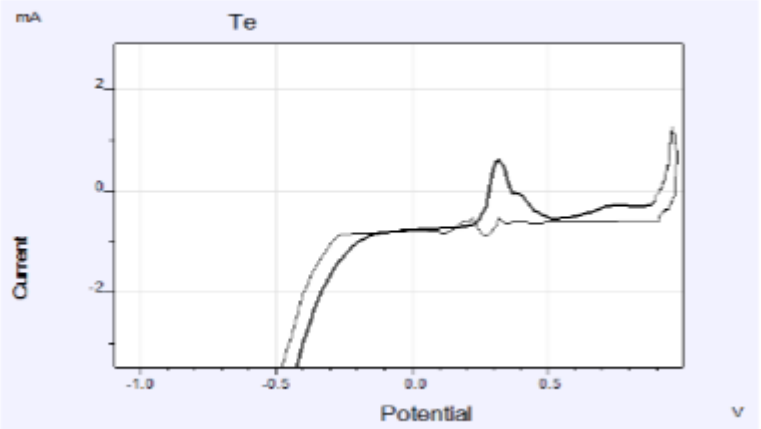

Fig. 7: Cyclic polarization curves of tellurium on Ni electrode in the electrolyte containing (mol/l): $1 \cdot 10^{-3}$ TeO_2 +1,5H_2SO_4+1,5HCl; pH=0.5. temperatur 75°C; (scanrate V=0,005 VS^{-1})

Thus, according to the experiments the electrolyte with following composition was proposed to produce thin tellurium films from chloride-sulfate solutions. Electrolyte composition is as follows (mol/l): 0,01TeO_2+1,5H_2SO_4+1,5HCl, i_k=1–4 mA/sm² , t=75°C, pH=0,5

IV. CONCLUSION

1. With an increase in the concentration of HCl in the electrolyte from 0.5 mol/l to 4 mol/l, the cathodic deposition of tellurium is facilitated, the polarization curves are shifted to the positive side. Thus, in this case, it can be assumed that with an increase in the HCl concentration in solution, partially hydrolyzed tellurium ions dissolve and at 2–3 mol/l HCl - $TeCl_4$ is formed, which dissociates well into ions, that causes the polarization curves to shift to the positive side.
2. Therefore, the experiments carried out in solutions containing chloride-sulfate ions show that in the initial stages of the cathodic process the main role is played by chemical difficulties, and at negative potentials of the process they are limited by diffusion polarization.
3. Based on the results, it can be concluded that at cathodic potentials up to 0.2 V, the process of tellurium deposition from a chloride-sulfate electrolyte is accompanied mainly by chemical polarization and the effective activation energy at these potentials reaches 40 kJ/mol, and at a potential 0.30–0.25 V the process is controlled by mixed kinetics.
4. The small value of the effective activation energy (12 KJ/mol) in the range of cathodic potentials (+0.2) - (+0.1) V and its insignificant independence from the potential show that in this case the rate of the cathodic process is limited only by diffusion of discharging ions to the cathode surface.

REFERENCES

1. Alekperov A.I. Electrochemistry of selenium and tellurium. Russian Chemical Reviewer. Moscow. Russia. 1974. V 43. IS.4, P. 585-593.
2. Bigelis V.M., Bykova E.M., Abrarov O.A. Stationary and equilibrium potentials of tellurium in fluoride-sulfate electrolytes. J. Electrochemistry. Moscow. Russia. 1976. V.12. P.139–142.

3. Bigelis V.M., Kim G.N., Navalikhin L.V. Influence of the electrolysis regime on the properties of tellurium coatings obtained from hydrochloric acid baths. J.Electrochemistry. Moscow. Russia. 1982. №11. P.1457–1461.
4. Bigelis V.M., Kim G.N., Abrarov O.A. et al. Influence of the composition of fluoride electrolytes and the conditions of electrodeposition on some properties of tellurium. J.Electrochemistry. Moscow. Russia. 1981.V.17. №12. P.1798–1802.
5. El-Khouli A.A., Hafez M.A., Kenavi I.M. Electrodeposition of palladium, thallium and tellurium from baths of various compositions. Electrochemistry, 2006, v.42, No. 3, p.264-271 (Russian)
6. Lebed, A., Boychenko S.S., Shunin V.A. Production of selenium and tellurium at JSC "Uralelektromed" Yekaterinburg: Ural University Press, 2015.114 p. (Russian)
7. Munirathnam N.R,. Prasad D.S., Rao J.V., Prakash T.L. High purity tellurium production using dry refining processes. Bull. Mater. Sci. 2005. V. 28. № 4. P. 309-311.
8. Hageman, A.M., Harrison M.J., Fritz N. , Krehbiel T.N., White R., Patenaude J., McGregor D.S. Purification of tellurium to 6N using a multistage vacuum distillation method . Proc. of SPIE. 2007. V. 6707. P. 67070Z1-7.
9. Munirathnam N.R., Prasad D.S., Sudheer Ch., Singh A.J., Prakash T.L. Preparation of high purity tellurium by zone refining. Bull. Mater. Sci. 2002. V. 25. № 2. P. 79-83.
10. Avetisov, I.Kh., Mozhevitina E.N., Khomyakov A.V., Avetisov R.I., Zinovyev A.Yu. Region of homogeneity of zinc telluride. News of higher educational institutions. Materials of electronic engineering. 2013. V. 61. No. 1. S. 4-10. (Russian)
11. Dergacheva M.B., Statsyuk V.N., Vogel L.A. Electrodeposition of CdTe films from ammonium chloride buffer electrolyte. Journal.Appl. Chemistry. 2004. V. 77. No. 2. C. 230-234.(Russian)
12. Dergacheva M.B., Statsyuk V.N., Vogel L.A. Electrochemical reduction of tellurium (IV) on solid electrodes in neutral solutions. Electrochemistry. 2001. T. 37. No. 6. C. 734-737. (Russian)
13. Ibishev K.S., Belyaev S.V., Kargina N.A. Temirgaliev S.M. Electrochemical reduction of tellurate ion using a high-voltage pulsed discharge. Modern methods in theoretical and experimental electrochemistry. II International Scientific Conf. Abstracts of reports. PLYOS 2010. Ivanovo June 21-25. C. 151. (Russian)
14. Kadyrov R.K., Rasulov K.R. Electrodeposition of tellurium from sulfate electrolytes in an ultrasonic field. Electrochemistry. 1972. No. 2. C. 1843-1845. (Russian)
15. Santos M.C., Machado S.A. Voltammetric and nano gravimetric study of Te underpotential deposition on Pt in perchloric acid medium. Electrochim. Acta. 2005. 50. № 11. P. 2289-2295.
16. Zhu W., Yang J.Y., Zhou D.X., Bao S.Q., Fan X.A., Duan X.K. Electrochemical characterization of the underpotential deposition of tellurium on Au electrode. Electrochim. Acta. 2007. 52. №11. P. 3660-13.
17. Fishman V.A., Liner V.I., Yerusalim Chick I.G. Study of the electrochemical behavior of tellurium. Electrochemistry. No. 5. 1969. C. 530-533. (Russian)Chizhikov D.M., Happy V.P. Tellurium and tellurides. M: "Nauka", 1966. 279s.
18. Mamedov M.N. Polarization during the deposition of tellurium from fluoroborate solutions. Azerbaijan Chem. Journal. 2000. No. 2. pp. 94-96. (Russian)
19. Salakhova E.A., Novruzova F.S., Majidzadeh V.A. Electrodeposition of thin tellurium coatings from chloride-borate electrolyte. Azerbaijan chem. jour. No. 4. 2005. C. 182-186(Russian)
20. E. Rudnik, j. Sobesto. Cyclic voltammetric studies of tellurium in diluted HNO_3 solutions. Archives of metallurgy and materials. volume 56, 2011, issue 2. DOI:10.2478/v10172-011-0030-z.

21. Samuel C. Perry, Joshua White , Iris Nandhakumar. Template-free electrochemical deposition of tellurium nanowires with eutectic solvents. Electrochimica Acta. Volume 439, 20 january 2022. https://doi.org/10.1016/j.electacta.2022.141674
22. Yan Li, Ye Zhang. Flexible Tellurium-Based Electrode for High-Performance Lithium-Tellurium Battery. Nanomaterials 2021, *11*(11), 2903; https://doi.org/10.3390/nano11112903
23. Yifei Yang, Mingkun Xu, Shujing Jia, Bolun Wang, Lujie Xu, Xinxin Wang, Huan Liu, Yuan Shuang Liu, Yuzheng Guo, Lidan Wang, Shukai Duan, Kai Liu, Min Zhu, Jing Pei, Wenrui Duan, Dameng Liu & Huanglong Li. A new opportunity for the emerging tellurium semiconductor: making resistive switching devices. Nature Communications. Volume 12, Article number: 6081 (2021) https://doi.org/10.1038/ s41467-021-26399-1 .

Great Britain Journal Press Membership

For Authors, subscribers, Boards and organizations

Great Britain Journals Press membership is an elite community of scholars, researchers, scientists, professionals and institutions associated with all the major disciplines. Great Britain memberships are for individuals, research institutions, and universities. Authors, subscribers, Editorial Board members, Advisory Board members, and organizations are all part of member network.

Read more and apply for membership here:
https://journalspress.com/journals/membership

For Authors

Author Membership provide access to scientific innovation, next generation tools, access to conferences/seminars/ symposiums/webinars, networking opportunities, and privileged benefits. Authors may submit research manuscript or paper without being an existing member of GBJP. Once a non-member author submits a research paper he/she becomes a part of "Provisional Author Membership".

For Institutions

Society flourish when two institutions Come together." Organizations, research institutes, and universities can join GBJP Subscription membershipor privileged "Fellow Membership" membership facilitating researchers to publish their work with us, become peer reviewers and join us on Advisory Board.

For Subscribers

Subscribe to distinguished STM (scientific, technical, and medical) publisher. Subscription membership is available for individuals universities and institutions (print & online). Subscribers can access journals from our libraries, published in different formats like Printed Hardcopy, Interactive PDFs, EPUBs, eBooks, indexable documents and the author managed dynamic live web page articles, LaTeX, PDFs etc.

GO GREEN AND HELP
SAVE THE ENVIRONMENT

JOURNAL AVAILABLE IN

PRINTED VERSION, INTERACTIVE PDFS, EPUBS, EBOOKS, INDEXABLE DOCUMENTS AND THE AUTHOR MANAGED DYNAMIC LIVE WEB PAGE ARTICLES, LATEX, PDFS, RESTRUCTURED TEXT, TEXTILE, HTML, DOCBOOK, MEDIAWIKI MARKUP, TWIKI MARKUP, OPML, EMACS ORG-MODE & OTHER

SCAN TO KNOW MORE

support@journalspress.com
www.journalspress.com

*THIS JOURNAL SUPPORT AUGMENTED REALITY APPS AND SOFTWARES